Execution and reliability of slip resistant connections for steel structures using CS and SS (SIROCO)

Version	Date of Issue	Purpose	Author	Technical Reviewer	Approved
01	12.3.2018	First draft for internal review	TPM	LEA	
02	16.3.2018	Issue to RFCS and TGS8	TPM	ES	MYI

EUROPEAN COMMISSION

Research Programme of
The Research Fund for Coal and Steel - Steel RTD

Creep and stress relaxation behavior of stainless steel plates at room temperature

Timo Manninen, Johan Pilhagen

Abstract

The present report summarizes the test results obtained from creep and stress relaxation testing of commercial austenitic, ferritic and duplex stainless steels. The objective of this work was to determine basic information on room temperature creep and stress relaxation behavior of plate materials in preloaded slip-resistant connections made of stainless steel. The test materials were hot-rolled 1.4003 and 1.4404 sheets and 1.4162 and 1.4462 plates.

Tensile tests with widely different loading rates ranging from 10^{-6} to 10^{-2} 1/s were performed to characterize the influence of loading rate on the stress-strain response of materials. Short-term and long-term uniaxial constant load creep tests were carried out with different load levels to investigate the creep behavior of plates. Additionally, a small number of stress-relaxation tests with repeated re-loading were carried out to simulate the influence of possible retightening of bolts.

Room temperature creep deformation was observed for the tested stainless steels at load levels at and above 0.50xRp0.2. The constant load creep behavior after sufficient time could be described by the logarithmic creep model. The logarithmic creep was dependent on the load level but independent on the initial loading rate. No secondary creep was observed. A state of the art viscoplastic material model was developed for modelling the creep and stress relaxation behavior of stainless steels at room temperature. Although one can observe creep in uniaxial tensile testing, the stress in plates in a preloaded connection is too low to give any significant contribution to the loss of preload. It was also concluded that the main contribution to the loss of preload in a preloaded stainless steel connection is the stress relaxation of the bolts.

Key words: Creep, Stress relaxation, 1.4003, 1.4404, 1.4162, 1.4462, SIROCO

Tornio R&D Center

outokumpu
high performance stainless steel

Creep and stress relaxation behavior of stainless steel plates at room temperature
Timo Manninen, Johan Pilhagen

2018-0042
2017-01-02
Technical report
Public

Page 1 of 69

TORNIO R&D CENTER

Contents

	Creep and stress relaxation behavior of stainless steel plates at room temperature Timo Manninen, Johan Pilhagen	2018-0042 2017-01-02 Technical report Public	Page 2 of 69

TORNIO R&D CENTER

1. Introduction

Creep deformation is defined as the time-dependent inelastic strain that occurs when material is subjected to sustained loading. In contrast to plastic flow, creep can occur also when stresses are below the yield strength of the material. Although creep deformation can occur at any temperature, creep deformations of crystalline solids such as metals and ceramics are typically very small at room temperature. Therefore, most creep studies have been concentrated in creep at high temperature. Creep at low temperatures has received less attention since structures "generally neither fail nor experience large creep deformations at low temperatures". The creep deformation of individual structural members at room temperature under allowable design stresses is usually remarkably small. Therefore, room temperature creep does not usually affect the design of individual structural elements.

Preloaded slip-resistant connections are used when deformations in the bolted connections must be limited to predefined values either for serviceability or ultimate limit reasons. Typical applications are found e.g. in bridges, cranes, radio masts and wind turbine towers. Essential characteristics of these connections are the level of preload in the bolts and the slip factor. The slip factor is influenced by the characteristics of contacting surfaces and by level of preload. For this reason, the level of preload in the bolts needs to be guaranteed over the whole service life of the structure. Loss of preload due to room temperature stress relaxation in the preloaded bolts and creep in the connected plates must be accounted for and taken into account in the design rules over the whole service life of the structure.

Slip-resistant connections have been used for carbon steel connections for several decades. No rules exist for design and execution of preloaded slip-resistant connections made of stainless steel. The lack of these design rules is currently limiting the use of stainless steel is certain types of structures.

The RFCS funded project Execution and Reliability of Slip-Resistant Connections for Steel Structures using Carbon Steel and Stainless Steel (SIROCO) aims to close the gap in the knowledge and generate guidance for design, preloading and execution of slip-resistant connections made of stainless steel.

The present report summarizes the test results obtained from creep and stress relaxation testing of commercial austenitic and ferritic stainless steels. The objective of this work was to determine basic information on room temperature creep and stress relaxation behavior of plate materials in preloaded slip-resistant connections made of stainless steel. The test materials were hot-rolled 1.4003 and 1.4404 sheets and hot-rolled 1.4162 and 1.4462 plates. The ferritic 1.4003 and austenitic 1.4404 test materials were studied at Outokumpu R&D in Tornio. The 1.4162 and 1.4462 duplex plates were studied at Outokumpu R&D in Avesta.

Uniaxial tension tests were carried out on samples orientated in 0°, 45° and 90° angles with respect to the rolling direction to characterize the basic mechanical properties of test material. Tensile tests with widely different loading rates ranging from 10^{-6} to 10^{-2} 1/s were used to characterize the influence of loading rate on the stress-strain response of materials. Short-term and long-term constant uniaxial load creep tests were carried out with different load levels to investigate the creep behavior of plates. Additionally, stress-relaxation tests with constant load and with repeated re-loading were carried out to investigate the stress-relaxation behavior of the ferritic and austenitic test materials. The test results contain basic information on the creep and stress-relaxation behavior of austenitic, ferritic and duplex materials at room temperature. The test results were used to define an empirical creep model and a state of the art material model for numerical simulation of preloaded slip-resistant connections.

TORNIO R&D CENTER

Creep and stress relaxation behavior of stainless
steel plates at room temperature
Timo Manninen, Johan Pilhagen

2018-0042
2017-01-02
Technical report
Public

Page 3 of 69

2. Materials

2.1 The austenitic and the ferritic material

The test materials were hot-rolled grade 1.4003 and 1.4404 sheets with the thickness of 8 mm. Both test materials were produced by Outokumpu. The grade 1.4003 is a low-chromium structural ferritic stainless steel. The grade 1.4404 is a molybdenum-alloyed austenitic stainless steel. The chemical composition of both test materials is given in Table 1. The mechanical properties of the test materials are summarized in Table 2. The grain size of the test materials was determined according to the standard ASTM E112-96. The grain size numbers were 11.6 and 7.9 in ASTM scale for the grade 1.4004 and 1.4003 test materials, respectively. Additionally, optical microscopy was carried out to study the microstructures of the test materials. The microstructures of both test materials correspond to those of typical commercial hot rolled stainless steels of type 1.4003 and 1.4404, Figure 1.

Table 1. Chemical composition of test materials according to material certificates (wt-%).

Grade	C	Si	Mn	P	N	Cr	Mo	Ni
1.4003	0.022	0.32	1.00	0.022	0.017	11.15	-	0.42
1.4404	0.018	0.45	0.85	0.040	0.044	16.6	2.04	10.1

Table 2. Mechanical properties of test materials according to material certificates.

Grade	Location in coil	Direction	Rp0,2 (MPa)	Rp1,0 (MPa)	Rm (MPa)	A5 (%)
1.4003	Beginning	Transversal	357	386	481	28.7
	End	Transversal	368	396	495	27.1
		Longitudinal	304	329	456	30.5
1.4404	Beginning	Transversal	283	328	592	52.0
	End	Transversal	286	336	592	51.0
		Longitudinal	280	315	583	52.7

ND

RD

100 µm

ND

RD

100 µm

1.4404   1.4003
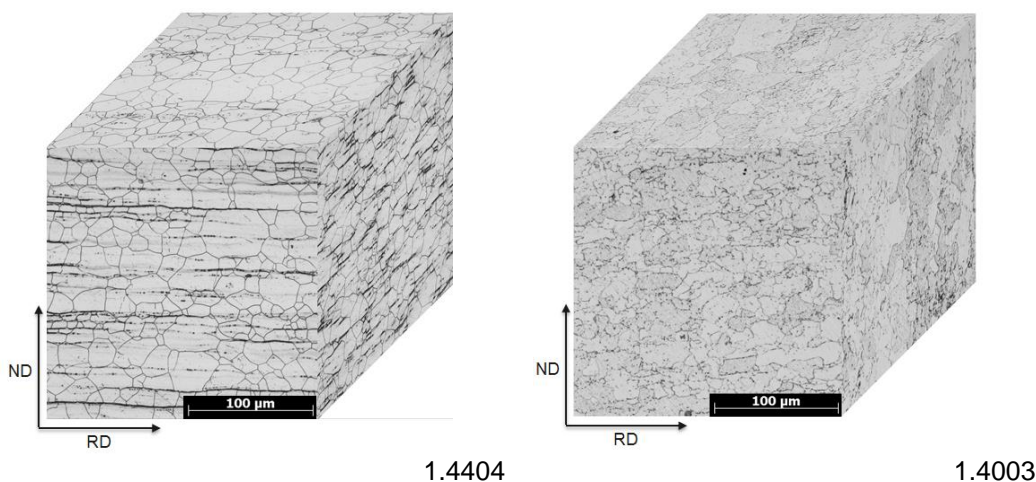
Figure 1. Microstructure of both test materials.

TORNIO R&D CENTER

Creep and stress relaxation behavior of stainless steel plates at room temperature
Timo Manninen, Johan Pilhagen

2018-0042
2017-01-02
Technical report
Public

Page 4 of 69

2.2   The duplex materials

Hot-rolled and annealed duplex plates of EN 1.4162 (lean duplex) and EN 1.4462 (duplex). Both plates were produced by Outokumpu. The plate thicknesses were 8.6 mm for 1.4162 and 8.0 mm for 1.4462. Table 3 shows the chemical composition of the duplex plates.

Table 3 Chemical composition of the duplex plates according to the material certificates (wt-%).

Grade	C	Si	Mn	P	N	Cr	Mo	Ni	Cu
1.4162	0.024	0.53	4.55	0.024	0.23	21.4	0.40	1.62	0.33
1.4462	0.017	0.44	1.60	0.024	0.17	22.64	3.14	5.81	0.24

The tensile properties of the plate material can be seen in Table 4, three tensile tests were performed on each type and the tested plated had continuous yielding behavior. The 1.4462 had higher proof and tensile strength while the 1.4162 had higher ductility.

Table 4 Mean tensile properties of the tested duplex plates.

Grade	Direction	E, GPa	$R_{p0.2}$, MPa	R_m, MPa	A, %
1.4162	Longitudinal	204	509	705	40.7
1.4462	Longitudinal	188	619	797	36.5
1.4162	Transversal	210	568	731	41.0
1.4462	Transversal	210	692	858	31.3

TORNIO R&D CENTER

---

3. Experimental techniques

3.1 Tensile testing of the austenitic and the ferritic material

The room temperature tensile testing was performed by means of a Zwick Z250 tensile testing machine with the capacity of 250kN. The tensile testing machine is equipped with GTM load cell 30971, hydraulic specimen grips and Zwick B06650 macro extensometer, Figure 2. The clamping of the sensor arms and the setting of the original gauge length L_0 is automatic with this extensometer type, Figure 3. The equipment is regularly calibrated according to standards SFS-EN ISO 7500-1:2004 and SFS-EN ISO 9513:2002.

Figure 2. Zwick Z250 tensile testing machine.

TORNIO R&D CENTER

Creep and stress relaxation behavior of stainless steel plates at room temperature
Timo Manninen, Johan Pilhagen

2018-0042
2017-01-02
Technical report
Public

Page 6 of 69

_____

Figure 3. Hydraulic specimen grips and Zwick macro extensometer.

The test piece geometry used in tensile tests is shown in Figure 4. This test piece geometry corresponds to type 1 in the annex B of EN ISO 6892-1. The original gauge length used for this test piece type is L0 = 50mm. The test pieces were fabricated by machining. Positioning and alignment of test pieces was done manually .
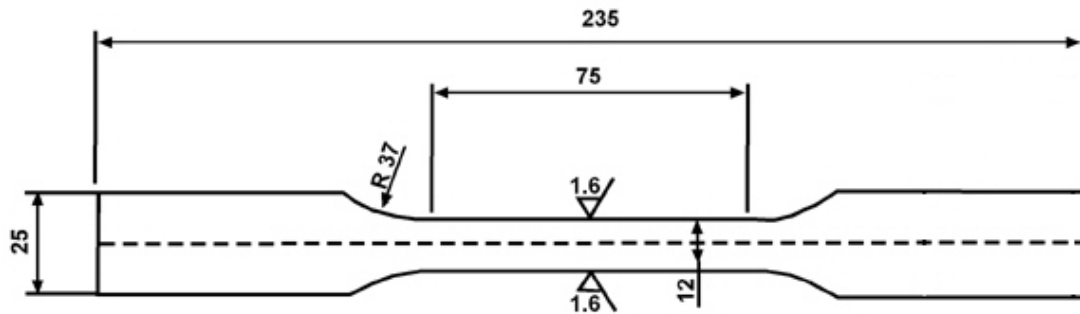
Figure 4. Test piece used for tensile testing. Dimensions are given in mm.

The tensile tests used for characterization of mechanical properties of test materials were carried out according to the tensile test standard EN ISO 6892-1. This testing standard specifies two different methods of controlling the machine rate in different parts of the tensile testing. The method A224 was used in the present work. The relevant strain rate values are summarized in Table 5.

Table 5. Loading rates used in the tensile tests used for determining the mechanical properties of test materials.

Range	Strain rate (s^{-1})	Relative tolerance
Elastic range	0.00025	± 20%
Proof stress	0.00025	± 20%
Tensile strength	0.0067	± 20%

	Creep and stress relaxation behavior of stainless	2018-0042	Page 7 of 69
outokumpu	steel plates at room temperature	2017-01-02	
	Timo Manninen, Johan Pilhagen	Technical report	
TORNIO R&D CENTER		Public	

_____

In addition to basic characterization of test materials, tensile tests were also used to investigate the rate-dependent and rate-independent strength of these plate materials. In these tests, different loading rates in the range from 10^{-7} 1/s to 10^{-2} 1/s were used.

The tensile testing machine used belongs to accuracy class 1. The accuracy of the results can be described by the following error measures:

- The relative error of the original gauge length is less than 1.0 %.
- The accuracy of one arm of the extensometer displacement is 3 µm or 1 % - whichever is larger.
- The error on the force value is less than 1.0 %.
- The resolution of the displacement of one arm of the extensometer is 0.6 µm.
- The resolution of the force sensor is 1 N.

3.2   Short-term creep testing of the austenitic and the ferritic material

The short-term room temperature testing was carried using the same tensile testing machine as the tensile tests. Precise axial alignment of test pieces is an essential prerequisite for accurate results in creep testing. Therefore, special precautions were taken to ensure perfect axial alignment of test pieces.

1. Test piece geometry having wide shoulders and centering holes was used for the tests, Figure 5. The original gauge length used for this test piece is L0 = 80 mm.
2. Special two-step fabrication procedure was used to manufacture the test pieces. In the first step, specimens with machining allowances were produced by laser cutting. Then in the second step the edges were machined. This fabrication procedure guarantees that the centering holes are accurately positioned in the axis of the specimen. Extremely good overall shape accuracy is also achieved.
3. Pin-end grips were used to attach the specimen to tensile testing machine. The pins position the specimen at the center of the grips. They also prevent transfer of bending moment from grips to the test piece. Figure 6 shows the short-term creep test specimen in the pin-end grips.
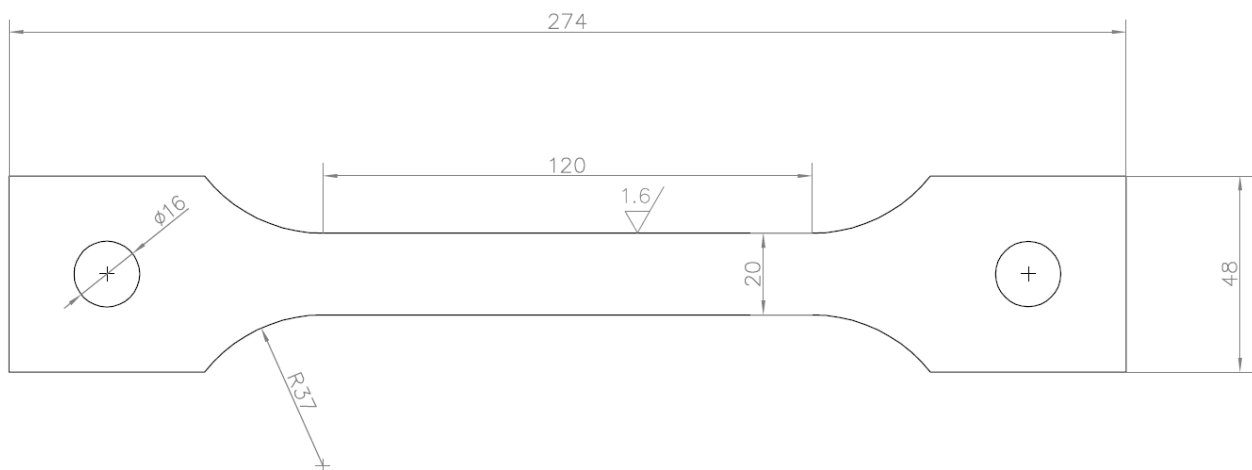

Figure 5. Test piece used in the short-term creep tests. Dimensions given in mm.

| | | Creep and stress relaxation behavior of stainless steel plates at room temperature | 2018-0042 | Page 8 of 69 |
| | | Timo Manninen, Johan Pilhagen | 2017-01-02 Technical report | |

outokumpu

TORNIO R&D CENTER

Public

_____

Figure 6. Short term creep test specimen in the pin-end grips.

The short term constant load creep tests were conducted with six different loading levels given in Table 6. The creep tests were carried out in the longitudinal direction. The load levels used are proportional to the 0.2 % proof stress value measured in the same direction, i.e. the 0° values given in Table 2. The duration of one creep tests was 12.5 hours.

Table 6. Loading levels used at short term constant load creep tests.

Nominal Stress	Repeats
(x $R_{p0,2}$)	(-)
0.300	3
0.475	3
0.650	3
0.825	3
1.000	3
1.200	3

The short-term creep tests were conducted under closed-loop force control. In the beginning of the test, the loading is applied with the target loading rate of 50 MPa/s. For the present test piece geometry, this loading rate corresponds to the strain rate of $\dot{e} = 0.00025 \ 1/s$ used in the elastic range in the standard tensile tests. When the specified target load was reached, it was maintained at this value throughout the 12.5-hour creep period.

In the ideal case, the loading would satisfy the following conditions:

1. The stress remains accurately constant at the target value throughout the actual creep period.
2. There is no overshoot in the load ramp-up stage.
3. The loading rate is constant during the load ramp-up stage.

The closed-loop force control used in the tensile testing machine is usually not capable of achieving all these targets simultaneously. The desired stress response in the constant load creep tests corresponds to step

		Creep and stress relaxation behavior of stainless steel plates at room temperature	2018-0042	Page 9 of 69
outokumpu		steel plates at room temperature	2017-01-02	
		Timo Manninen, Johan Pilhagen	Technical report	
TORNIO R&D CENTER			Public	

_____

change in the set point. Generally, the response of a closed-loop PID-control system to this kind of loading will contain features such as overshoot, damped oscillations, persistent offset from the set-point value and oscillation near the set point value. Some of these features are illustrated in Figure 7. Fortunately, the control response can be influenced by adjusting the gain parameters of the PID-controller. The adjustment process is known as tuning of the control loop.
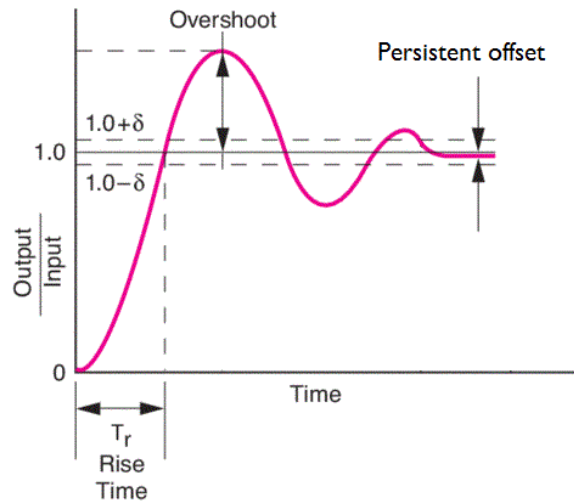

Figure 7. Schematic illustration describing the response of process variable to a step change in the set-point value in a process is controlled with a PID-controller.

In constant load creep tests, overshoot and damped oscillations are simply not acceptable. Therefore, the controller was tuned with the goal of having no overshoot and an accurately constant creep load with a minimal amount of oscillation around the specified target value. This was achieved with an overdamped controller with a low gain in the proportional term.

Figure 8 shows an example of the stress response obtained in the short-term constant load creep tests. Several important features can be observed in the figure. There is a small persistent offset between the creep stress and the target value of 280 MPa. This deviation is, however, smaller than the measurement error in the stress signal. There is also small continuous fluctuation in the stress signal, but he amplitude of the oscillation is also small. The state of constant load is approached gradually. The exact time, at which the load ramp-up stage has ended and the constant load creep has started, is somewhat controversial.

It is also worth noting that when the controller settings optimized for the creep testing, the stress rate will not be constant in the initial loading phase. The increase of the stress follows a smooth sigmoid curve instead of a straight line. Figure 9 shows a typical example of stress response in the loading phase and Figure 10 shows the corresponding stress-rate. It can be observed that there is notable variation in the stress and strain rates in the initial loading stage.

According to literature, the loading rate has an influence in the creep and stress relaxation testing. The effect is particularly strong in the beginning of the test and gradually vanishes with time. Therefore, the first 1800 seconds of the short-term creep tests will be excluded from the analysis of test results.

Creep and stress relaxation behavior of stainless
steel plates at room temperature
Timo Manninen, Johan Pilhagen

TORNIO R&D CENTER

2018-0042
2017-01-02
Technical report
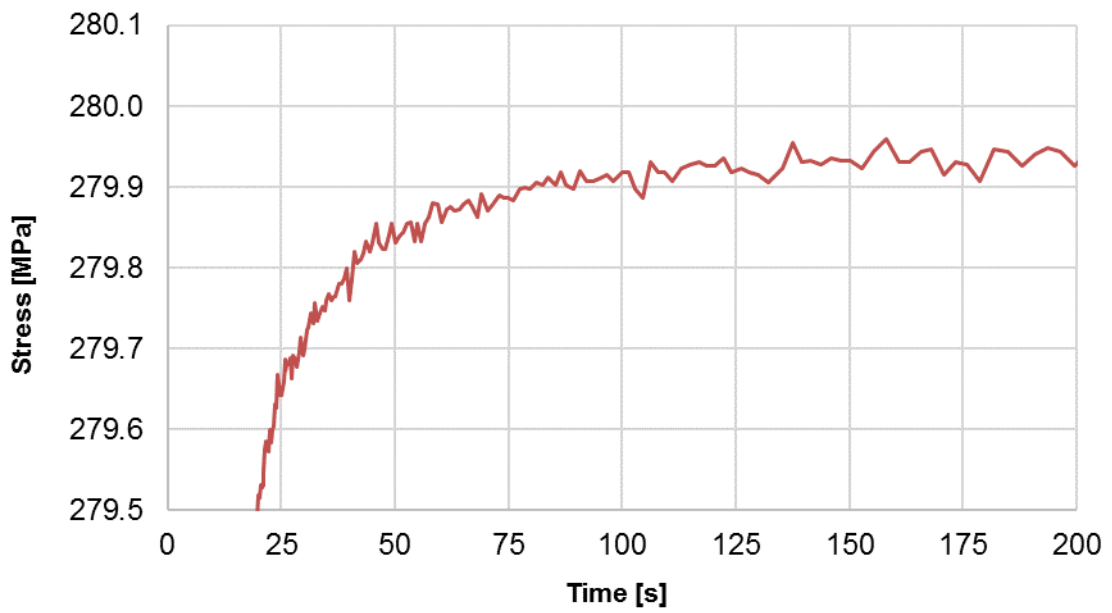Public

Page 10 of 69

_____

Figure 8. Typical stress response in the beginning of a short-term creep test. The creep load 280 MPa used in this case equals to 0.2 % proof stress of grade 1.4404 test material used.

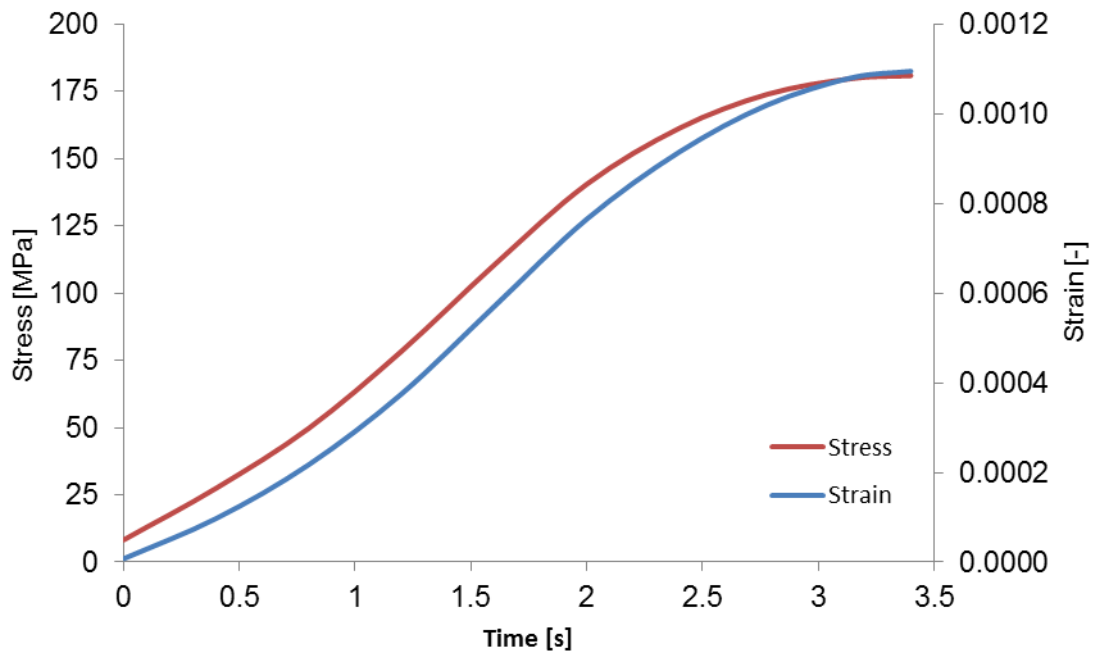|	Creep and stress relaxation behavior of stainless	2018-0042	Page 11 of 69
TORNIO R&D CENTER	steel plates at room temperature	2017-01-02	
	Timo Manninen, Johan Pilhagen	Technical report	
		Public	

_____

Figure 9. Evolution of stress and strain in the loading phase in the short-term constant load creep test for grade 1.4404 plate material. The creep load 182 MPa used in this case equals to 65 % of the 0.2 % proof stress of the material.
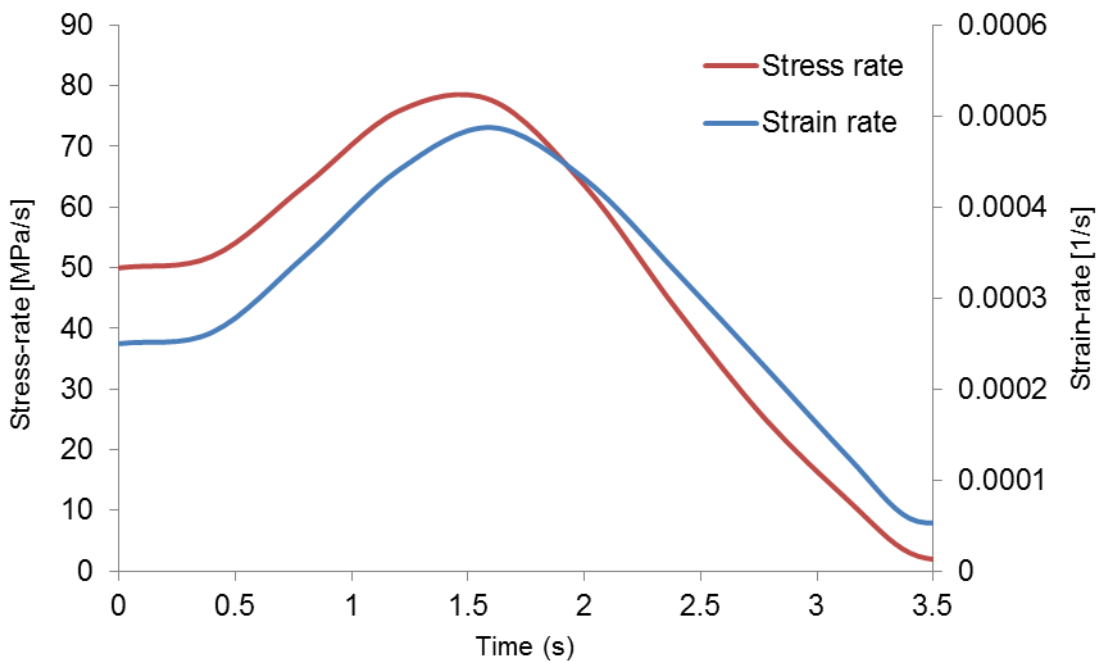

Figure 10. Stress-rate and strain-rate in the loading phase in the short-term constant load creep test for grade 1.4404 plate material. The creep load 182 MPa used in this case equals to 65 % of the 0.2 % proof stress of the material.

_____

3.3 Long-term creep testing of the austenitic and the ferritic material

The long-term constant load creep tests were carried using an in-house built lever-arm testing rig. The test piece geometry used in the long-term creep testing has similar wide shoulders and centering holes as the one used for the short-term creep tests, Figure 11. The test pieces used in the long-term creep tests were also fabricated with the same two-step manufacturing procedure. Pin-end grips were used to attach the specimen to the creep testing rig. These precautions ensure perfect axial alignment of the test pieces.
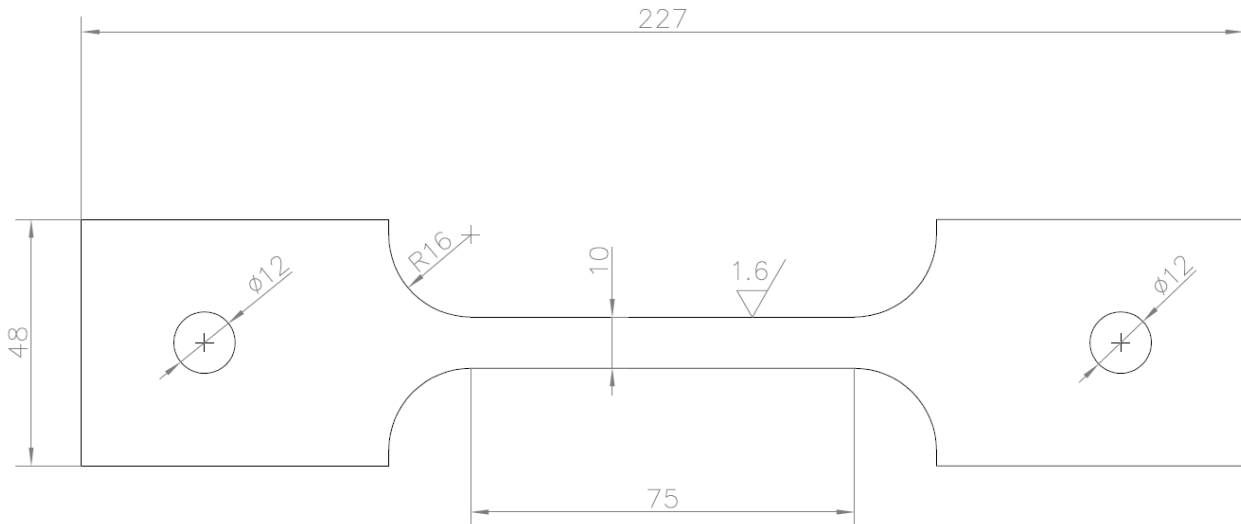

Figure 11. Test piece used in the long-term creep tests. Dimensions given in mm.

Strain was measured using strain gages. Two strain gages were attached exactly in the middle of the test piece, one gage on each side of the specimen. The type of strain gages was selected to minimize the influence of minor temperature variation in the laboratory. The selected strain gages are self-temperature compensated and delivered with a vinyl-coated three-wire cable. Austenitic and ferritic stainless steels have different coefficient of thermal expansion. Therefore, different strain gages had to be used for different test materials. The properties of strain gages are summarized in Table 7. The strain gages were used in a quarter bridge configuration. The gages were connected to separate channels of carrier frequency amplifier (Kyowa PCD-330B-F). The measurement frequency was 1 Hz and the measurement scale was set to 2 %. The variation of room temperature was measured with two K-type thermocouples attached to an unloaded specimen hanging freely from the testing rig.

Table 7. Strain gages used in long-term creep testing.

Grade	Gage producer and type	Temperature compensation	Gage length (mm)
1.4003	Kyowa KGF-10-120-C1-11L3M3R	11.7 $\mu\varepsilon/K$	10
1.4404	Kyowa KGF-10-120-C1-16L3M3R	16.2 $\mu\varepsilon/K$	10

The long-term constant load creep tests were conducted with three different loading levels. The loading levels were selected based on the results of the short-term creep tests. The selected loading levels are summarized in Table 8. The long-term creep tests were also carried out in the longitudinal direction. The load levels used are proportional to the 0.2 % proof stress value measured in the same direction.

	Creep and stress relaxation behavior of stainless	2018-0042	Page 13 of 69
	steel plates at room temperature	2017-01-02	
	Timo Manninen, Johan Pilhagen	Technical report	
TORNIO R&D CENTER		Public	

_____

Table 8. Loading levels used in the long-term constant load creep tests. The same loading levels were also included in the short-term creep tests.

Nominal Stress (x $R_{p0,2}$)	Repeats
0.650	3
0.825	3
1.000	3

In the Technical Annex, the duration of long-term constant load creep tests was 100 hours. For practical reasons, the testing period was, however, extended to approximately 150 hours. Steel weights were used for producing the specified axial force on the test pieces. The load was calibrated by means of HBM U2A load cell. The load cell belongs to accuracy class 0.5. The weights were lifted and lowered by means of a chain hoist. The loading was carried out as smoothly as possible. The strain measurement was started before the load was applied and the time used for assigning the load on the specimen was measured with a stopwatch.

Based on the technical specifications of strain gages and the carrier frequency amplifier it was estimated that the accuracy of the strains in the present test setup is approximately 1.1 %. This error consists mainly on the inaccuracy of the amplifier and drifting of the zero value with time. Other error sources seem to be insignificant compared to these two.

Processing of measurement data
A close inspection of the creep test results revealed that the creep strain signal contains an error signal correlated to variation of room temperature in the laboratory. Figure 12 shows an example of a creep test curve along with the temperature change measured from the specimen during the creep test. It can be clearly seen that the change of temperature also shows in the creep curve. Based on the nature of the creep process the creep strain should be monotonically increasing with time whereas in the example case shown below, the creep strain is occasionally also decreasing with time. A negative slope may typically occur at times when the room temperature is changing rapidly and the rate of creep deformation is slow.

The change of strain with changing temperature might be caused by thermal expansion of the specimen. But in the present case it can be observed that the specimen contracts when the temperature increases and elongates when the temperature decreases. This kind of negative thermal expansion cannot be explained by any physical process. Rather, it is most likely caused by the temperature sensitivity of the measurement system.
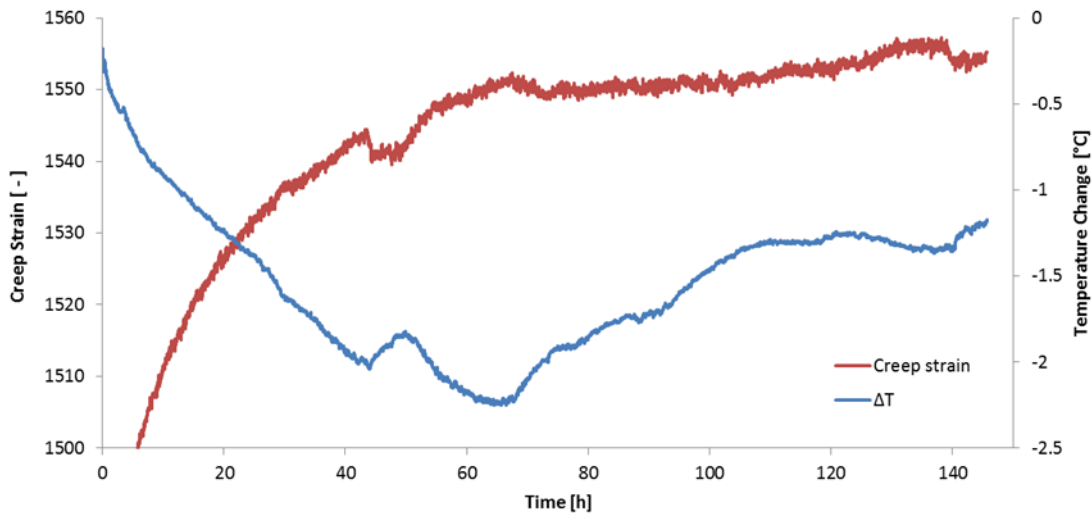
_____

Figure 12. Creep strain and room temperature change in 150-hour creep test with the load level of 182 MPa for grade 1.4404 plate material.

The main purpose of creep testing is to determine the rate of creep deformation as a function of time and stress. The rate of creep deformation is the slope of creep curve. Therefore, the first step in analyzing the creep test results is to differentiate the creep curve numerically.

Numerical differentiation of noisy signals is in general difficult since the noise and possible error signals are amplified in the differentiation operation. In the present case, the error signal related to change in the room temperature is amplified, and starts dominating over the actual creep process towards the end of the test period. Therefore, it is necessary to filter the error signal from the creep strain signal before the creep strain rate is calculated.

In the present work, a new numerical method was developed for processing the measurement data acquired during the long-term creep tests. All measurement data acquired in the long-term 150-hour creep tests was processed using this method. The method was derived based on analysis of measured signals.

The method developed for processing the data consists of the following three steps:

1. Data reduction.
2. Removing the temperature dependent part of the measurement signal.
3. Calculation of derivative.

The data reduction step consists of two sub-steps. First, 60 second running averages are calculated to remove the high frequency measurement noise from the creep strain signal. Certain amount of high frequency noise is clearly visible in the example curve shown in Figure 12. Then, in the second sub-step, measurement points (t_i, ε_i) are extracted from the averaged data. The time points are organized in the geometrical series

$$\begin{cases} t_0 = 1800 \ s \\ t_{i+1} = 1.05 \ t_i \end{cases} \qquad (1)$$

This arrangement on measurement points results in equal distance between points in the logarithmic time scale. In the present case, the time series generated with the series (1) will consist of nearly equidistance points in the double-logarithmic scale used for presenting the creep and creep rate curves.

In the second step, multilinear regression analysis is used to removing the temperature dependent part of the measurement signal. Let the observed creep signal time-series be denoted by x_k. The observed signal consists of the creep strain s_k, temperature correlated error e_k and zero-mean white noise w_k.

_____

$$x_k = s_k + e_k + w_k \tag{2}$$

The creep strain which is close to linear with respect to the logarithm of time is approximated with series

$$s_k = \alpha_0 + \alpha_1 \ln t_k + \alpha_2 (\ln t_k)^2 \tag{3}$$

where α_0, α_1, and α_2 are unknown constants. The temperature correlated error is proportional to the temperature change ΔT in the testing period

$$e_k = \beta \, \Delta T_k \tag{4}$$

where β is an unknown constant. It follows that the time series can be written as

$$x_k = \alpha_0 + \alpha_1 \ln t_k + \alpha_2 (\ln t_k)^2 + \beta \, \Delta T_k + w_k \tag{5}$$

The component w_k was assumed to be zero-mean white noise. Optimal values for the unknown parameters $\alpha_0, \alpha_1, \alpha_2$ and β can therefore be obtained by applying multilinear regression analysis to the problem

$$x_k = \alpha_0 + \alpha_1 \ln t_k + \alpha_2 (\ln t_k)^2 + \beta \, \Delta T_k \tag{6}$$

The results of the regression analysis will provide least squares estimates for the unknown parameters along with diagnostic information regarding the results. The multilinear regression analysis can be readily carried out e.g. by using the data analysis package in Microsoft Excel.

If P-value for the for the second independent variable ΔT is sufficiently small, say $P < 0.05$, the temperature dependent error can be estimated to be

$$e_k = \hat{\beta} \, \Delta T_k \tag{7}$$

where $\hat{\beta}$ is the least squares estimate for parameter β. The creep strain time-series, $\tilde{x}_k$ cleaned from the error caused by the changing temperature, can therefore be written as

$$\tilde{x}_k = x_k - \hat{\beta} \, \Delta T_k \tag{8}$$

In the third and final step, the creep rate is calculated. In the present work, the creep rate was calculated both using central difference approximation.

$$\dot{\varepsilon}_{k+\frac{1}{2}} = \frac{\tilde{x}_{k+1} - \tilde{x}_k}{t_{k+1} - t_k} \tag{9}$$

Negative creep rate values were neglected. The influence of different steps on the creep test data is illustrated in Figures 13 and 14.

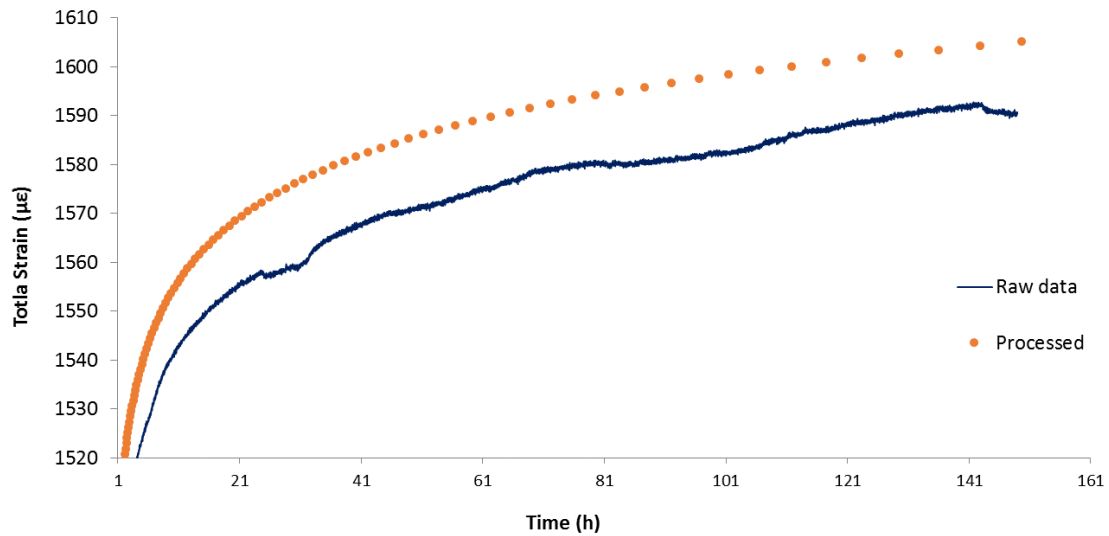|	Creep and stress relaxation behavior of stainless	2018-0042	Page 16 of 69
outokumpu ⃝	steel plates at room temperature	2017-01-02	
	Timo Manninen, Johan Pilhagen	Technical report	
TORNIO R&D CENTER		Public	

Figure 13. Creep strain in 150-hour creep test before and after processing with developed numerical method. The raw data is shown for reference. The same creep test as in Figure 12.
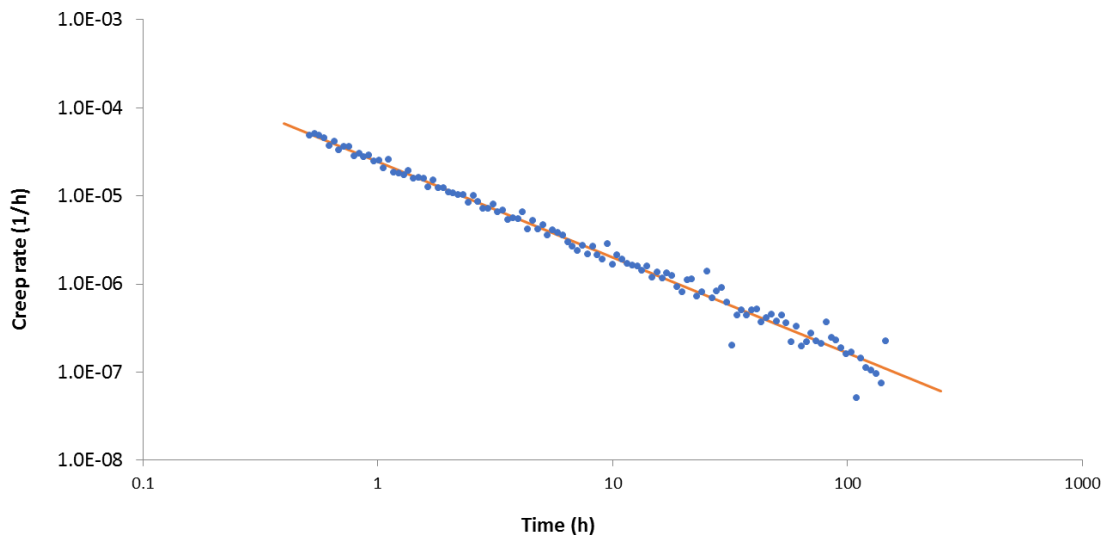

Figure 14. Creep strain rate calculated with developed numerical method for the example case discussed above and shown in Figures 12 -13. A logarithmic trend line fitted to the data is shown for reference.

3.4   Short-term stress relaxation testing with repeated reloading

The original testing plan outlined in the Technical Annex included short term creep tests with staircase loading for grade 1.4003 and 1.4404 plate materials. The purpose of these tests was to investigate material response in the case that the bolts are retightened once or several times during the execution procedure or during the service life. Once the results of the short term constant load creep tests were analyzed, it was, however, concluded that a repeated relaxation test would a better way of observing the material response under repeated loading. Therefore, creep tests with staircase loading were replaced by an equal number of repeated relaxation tests of grade 1.4003 and 1.4404 plate materials.

The short-term stress relaxation tests with repeated reloading were carried using the same tensile testing machine and the same test piece geometry as the short-term constant load creep tests. Two different

	Creep and stress relaxation behavior of stainless	2018-0042	Page 17 of 69
	steel plates at room temperature	2017-01-02	
	Timo Manninen, Johan Pilhagen	Technical report	
outokumpu			
TORNIO R&D CENTER		Public	

_____

loading rates were used. The loading phase was done with position control and the relaxation periods with strain control. The duration of one relaxation period was 3 hours and one test included four repeated relaxations. Figure 15 shows an example. Continuous 12-hour relaxation tests were also carried out for comparison purposes. The load levels and loading rates used are summarized in
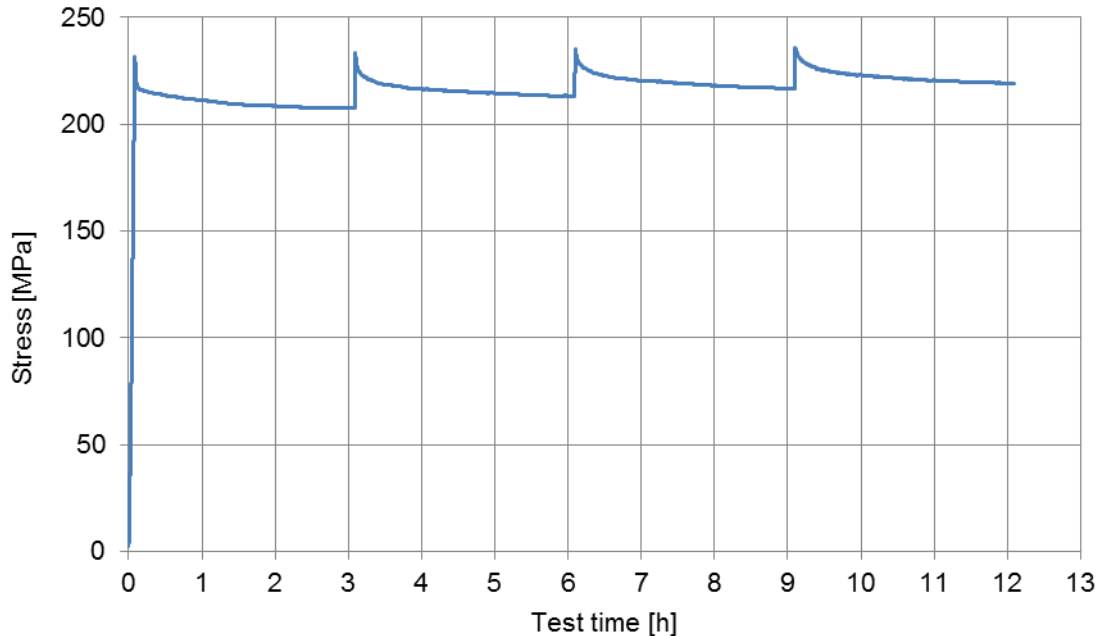Table 9.

Figure 15. Repeated relaxation test for grade 1.4404 plate material.

Table 9. Load levels and loading rates used in the repeated relaxation tests. Continuous 12-hour relaxation tests also were conducted for comparison purposes.

Grade	Nominal Stress (x $R_{p0,2}$)	Loading rate (MPa/s)	Test type	Repeats
1.4003	0.825	0.5	4 x 3h	2
	0.825	5.0	4 x 3h	2
	0.825	0.5	12h	2
1.4404	0.825	0.5	4 x 3h	2
	0.825	5.0	4 x 3h	2
	0.825	0.5	12h	2

3.5 Tensile and creep testing of the duplex materials

The testing system consisted of an electromechanical servo controlled machine from Dartec. The console was Doli EDC 120 and the testing software was Cyclic v8.11.02 from the Swedish company Inersjö Systems AB. The load cell used was a 250 kN class 0.5. The LVDT for the position had class 0.5. The extensometer used was a class 0.5 macro extensometer from Zwick/Roell. The specimens used was flat specimens with cross-section of 12.5xthickness mm² and 110 mm parallel length in compliance with ISO 6892-1. The extensometer gauge length was of proportional length.

_____

The tensile testing was based on EN ISO 6892-1:2009 B11. The relevant rate values are summarized in Table 10.

Table 10 Loading rates used in the tensile tests of the duplex materials for determining the mechanical properties.

Range	Stress rate, MPa/s	Strain rate, s^{-1}	Relative tolerance
Elastic range	11		
Proof stress		0.001	
Tensile strength		0.0067	± 20%

For the creep testing, similar specimens as for the tensile testing were used. The specimens were loaded to an initial tensile stress of 0.50, 0.65, 0.83, 1.00 and 1.20 times the measured $R_{p0.2}$ (Table 4) and thereafter held at constant load for various amount of time at room temperature conditions and then unloaded and removed. The testing direction was longitudinal.

Three types of initial loading rates were used: 2 MPa/s up to 10 MPa from the specified initial stress and 0.5 MPa/s thereafter, constant crosshead speed with resulting strain rate of 10^{-5} 1/s and 10^{-4} 1/s. Least linear square fitting was used for evaluating the resulting strain rate under constant crosshead speed, see Table 11. For the constant crosshead speed, two speeds were used for the higher load levels due to the non-linear deformation behavior of the plates where the lower speed was used at higher strains. As seen in Table 11 this manual may of achieving constant strain rate was not perfect at higher strains but was deemed good enough. In this report, the loading rates for the duplex plates are referred to as 2 MPa/s, 10^{-5} 1/s and 10^{-4} 1/s.

Table 11 Resulting strain rate during constant crosshead speed.

Grade	xRp0.2	Strain rate, 1/s	R2	Strain rate, 1/s	R2
1.4162	0.65	1.0×10^{-4}	1.000	9.7×10^{-6}	0.999
	0.83	1.0×10^{-4}	0.998	1.1×10^{-5}	0.996
	1.00	8.5×10^{-5}	0.989	8.7×10^{-6}	0.997
1.4462	0.65	1.0×10^{-4}	1.000	1.0×10^{-5}	0.999
	0.83	1.1×10^{-4}	0.999	1.1×10^{-5}	0.997
	1.00	9.3×10^{-5}	0.997	9.3×10^{-6}	0.998

The initial loading rate as a function of strain for the initial loading can be found in Figure 16. The sudden decrease of strain rate for the constant stress rate loading was due to the change to 0.5 MPa/s close to the end of loading, Figure 16a. Figure 16b shows the load levels 0.50 to 0.83xRp02. The highest strain rate during the initial loading was achieved for the 1.20xRp0.2 at the loading rate of 2 MPa/s, see Figure 16c.

The creep test consisted of different programming blocks in the software used for controlling the electromechanical testing machine. When the specified stress was reached, the software proceeded to the next block which keeps the load constant. The standard deviation for keeping constant load were 0.04 MPa for the 1.4162 and 0.06 MPa for the 1.4462, this indicates high precision for maintaining constant load for the used test setup. For the creep test of the two duplex materials the transition from initial loading to constant load was almost instantaneous and without over-shooting as shown in Figure 17. Due to this it was possible to distinguish the initial creep from the logarithmic creep (see chapter 5.2).

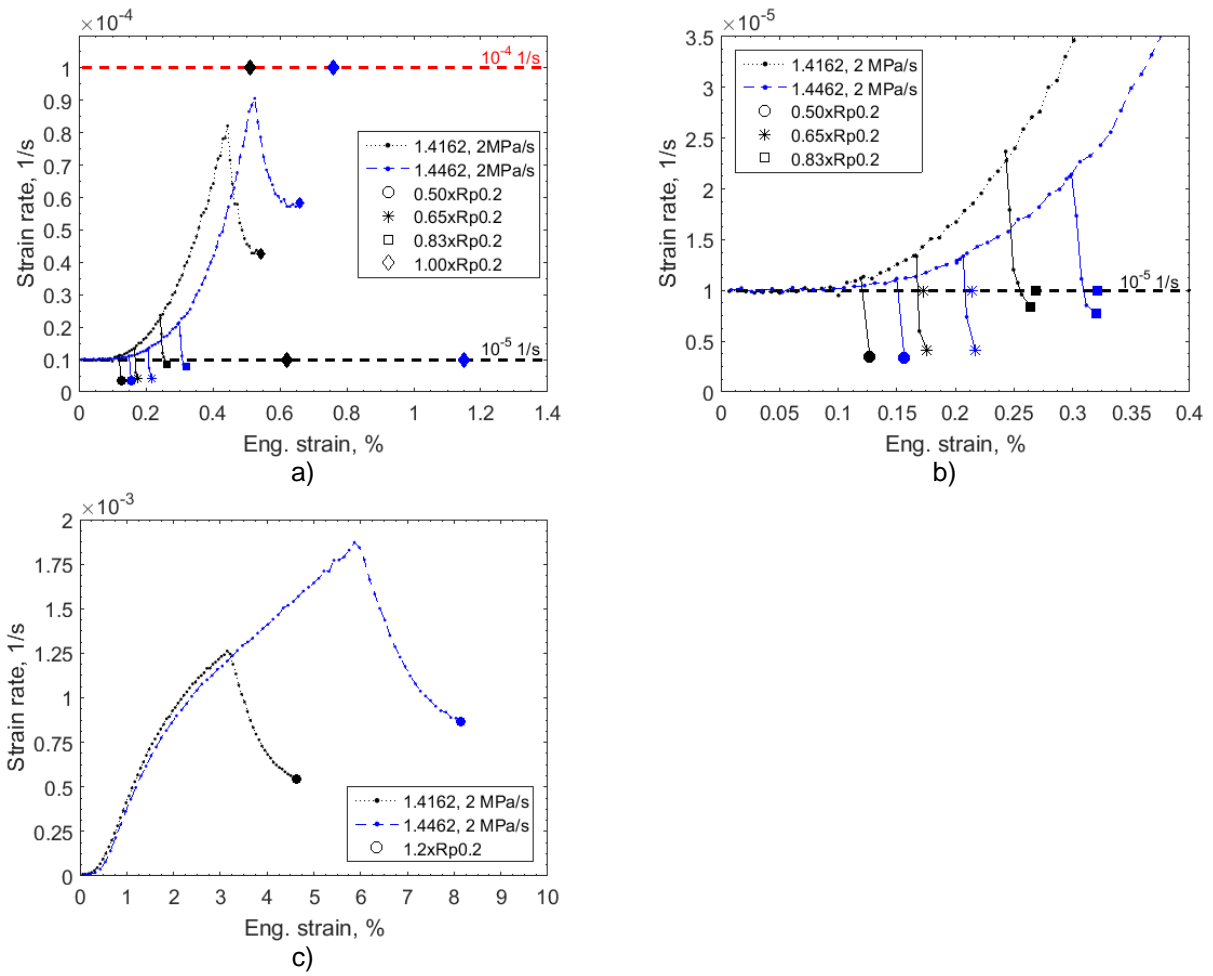| outokumpu	Creep and stress relaxation behavior of stainless steel plates at room temperature Timo Manninen, Johan Pilhagen	2018-0042 2017-01-02 Technical report Public	Page 19 of 69

TORNIO R&D CENTER

Figure 16 Initial loading rates as a function of engineering strain. a) Load levels up to $1.00xR_{p0.2}$, b) load levels between 0.50 and $0.83xR_{p0.2}$, c) $1.20xR_{p.02}$ load level. The markers indicate the strain and strain rate at the start of the creep testing (constant load).
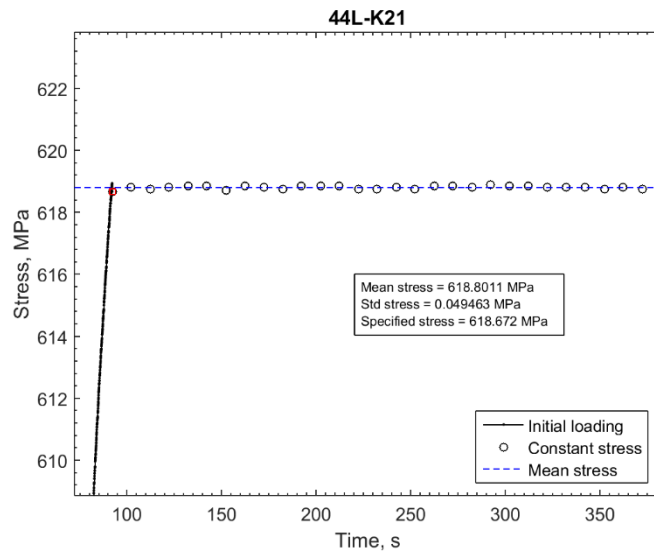
Figure 17 The transition from the initial loading to the constant load condition.

	Creep and stress relaxation behavior of stainless steel plates at room temperature Timo Manninen, Johan Pilhagen	2018-0042 2017-01-02 Technical report Public	Page 20 of 69

TORNIO R&D CENTER

_____

The creep testing was performed in room temperature condition where the ambient temperature in the room changed with the day-night cycle and outdoor condition. No climate chamber was available so no control over the ambient temperature was possible which caused interference with the creep testing for the 0.50 to 0.83xRp0.2 load levels. Hydraulic grips were used for clamping the specimen where the pressure was maintained from a hydraulic pump. The configuration was such that the pump increased the pressure to 200 bar and then was idle until the pressure had decreased to 190 bar at which the pump becomes active again. This cycle took approximately 30 s. Due to the machine was operated in closed-loop control using the force signal no stress changes was observed due to the retightening but it is likely that the measured strain was affected. However, this effect was significant lesser than the influence of the temperature variation.

One may conclude that for creep testing at room temperature conditions, pin-loaded specimen is preferred and that the ambient temperature needs to be controlled, especially for testing for long periods of time or at low load levels.

TORNIO R&D CENTER

Creep and stress relaxation behavior of stainless steel plates at room temperature
Timo Manninen, Johan Pilhagen

2018-0042
2017-01-02
Technical report
Public

Page 21 of 69

___

4. Results

4.1 Standard tension tests of the austenitic and the ferritic material

The mechanical properties of the test materials were measured according to the testing standard EN ISO 6892-1 A224 in different angles to the rolling direction. The results are summarized in Table 12. The values are average values for three repeats. The measured stress-strain curves are shown in Figures 18 and 19.

The tensile testing standard EN ISO 6892-1 method A224 specifies that a slow loading rate loading rate is used for determining the proof stress values and another, higher loading rate is used for determining the tensile strength. The change loading rate shows as a sharp step in the stress-strain curves. The step is clearly visible in Figures 18 and 19.

Table 12. Mechanical properties of test materials measured in different angles to the rolling direction.

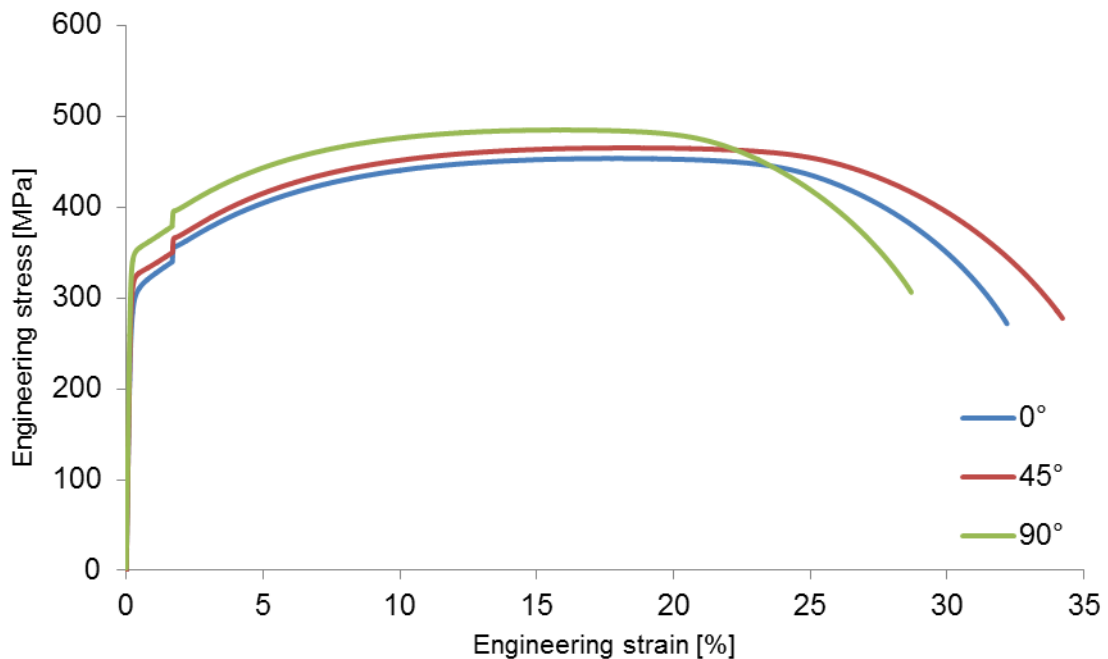| Grade	Testing direction (°)	Rp0,1 (MPa)	Rp0,2 (MPa)	Rp1,0 (MPa)	Rm (MPa)	Ag (%)	A50 (%)	A5 (%)
1.4003	0	291	304	329	456	17.3	31.9	30.5
1.4003	45	318	326	340	465	17.9	34.1	32.5
1.4003	90	345	352	369	486	15.6	28.9	27.7
1.4404	0	263	280	315	583	39.5	54.1	52.7
1.4404	45	263	280	321	573	39.5	54.6	53.1
1.4404	90	277	293	333	596	38.9	52.4	51.1

Figure 18. Stress strain curves measured for grade 1.4003 test material in the rolling direction (RD), transverse direction (TD) and in 45° angle to the rolling direction (45°).
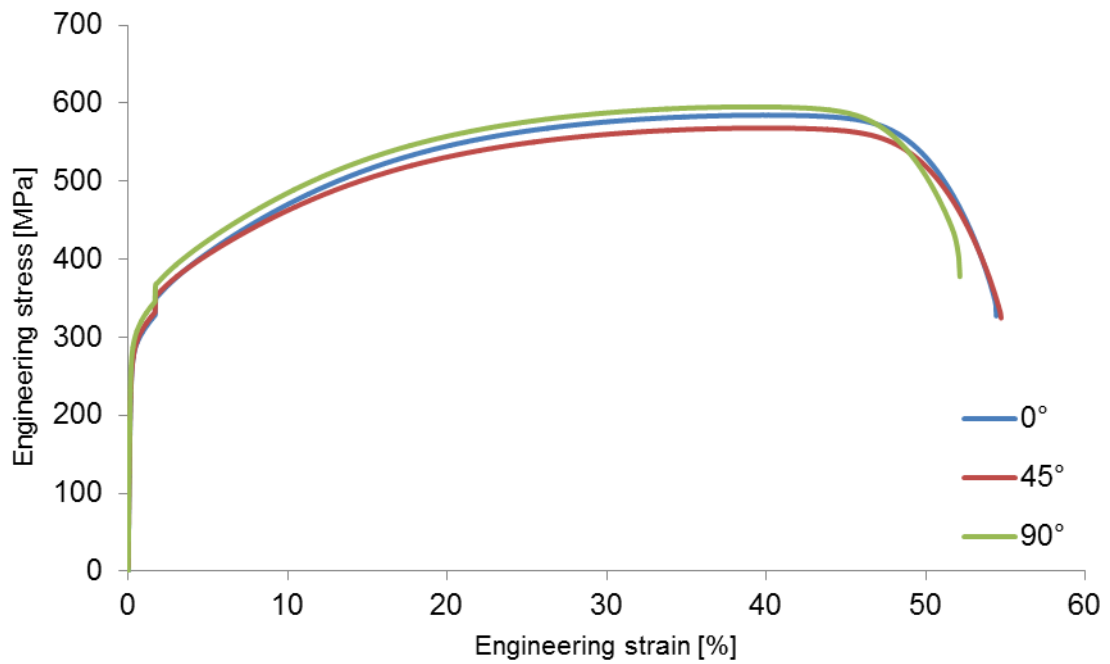
Figure 19. Stress strain curves measured for grade 1.4404 test material in the rolling direction (RD), transverse direction (TD) and in 45° angle to the rolling direction (45°).

_____

4.2 Tension tests of the austenitic and the ferritic material with different loading rates

Non-standard tensile tests with different constant loading rates in the range from 10^{-7} 1/s to 10^{-2} 1/s were carried out to investigate the rate-dependent and rate-independent strength of all plate materials. The results show that the strength of the material increases with increasing loading rate, Figure 20 to Figure 23. It can also be observed that the distance between the curves remains constant. Therefore, the rate-dependent part of the strength is independent of the plastic strain.

The results suggest that the material response follows the theory of viscoplasticity based on overstress. The overstress viscosity function can be accurately described with the power-law type viscosity function

$$\dot{\varepsilon}_p = \left(\frac{\sigma - \sigma_0}{D}\right)^n \tag{10}$$

where D and n are material parameters, and σ_0 is the rate-independent (static) strength of the material. The 0.2 % proof stress values measured with different loading rates were used to determine the values for the unknown parameters by means of the non-linear least squares (NLSQ) method. The optimal values are summarized in Table 13. The coefficient of determination obtained with the viscosity function is equal to or higher than $R^2 = 0.98$ for all studied materials. Figure 24 to Figure 26 show the measured data and the fitted viscosity function for both plate materials. It can be concluded that the power-law viscosity function can describe the measurement data with good accuracy.

Table 13. Parameters of the power-law viscosity function for all studied plate materials. The Rp0.2 value in the rightmost column specifies the 0.2 % proof stress of each material in standard tension tests.

Grade	D (MPa)	n (-)	σ_0 (MPa)	Rp0.2 (MPa)
1.4003	130	11	241	304
1.4404	110	15	218	280
1.4162	329	30	256	509
1.4462	313	24	382	619

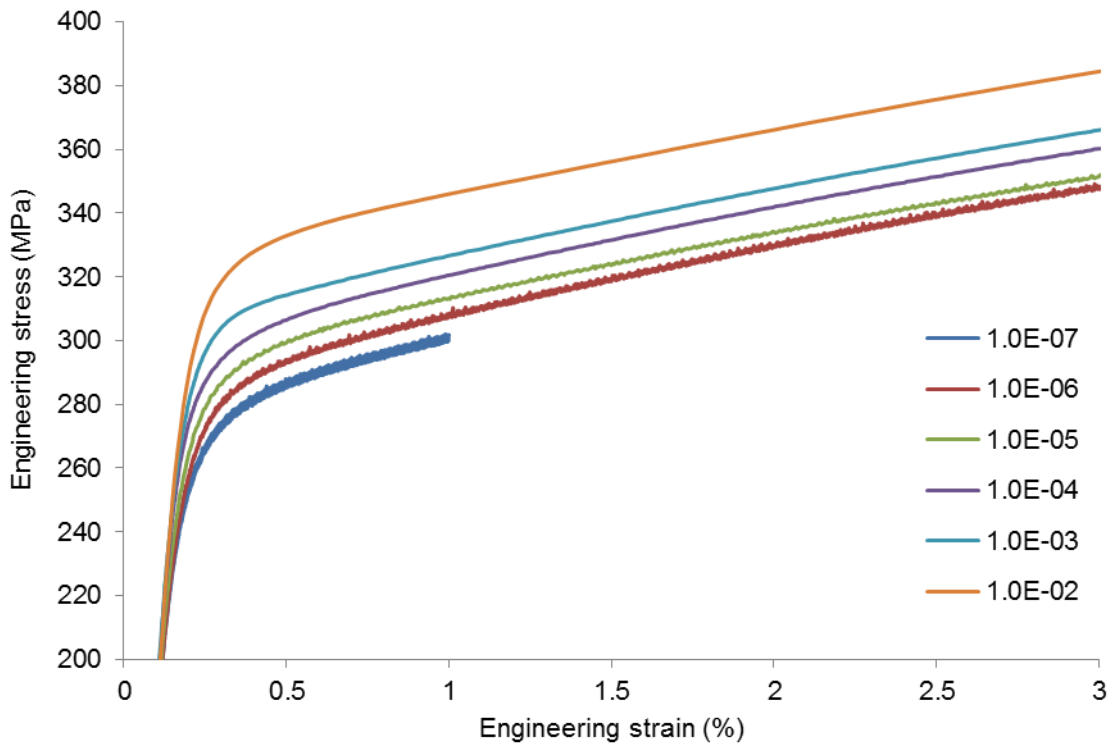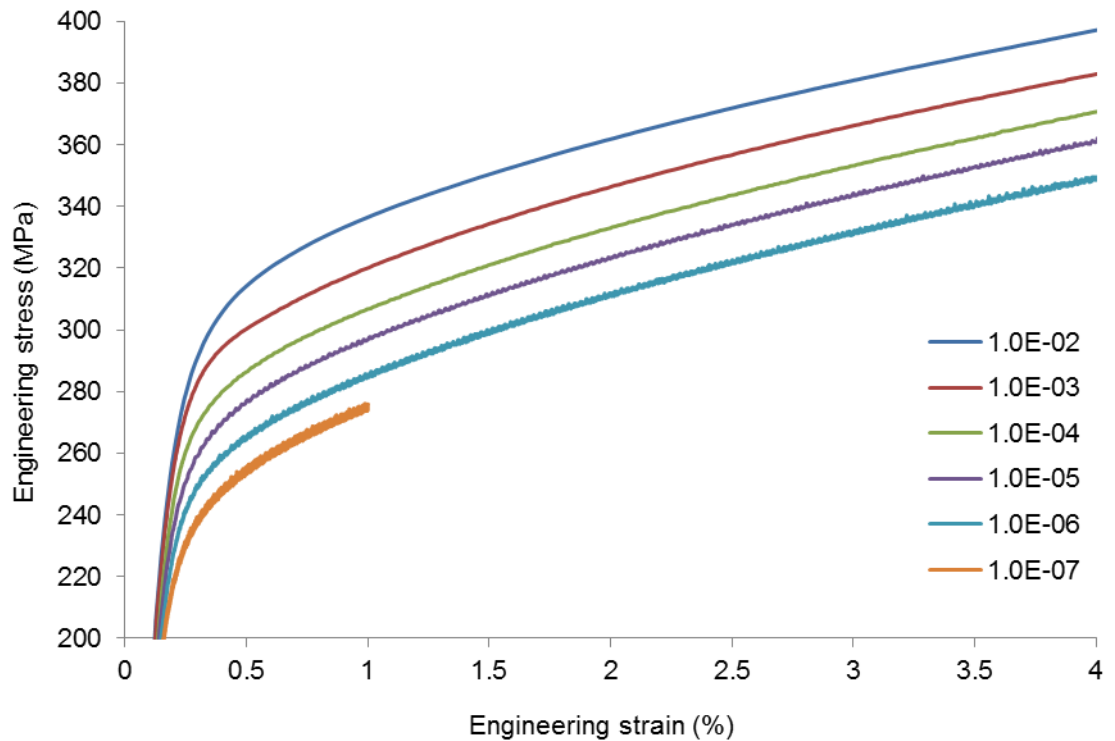| | Creep and stress relaxation behavior of stainless | 2018-0042 | Page 24 of 69 |
outokumpu	steel plates at room temperature	2017-01-02	
	Timo Manninen, Johan Pilhagen	Technical report	
TORNIO R&D CENTER		Public	

_____

Figure 20. Stress-strain curves for grade 1.4003 plate material measured using different loading rates.

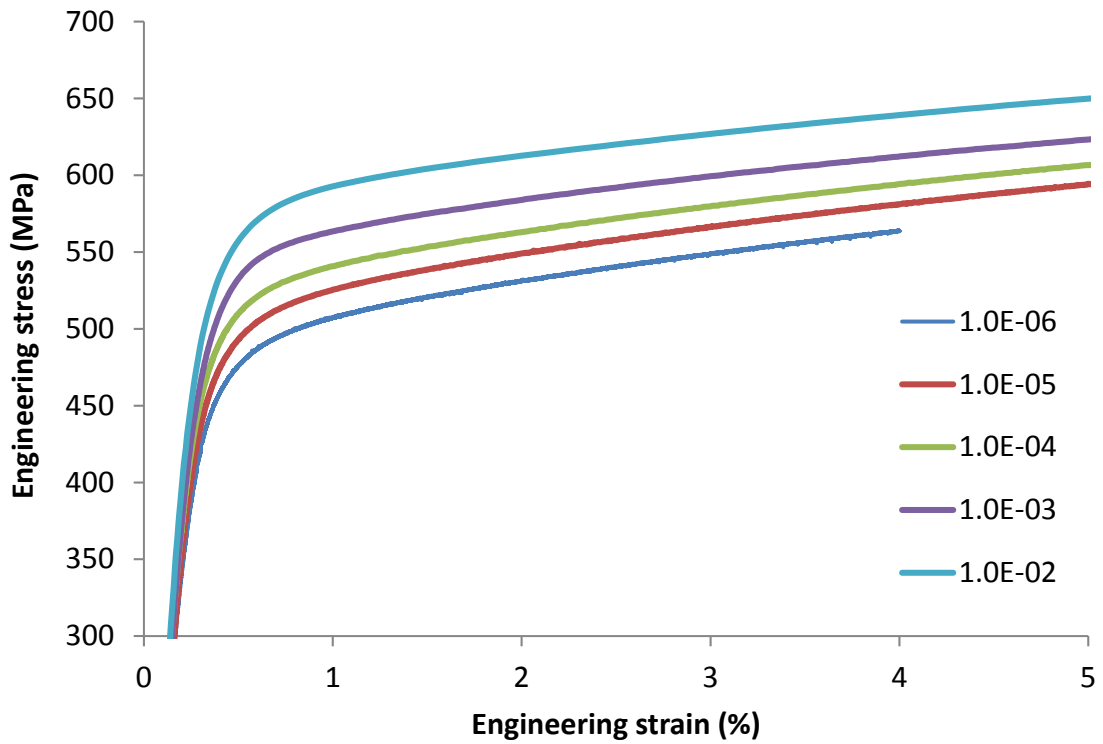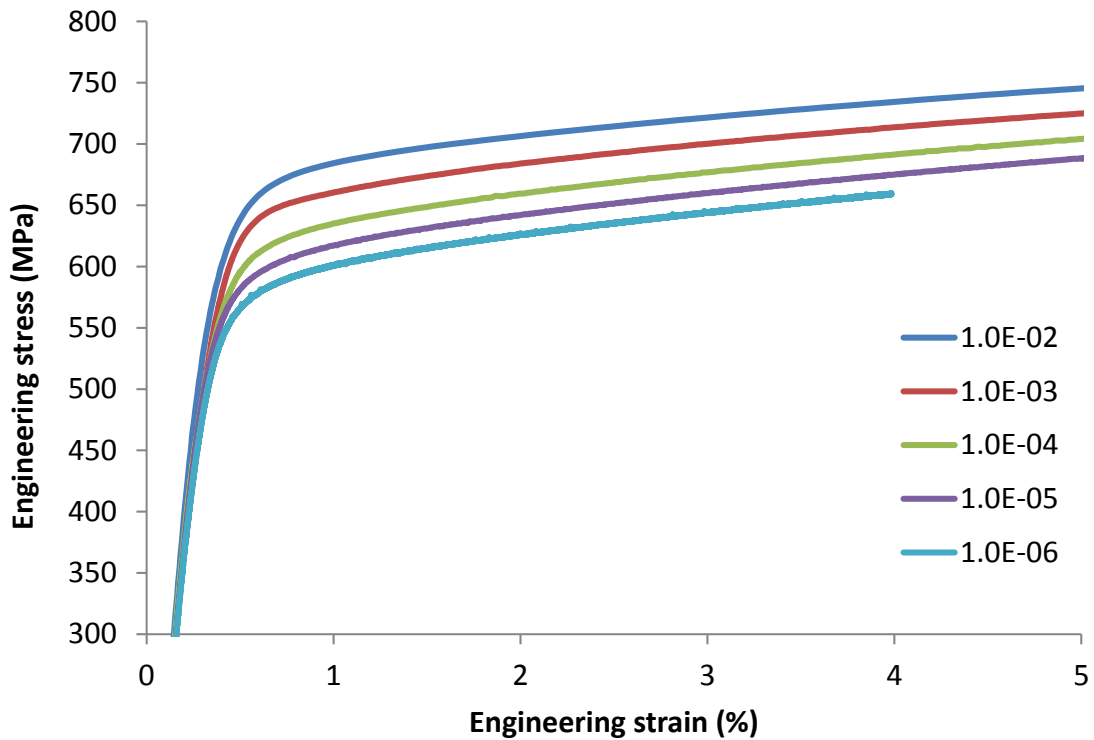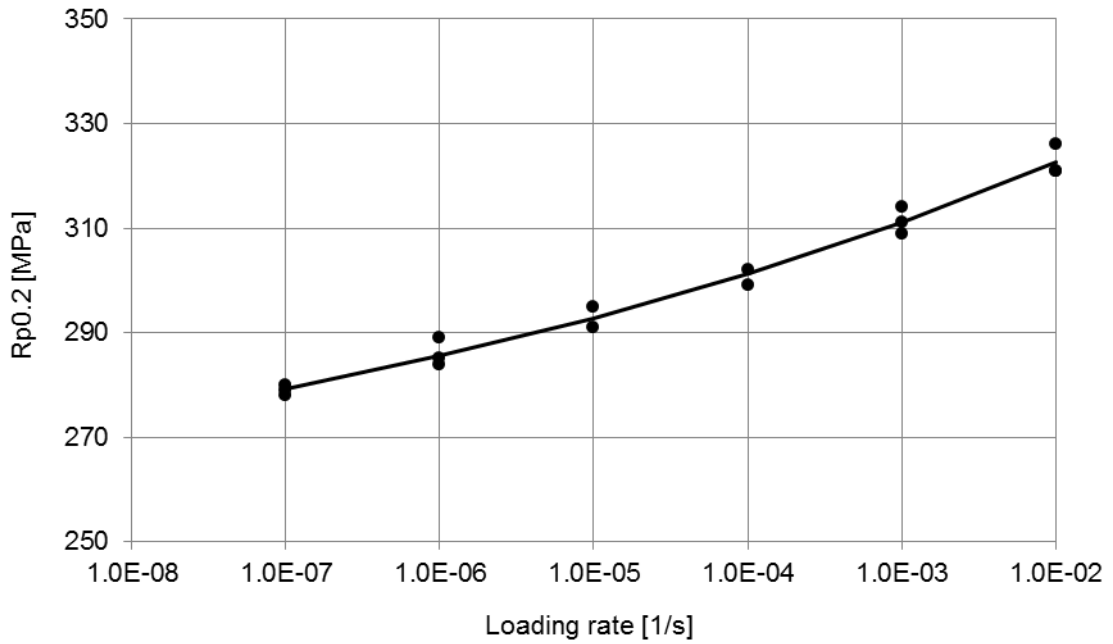*Figure 21. Stress-strain curves for grade 1.4404 plate material measured using different loading rates.*

Figure 22. Stress-strain curves for grade 1.4162 plate material measured using different loading rates.

Figure 23. Stress-strain curves for grade 1.4462 plate material measured using different loading rates.

	Creep and stress relaxation behavior of stainless	2018-0042	Page 26 of 69
outokumpu	steel plates at room temperature	2017-01-02	
	Timo Manninen, Johan Pilhagen	Technical report	
TORNIO R&D CENTER		Public	

_____

Figure 24. The influence of loading rate on the 0.2 % proof stress of grade 1.4003 plate material. Experimental data presented by circles, power-law viscosity function by continuous line.
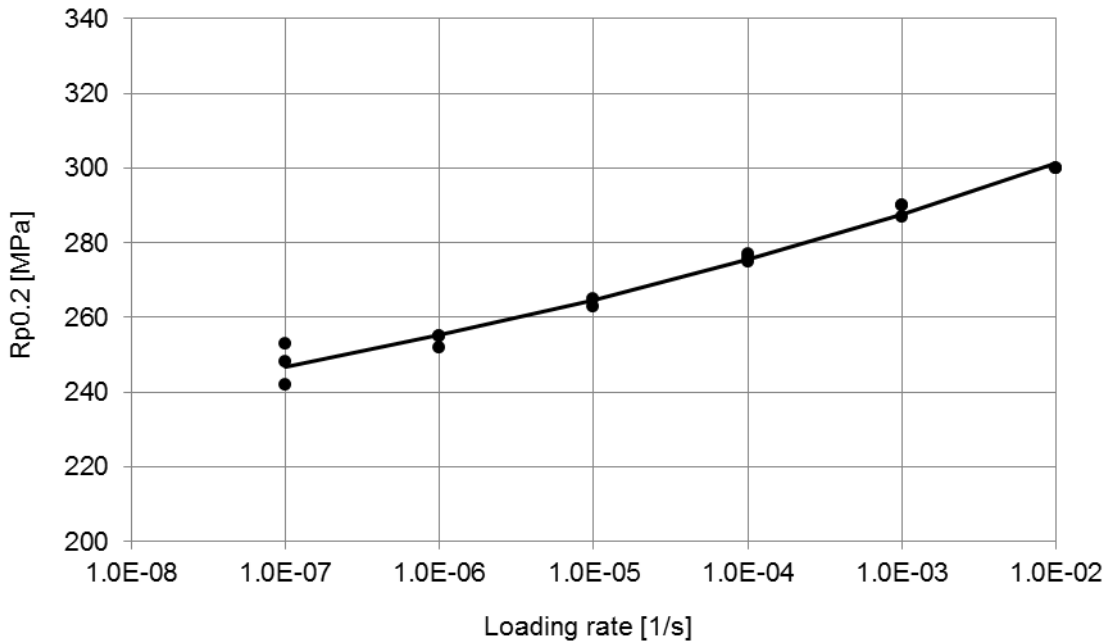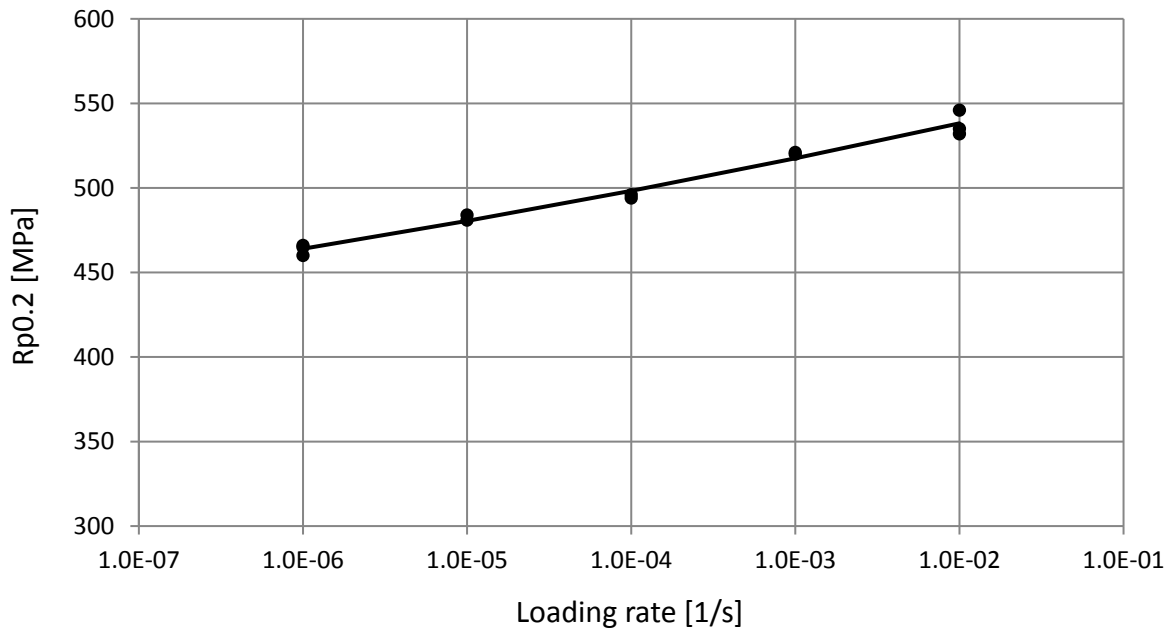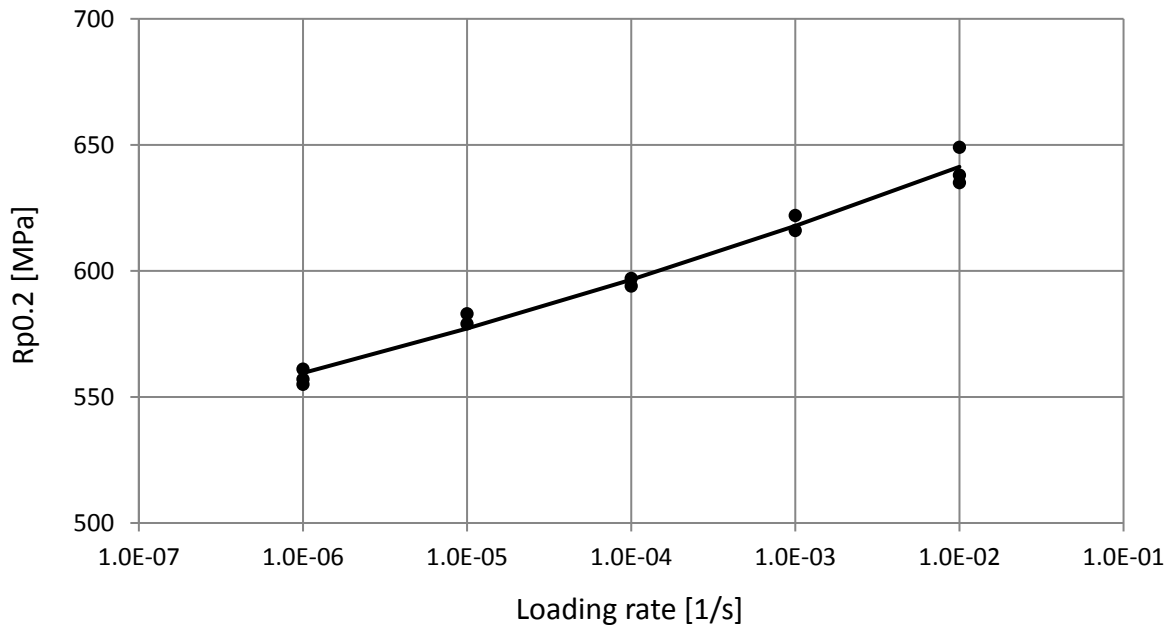

Figure 25. The influence of loading rate on the 0.2 % proof stress of grade 1.4404 plate material. Experimental data presented by circles, power-law viscosity function by continuous line.

outokumpu

TORNIO R&D CENTER

Creep and stress relaxation behavior of stainless
steel plates at room temperature
Timo Manninen, Johan Pilhagen

2018-0042
2017-01-02
Technical report
Public

Page 27 of 69

Figure 25. The influence of loading rate on the 0.2 % proof stress of grade 1.4162 plate material. Experimental data presented by circles, power-law viscosity function by continuous line.

Figure 26. The influence of loading rate on the 0.2 % proof stress of grade 1.4462 plate material. Experimental data presented by circles, power-law viscosity function by continuous line.

_____

4.3 Short term constant load creep tests of the austenitic and the ferritic material

Short term constant load creep tests were conducted on six different load levels. The load levels were defined as percentage of the 0.2 % proof stress in the longitudinal direction. The stress levels used on short term constant load creep tests on grade 1.4003 and 1.4404 plate materials are summarized in Table 14.

Table 14. Load levels used for short term creep tests.

Load case (-)	Stress (% of $R_{p0,2}$)	Stress for 1.4003 (MPa)	Stress for 1.4440 (MPa)
1	30.0	91	84
2	47.5	144	133
3	65.0	198	182
4	82.5	251	231
5	100.0	304	280
6	120.0	365	336

The strain measured as a function of time in short-term constant load creep testing of grade 1.4003 plate material is shown in the Figures 27 - 30. No creep deformation was observed with the two lowest load levels for grade 1.4003 plate material. Furthermore, creep deformation was extremely slow, almost below detection limit, for load level number three, which corresponds to 65 % of the 0.2 % proof stress of the material. In load levels 3 and 4, which correspond to 65 % and 82.5 % of the 0.2 % proof stress of the material, respectively, the creep strain occurring after the initial load stage was of the same order of magnitude with the resolution of the extensometer used. This results in the step-like appearance of creep curves in the Figures 28 and 27. The size of the steps equals to the resolution of the extensometer, which equals to $\Delta\varepsilon = 7.5 \cdot 10^{-6}$ for this test setup.

The strain measured in short-term constant load creep testing of grade 1.4404 plate material is shown in the Figures 31 to 34. It can be concluded that the creep behavior of grade 1.4404 plate material in short term creep tests was qualitatively similar to that of grade 1.4003. No creep deformation was observed with the lowest two load levels. Furthermore, creep deformation was extremely slow with the load level number three, which corresponds to 65 % of the 0.2 % proof stress of the material. In load cases 3 and 4, which correspond to 65 % and 82.5 % of the 0.2 % proof stress of the material, the creep strain occurring after the initial load stage was of the same order of magnitude with the resolution of the extensometer used. This causes the step-like appearance of creep curves in the Figures 32 and 31.
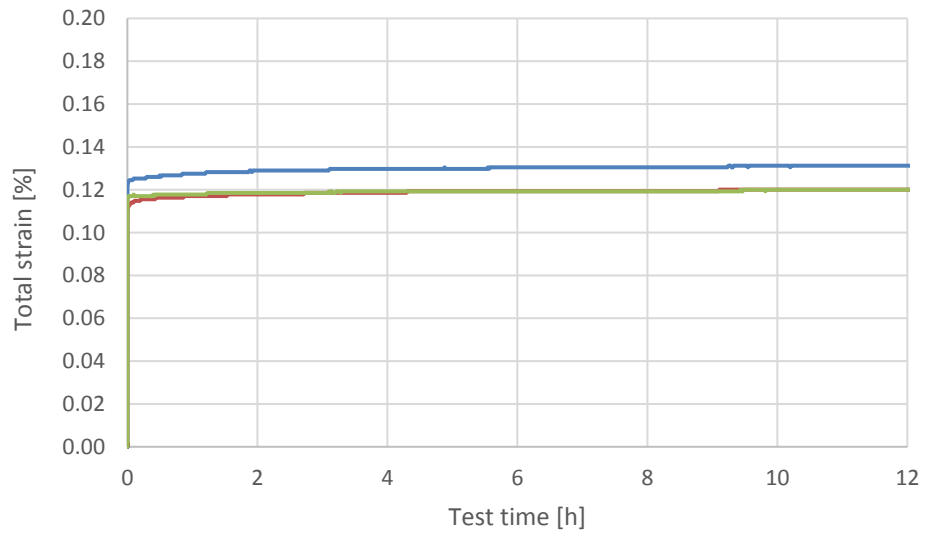
_____

Figure 27. Strain in short-term creep testing of grade 1.4003 material with the load level of 0.65xRp0.2.
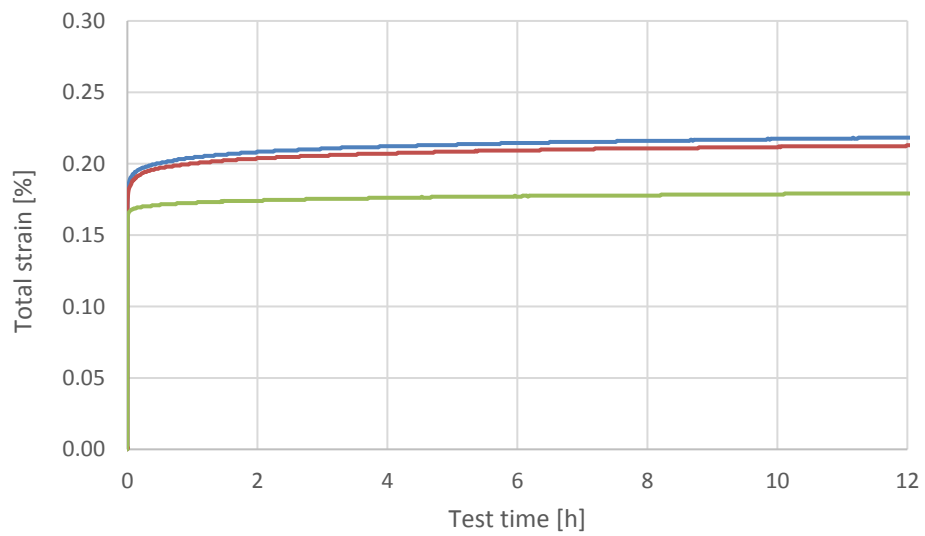

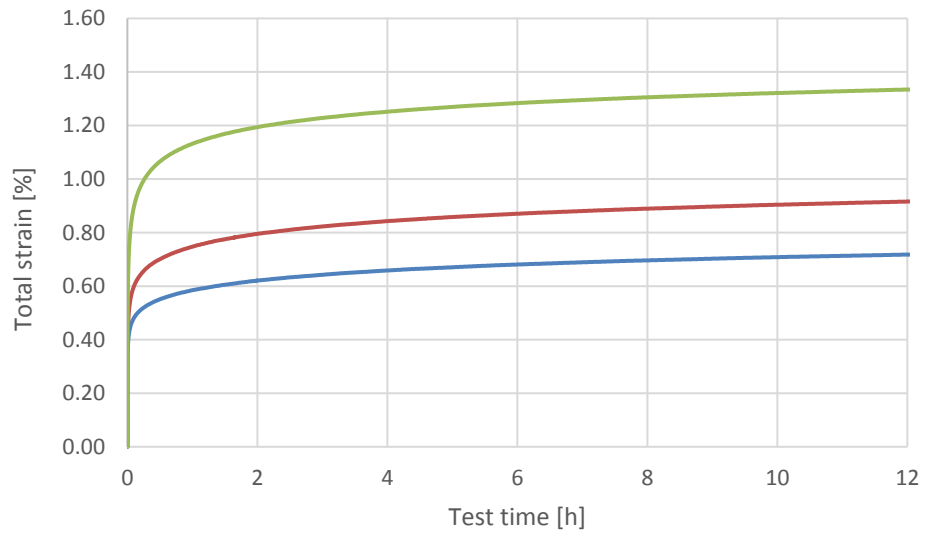*Figure 28. Strain in short-term creep testing of grade 1.4003 material with the load level of 0.825xRp0.2.*

Creep and stress relaxation behavior of stainless
steel plates at room temperature
Timo Manninen, Johan Pilhagen

TORNIO R&D CENTER

2018-0042
2017-01-02
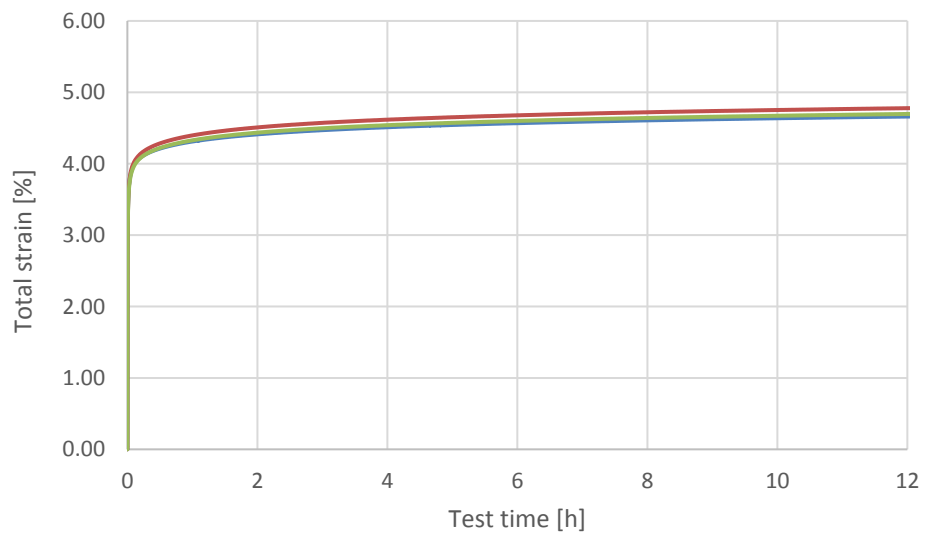Technical report
Public

Page 30 of 69

_____

Figure 29. Strain in short-term creep testing of grade 1.4003 material with the load level of 1.0xRp0.2.

Figure 30. Strain in short-term creep testing of grade 1.4003 material with the load level of 1.2xRp0.2.

TORNIO R&D CENTER

Creep and stress relaxation behavior of stainless
steel plates at room temperature
Timo Manninen, Johan Pilhagen

2018-0042
2017-01-02
Technical report
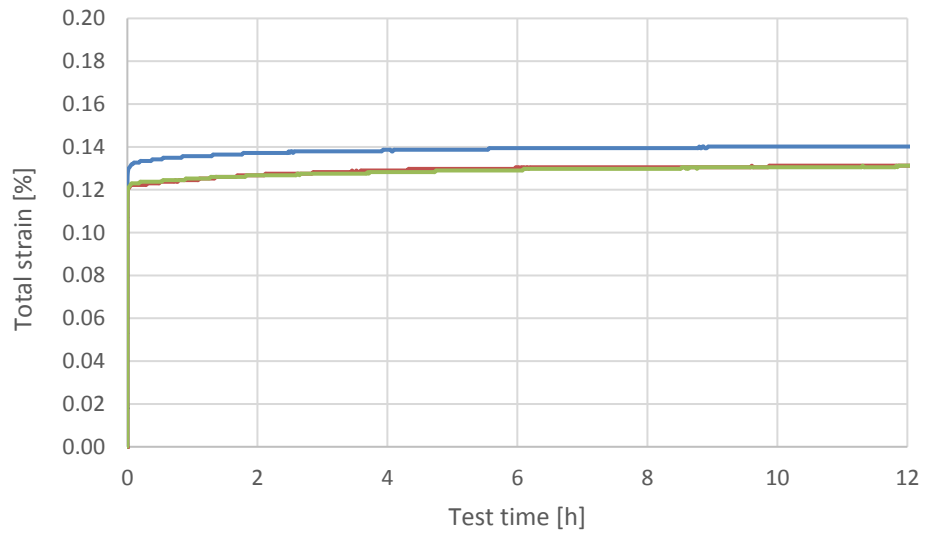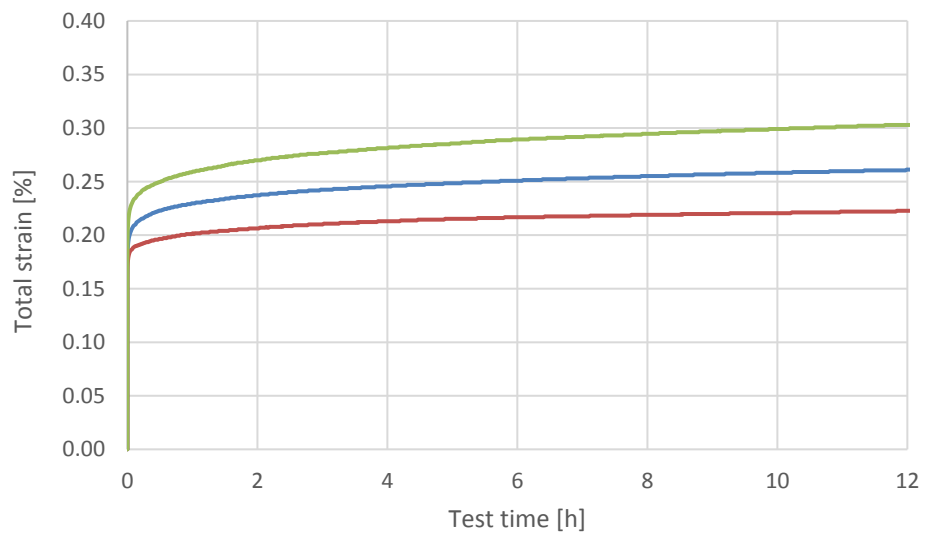Public

Page 31 of 69

_____

Figure 31. Strain in short-term creep testing of grade 1.4404 material with the load level of 0.65xRp0.2.

Figure 32. Strain in short-term creep testing of grade 1.4404 material with the load level of 0.825xRp0.2.
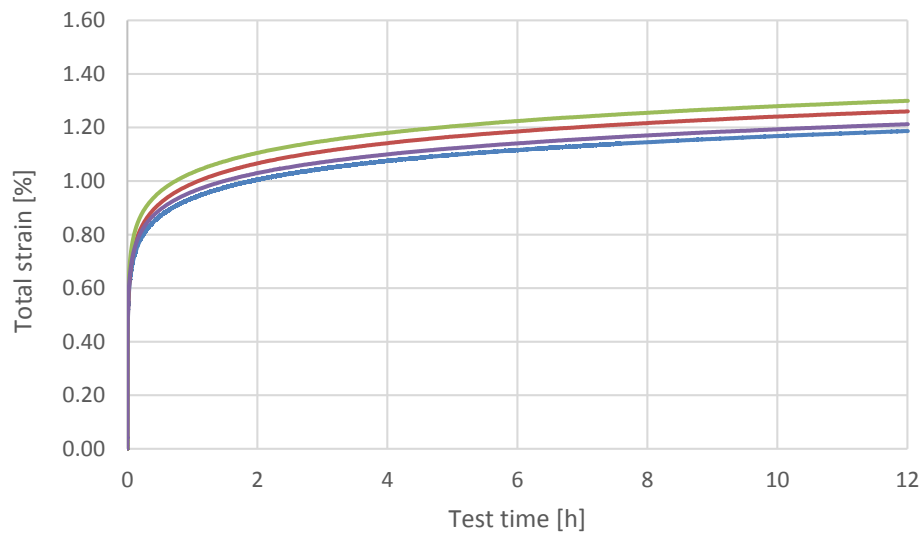
TORNIO R&D CENTER

Creep and stress relaxation behavior of stainless
steel plates at room temperature
Timo Manninen, Johan Pilhagen

2018-0042
2017-01-02
Technical report
Public

Page 32 of 69

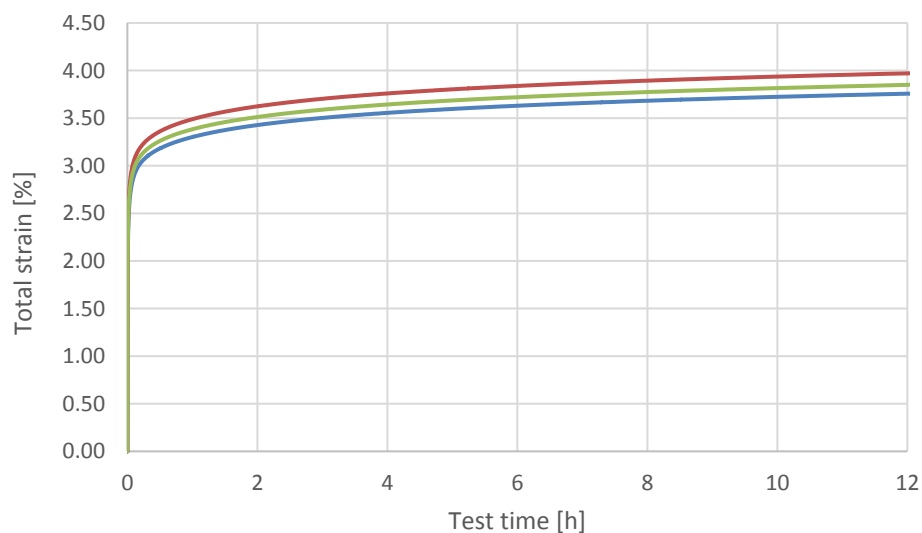*Figure 33. Strain in short-term creep testing of grade 1.4404 material with the load level of 1.0xRp0.2.*

Figure 34. Strain in short-term creep testing of grade 1.4404 material with the load level of 1.2xRp0.2.

The creep strain rates were calculated by Juhani Rantala of VTT by means of the seven-point incremental polynomial method described in ASTM E399. The calculated creep strain rates are given in the Figures 35 - 42. The results are summarized in Figures 43 and 44. It can be observed that the creep rate curves form a sequence of straight lines in the double logarithmic scale and that the slope of the lines is approximately equal to $k = -1$. Therefore, the short-term creep behavior of grade 1.4003 and grade 1.4404 plate materials follows the logarithmic creep law. It can also be observed that creep deformation decreases with decreasing external loading. No secondary creep was observed in these tests. In the end of the creep test, the rate of creep deformation becomes extremely slow. This shows as noise in the lowermost curves. Since the test piece geometry was optimized for high resolution in strain measurement, the measurements could capture the creep deformation down to the level of 10^{-10} 1/s.
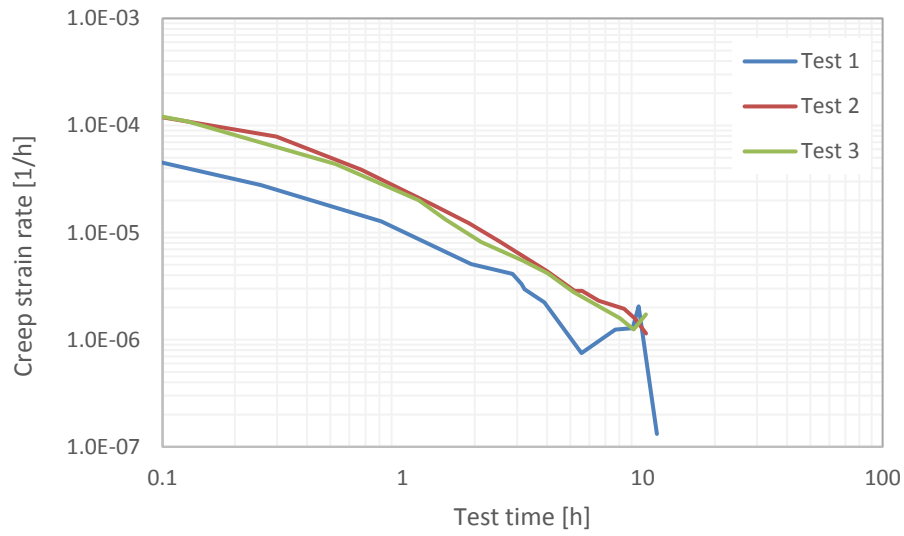
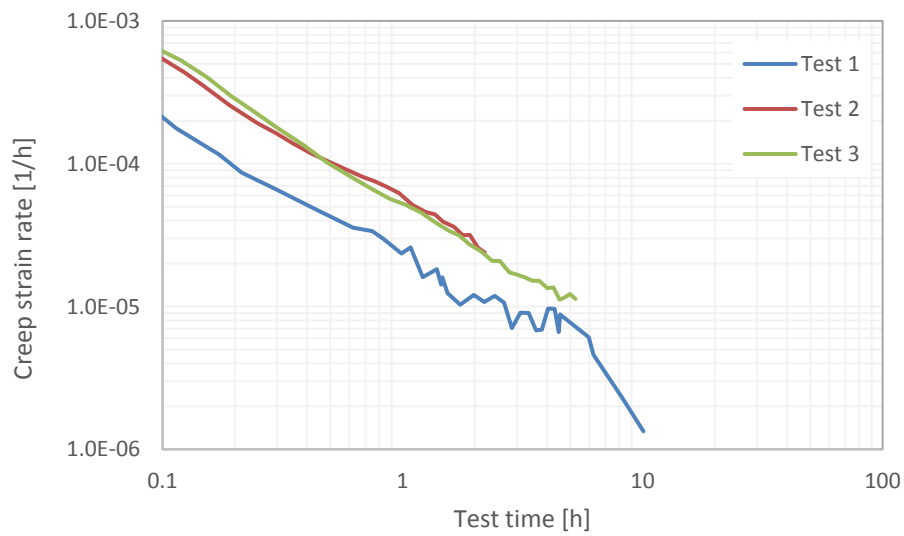| | Creep and stress relaxation behavior of stainless steel plates at room temperature | 2018-0042 | Page 33 of 69 |
outokumpu	steel plates at room temperature	2017-01-02	
	Timo Manninen, Johan Pilhagen	Technical report	
TORNIO R&D CENTER		Public	

_____

Figure 35. Creep rate curves for grade 1.4003 material with the load level of 0.65xRp0.2.

Figure 36. Creep rate curves for grade 1.4003 material with the load level of 0.825xRp0.2.

Creep and stress relaxation behavior of stainless
steel plates at room temperature
Timo Manninen, Johan Pilhagen

TORNIO R&D CENTER

2018-0042
2017-01-02
Technical report
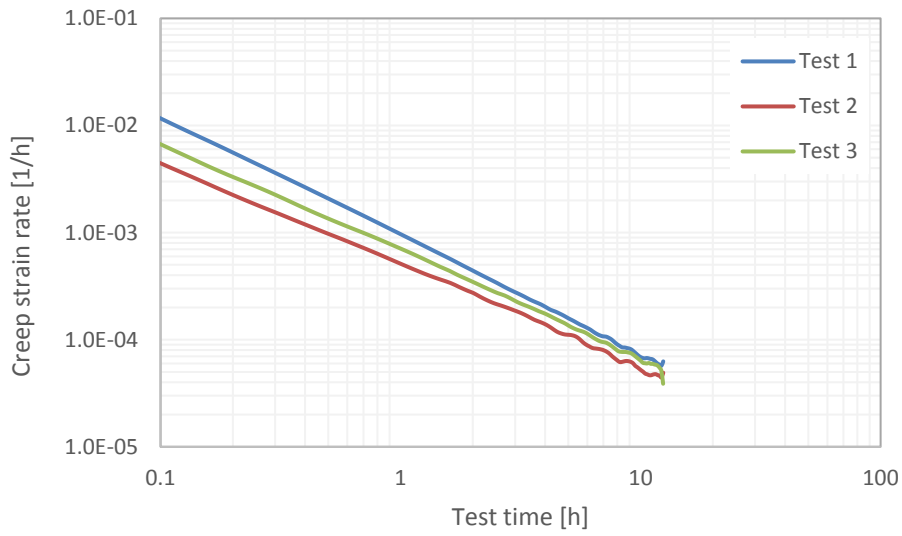Public

Page 34 of 69

_____

Figure 37. Creep rate curves for grade 1.4003 material with the load level of 1.0xRp0.2.

Figure 38. Creep rate curves for grade 1.4003 material with the load level of 1.2xRp0.2.
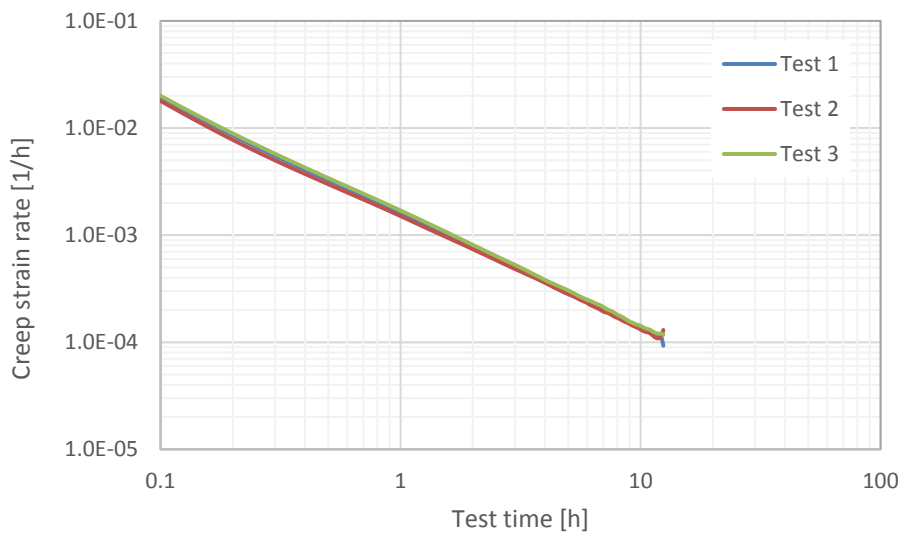
_____

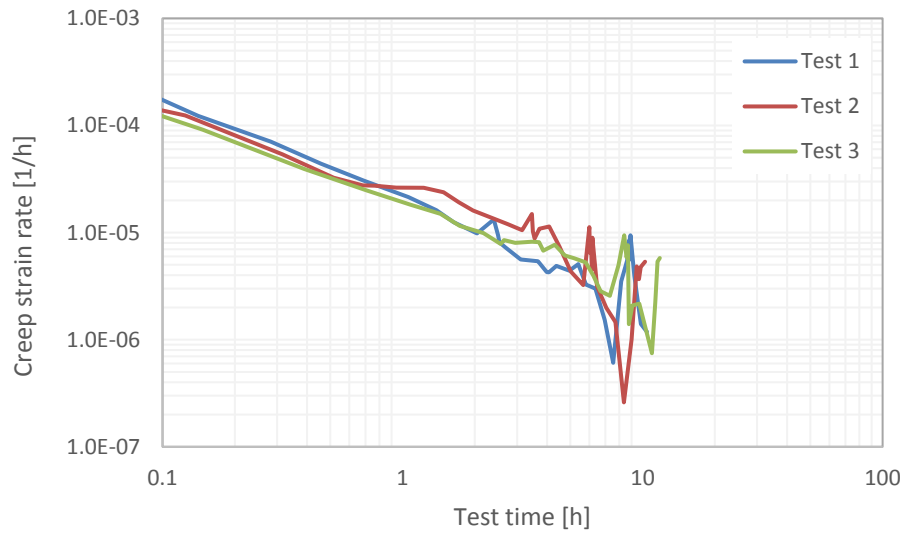*Figure 39.Creep rate curves for grade 1.4404 material with the load level of 0.65xRp0.2.*

Figure 40. Creep rate curves for grade 1.4404 material with the load level of 0.825xRp0.2.

	Creep and stress relaxation behavior of stainless steel plates at room temperature	2018-0042	Page 36 of 69
	Timo Manninen, Johan Pilhagen	2017-01-02	
outokumpu		Technical report	
TORNIO R&D CENTER		Public	

_____

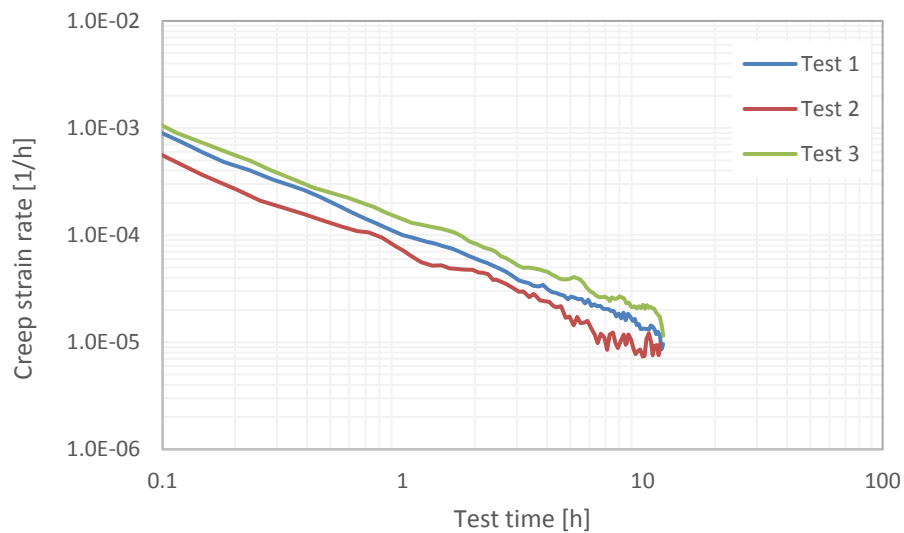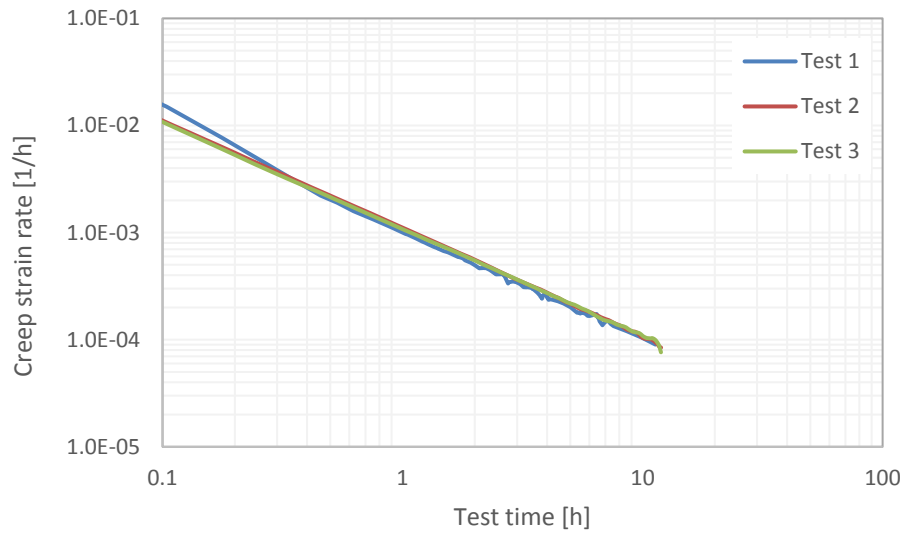*Figure 41. Creep rate curves for grade 1.4404 material with the load level of 1.0xRp0.2.*
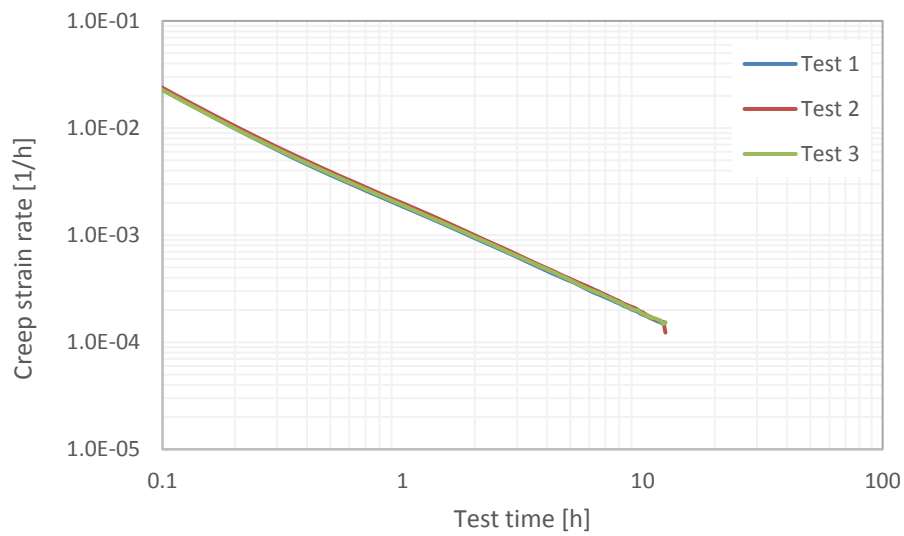

Figure 42. Creep rate curves for grade 1.4404 material with the load level of 1.2xRp0.2.
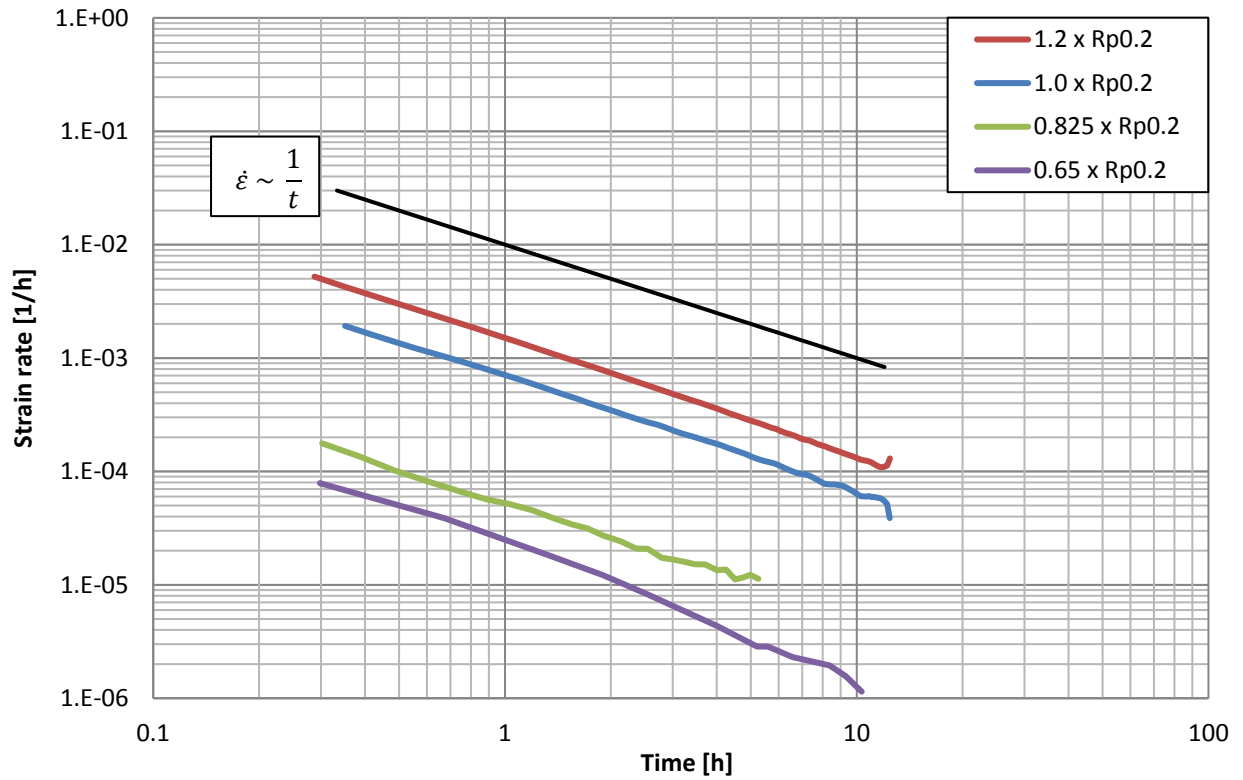
Figure 43. The rate of creep deformation for 1.4003 in short term 12-hour constant load creep test. The curve $\dot{\varepsilon} \sim (1/t)$, which corresponds to logarithmic creep behavior is shown for reference.

outokumpu

TORNIO R&D CENTER

Creep and stress relaxation behavior of stainless
steel plates at room temperature
Timo Manninen, Johan Pilhagen

2018-0042
2017-01-02
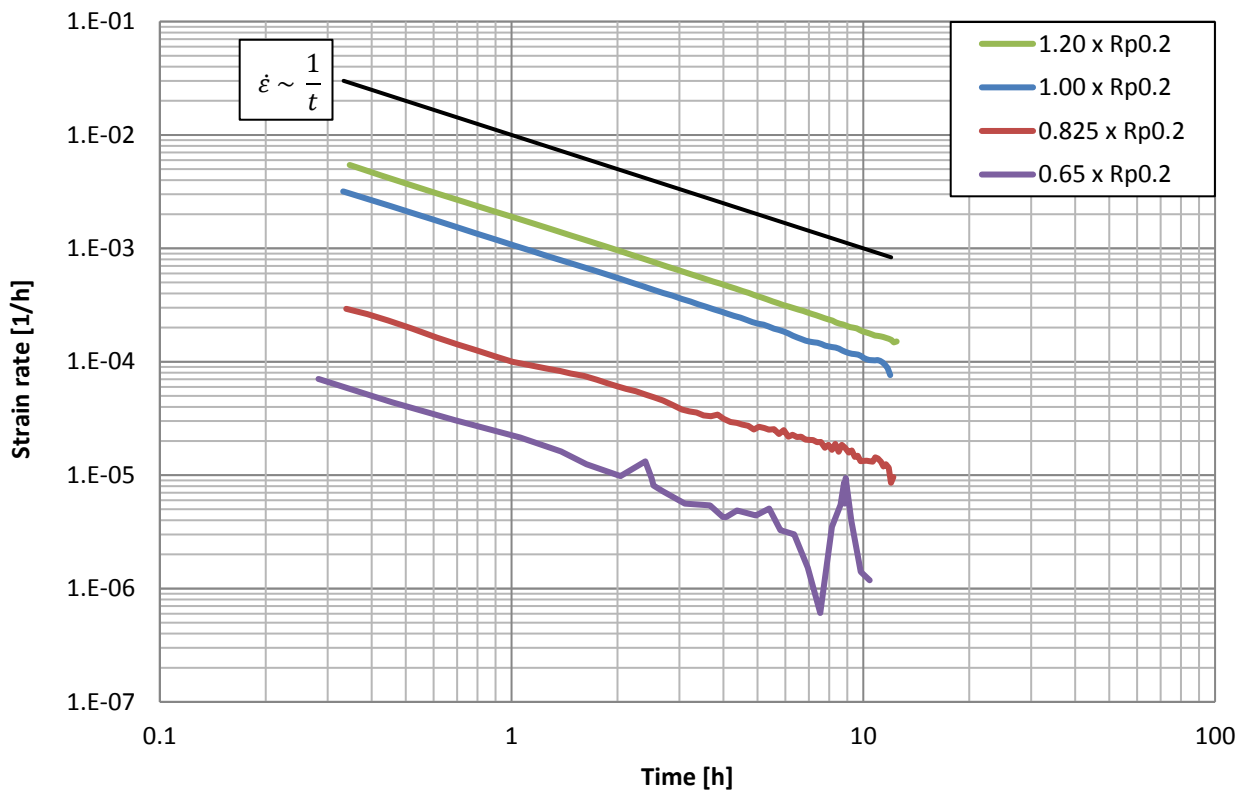Technical report
Public

Page 38 of 69

_____

Figure 44. The rate of creep deformation for 1.4404 in short term 12-hour constant-load creep test. The curve $\dot{\varepsilon} \sim (1/t)$, which corresponds to logarithmic creep behavior, is shown for reference.

4.4 Long term constant load creep tests with dead weight loading

The long-term creep tests were carried our using a dead-weight lever-arm testing rig for the austenitic and ferritic material. Tests were conducted with the three loading levels summarized in Table 15.

Table 15. Load levels used for long-term creep tests.

Load case	Stress	Stress for 1.4003	Stress for 1.4440
(-)	(% of $R_{p0,2}$)	(MPa)	(MPa)
L1	65.0	198	182
L2	82.5	251	231
L3	100.0	304	280

The total strain measured in long term constant load creep testing of grade 1.4003 and 1.4404 plate materials is shown in Figures 45 - 52. The creep strain rate curve, calculated using the method described in chapter 3.3, are shown in Figures 53 - 58. Comparison of creep strain rate curves obtained with different load levels are summarized in Figures 59 and 60. The characteristics of the long-term creep tests reveal no new features in the creep deformation of these material. No signs of secondary creep were observed. The creep rate curves formed a sequence of straight lines in the double logarithmic scale. The slope of the lines is approximately equal to k = -1. Therefore, the material behavior observed can be described with the same power-law or logarithmic creep models as that observed in the in the short-term creep testing of same materials.

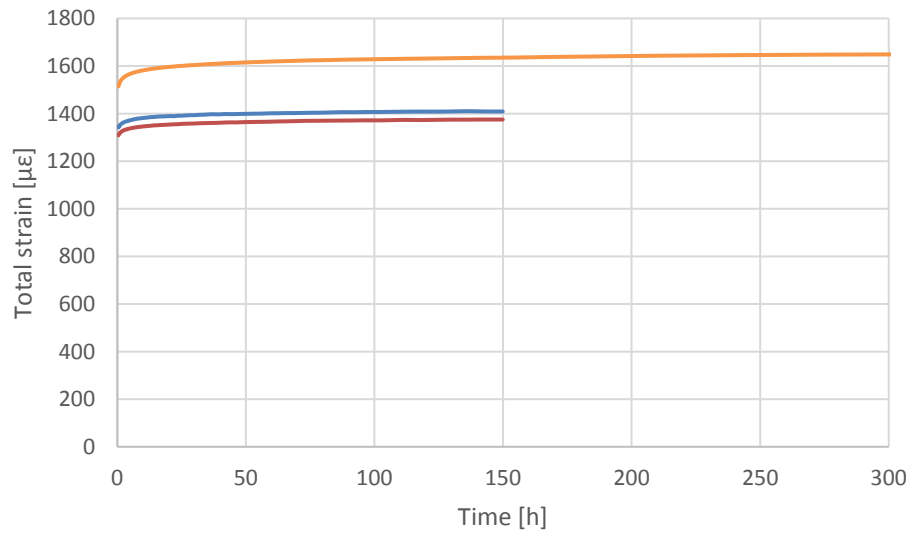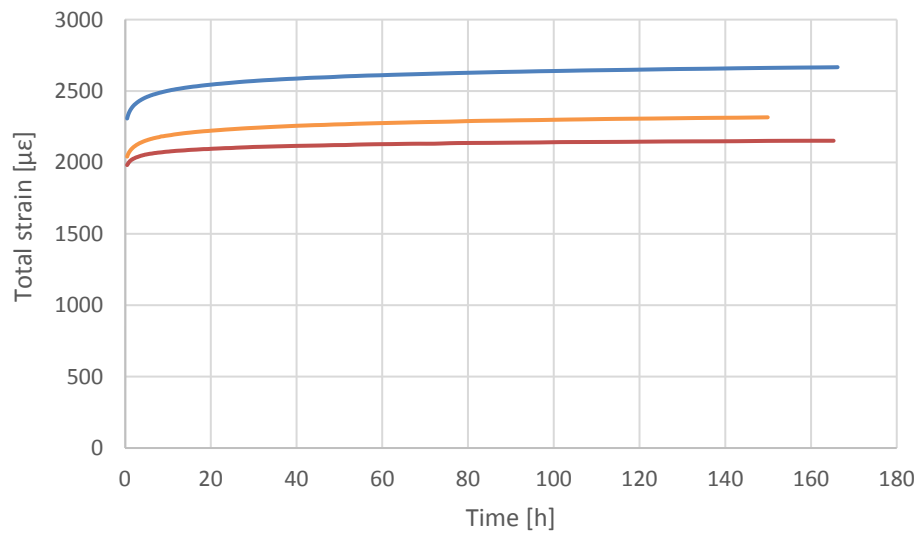| | Creep and stress relaxation behavior of stainless steel plates at room temperature
Timo Manninen, Johan Pilhagen | 2018-0042
2017-01-02
Technical report
Public | Page 39 of 69 |

TORNIO R&D CENTER

_____

Figure 45. Creep strain in long-term creep testing of grade 1.4003 plate material with the load level of 0.65xRp0.2.

Figure 46. Creep strain in long-term creep testing of grade 1.4003 plate material with the load level of 0.825xRp0.2.

	Creep and stress relaxation behavior of stainless steel plates at room temperature Timo Manninen, Johan Pilhagen	2018-0042 2017-01-02 Technical report Public	Page 40 of 69

TORNIO R&D CENTER

_____

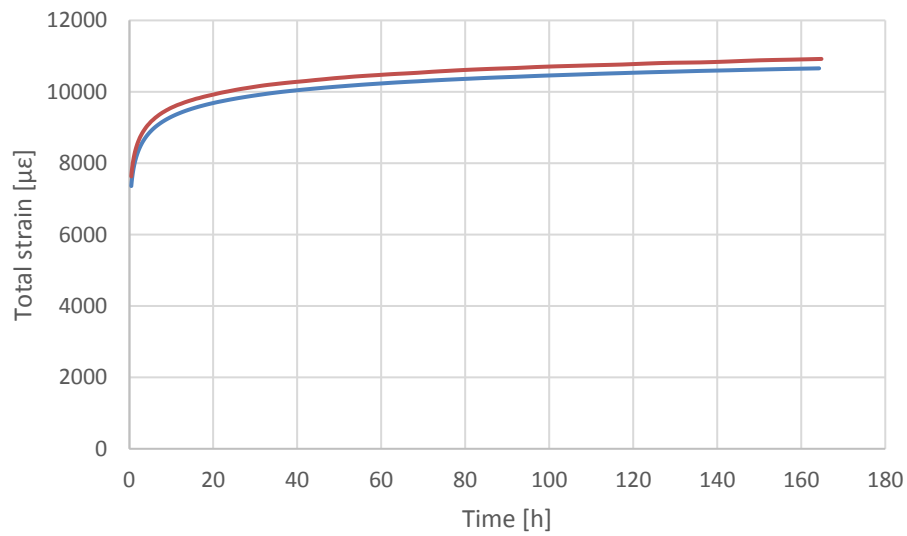*Figure 47. Creep strain in long-term creep testing of grade 1.4003 plate material with the load level of 1.0xRp0.2.*
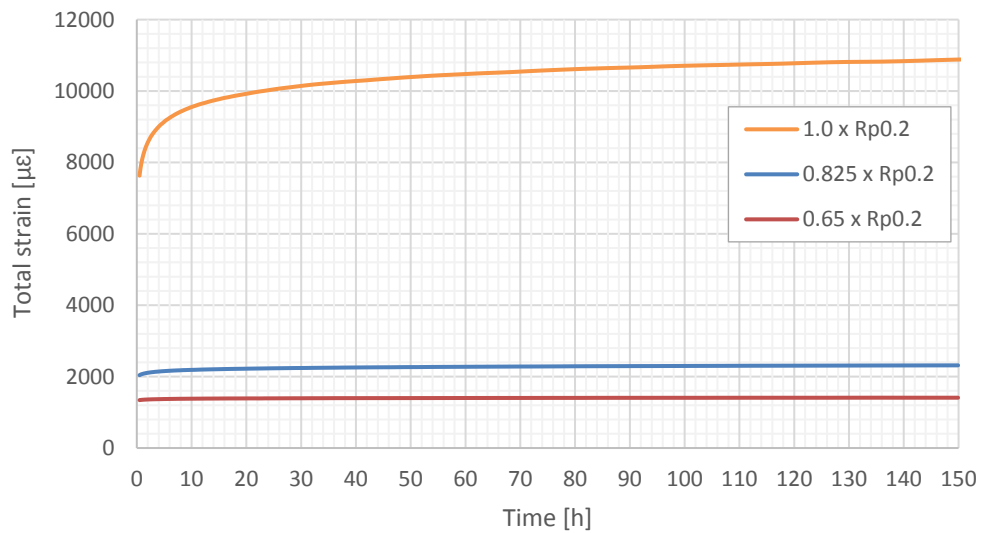

Figure 48. Comparison of creep strain in long-term creep testing of grade 1.4003 plate materials with different load levels.

_____

Figure 49. Creep strain in long-term creep testing of grade 1.4404 plate material with the creep load of 0.65xRp0.2.
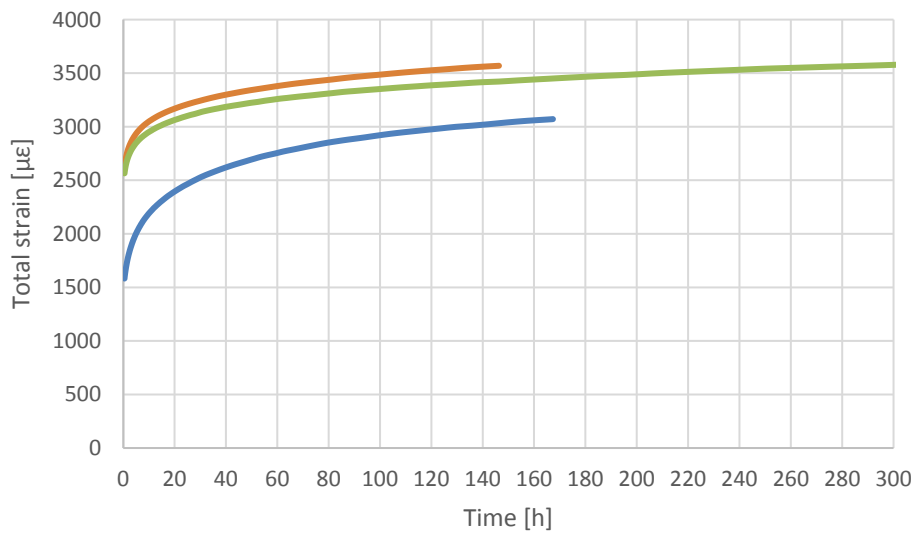
Figure 50. Creep strain in long-term creep testing of grade 1.4404 plate material with the creep load of 0.825xRp0.2.

_____
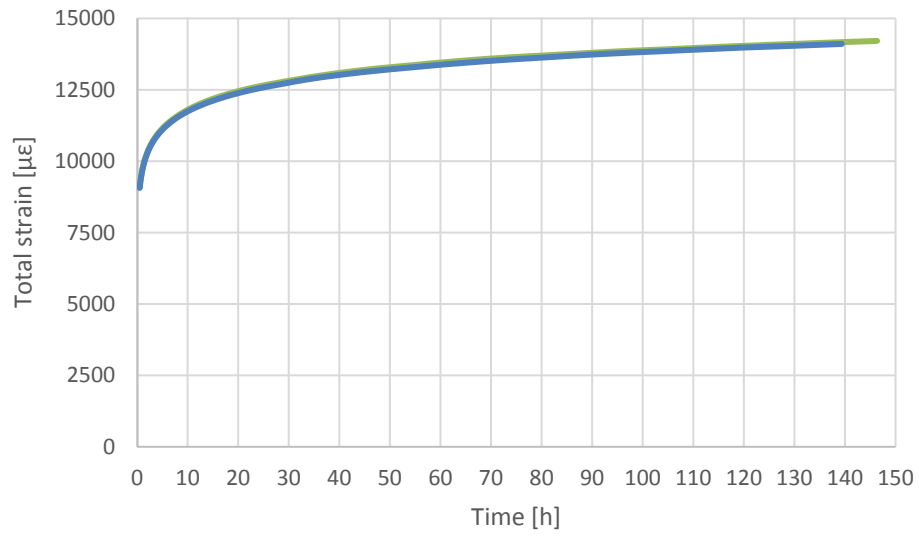
Figure 51. Creep strain in long-term creep testing of grade 1.4404 plate material with creep load of 1.0xRp0.2.
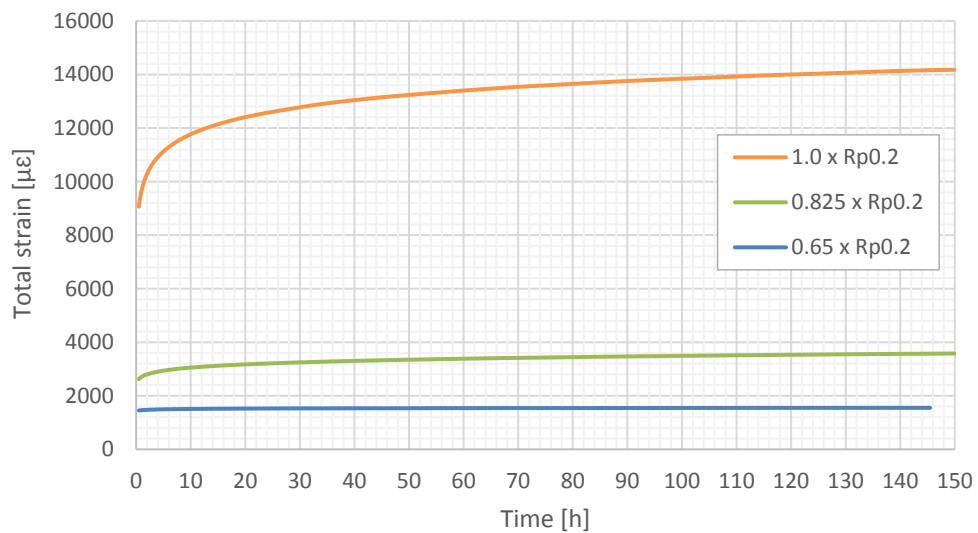
Figure 52. Comparison of creep strain in long-term creep testing of grade 1.4404 plate materials with different load levels.

_____
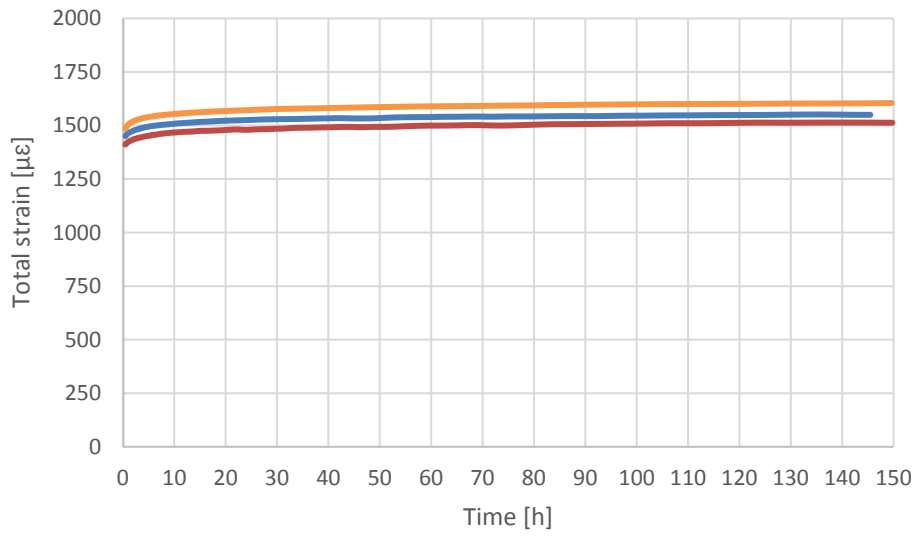

Figure 53. Creep strain rate for grade 1.4003 material in long-term test with the load level of 0.65xRp0.2.

Figure 54. Creep strain rate for grade 1.4003 material in long-term test with the load level of 0.825xRp0.2.

TORNIO R&D CENTER

Creep and stress relaxation behavior of stainless
steel plates at room temperature
Timo Manninen, Johan Pilhagen

2018-0042
2017-01-02
Technical report
Public

Page 44 of 69

_____

Figure 55. Creep strain rate for grade 1.4003 material in long-term test with the load level of 1.0xRp0.2.

Figure 56. Creep strain rate for grade 1.4404 material in long-term test with the load level of 0.65xRp0.2.

	Creep and stress relaxation behavior of stainless steel plates at room temperature	2018-0042	Page 45 of 69
outokumpu	steel plates at room temperature	2017-01-02	
	Timo Manninen, Johan Pilhagen	Technical report	
TORNIO R&D CENTER		Public	

_____

Figure 57. Creep strain rate for grade 1.4404 material in long-term test with the load level of 0.825xRp0.2.
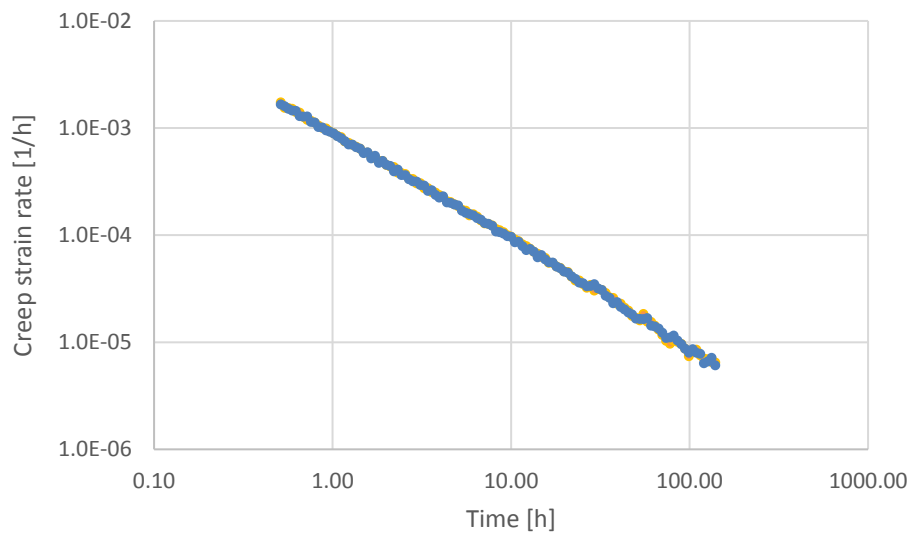
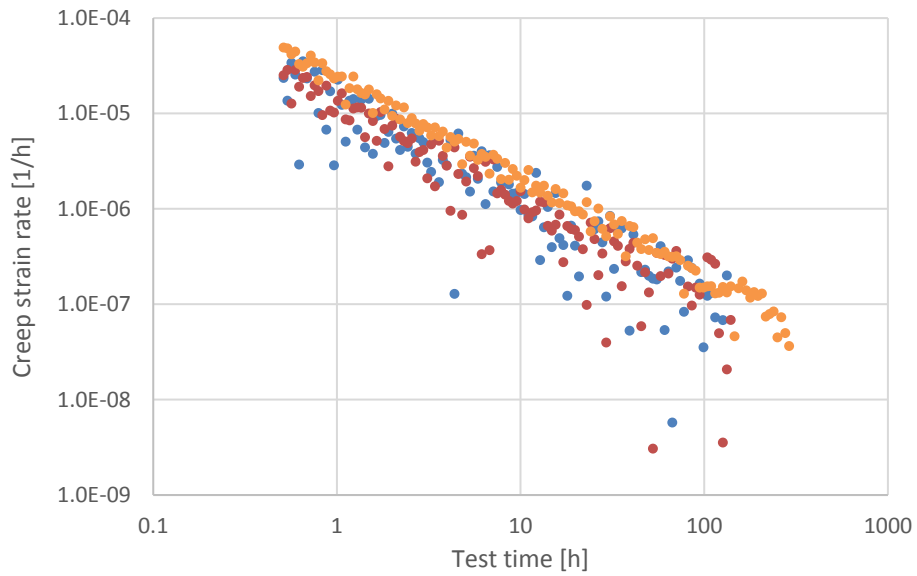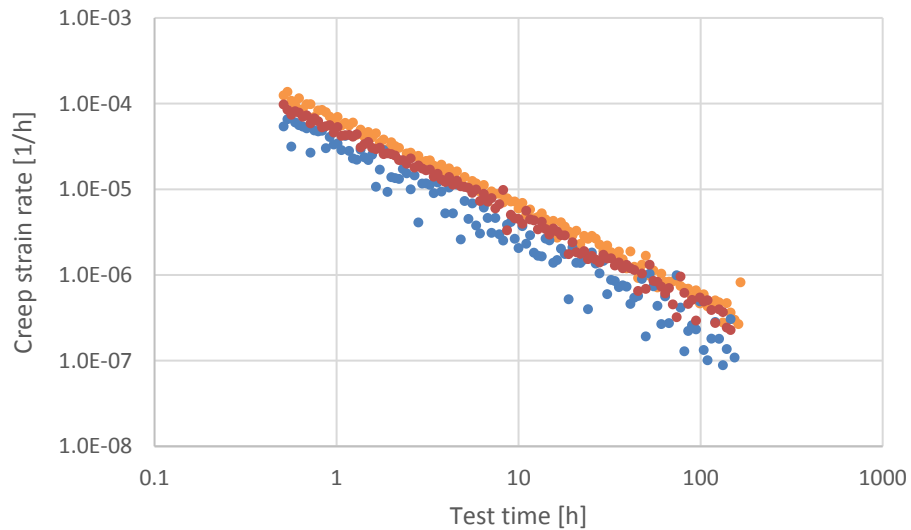*Figure 58. Creep strain rate for grade 1.4404 material in long-term test with the load level of 1.0xRp0.2.*
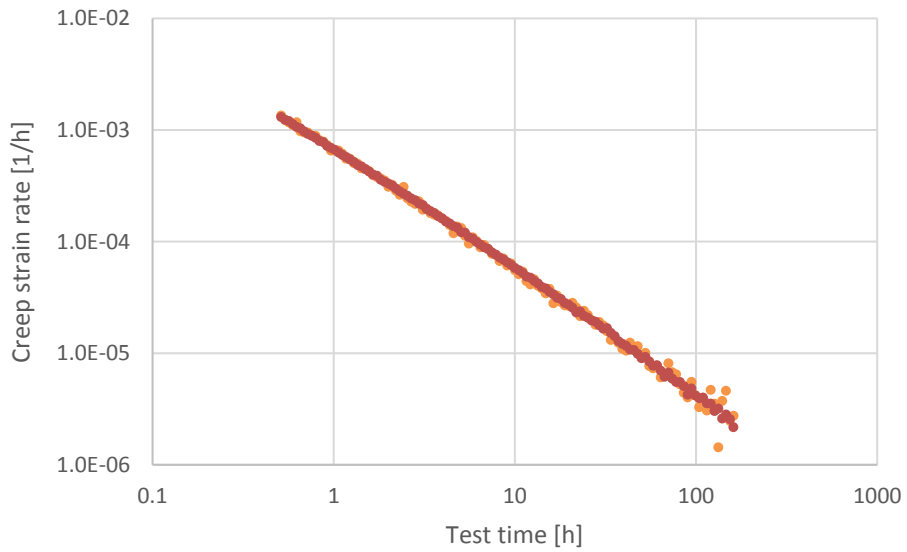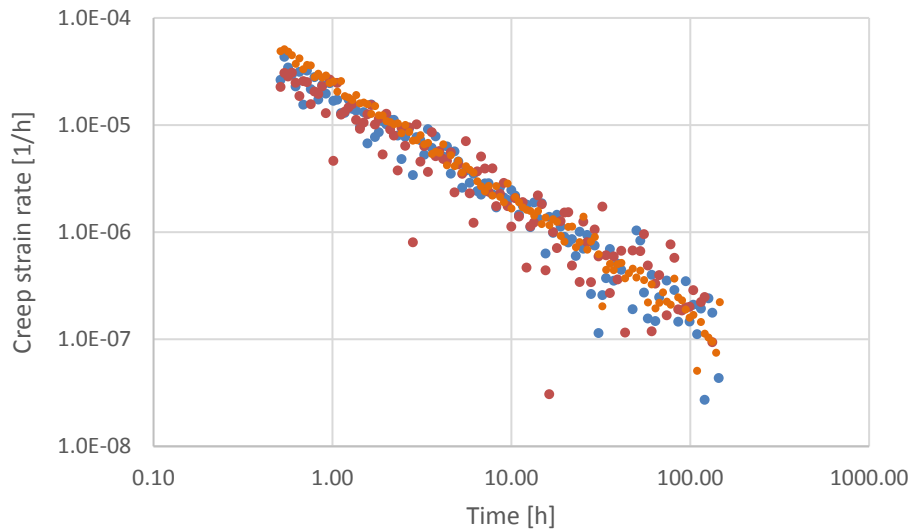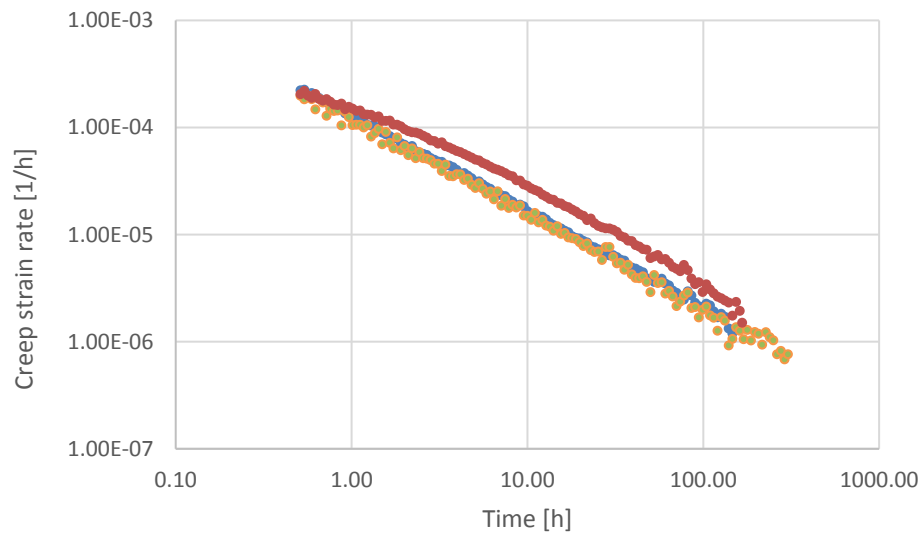
_____
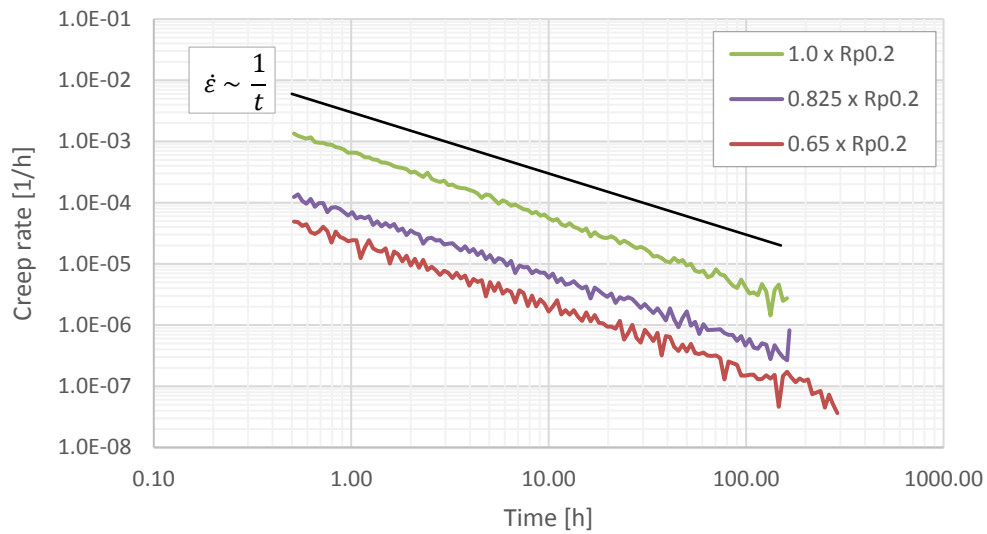
Figure 59. The rate of creep deformation for grade 1.4003 plate material in long term constant load creep test. The curve $\dot{\varepsilon} \sim \left(\frac{1}{t}\right)$, which corresponds to logarithmic creep behaviour, is shown for reference.
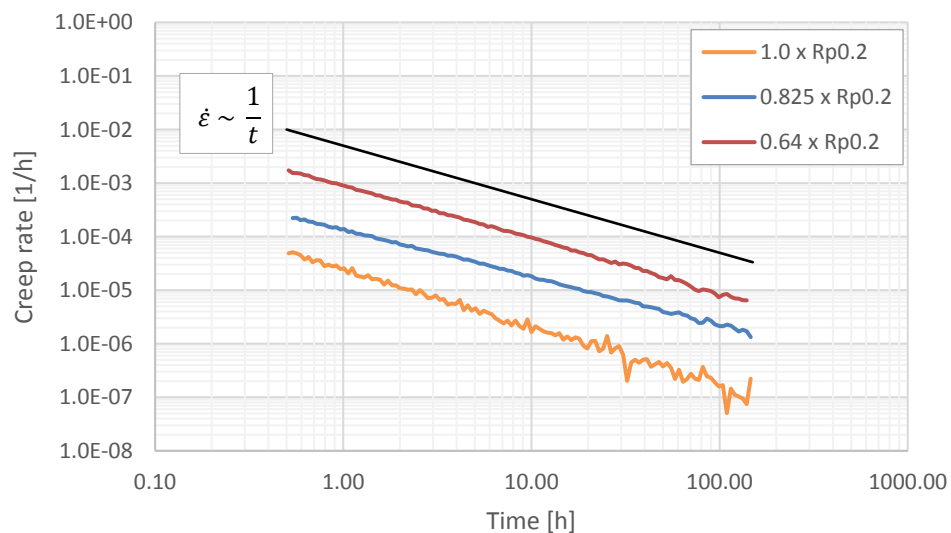
Figure 60. The rate of creep deformation for grade 1.4404 plate material in long term constant load creep test. The curve $\dot{\varepsilon} \sim \left(\frac{1}{t}\right)$, which corresponds to logarithmic creep behavior, is shown for reference.

It is noteworthy that the testing rig used for the long-term dead-weight creep tests does not enable accurate control of loading rate nor accurate determination of the time-zero value for the actual creep period. Possible differences in the loading rate have a direct influence on the strain occurring in the loading phase on the test. The strain induced during the loading stage will decrease with increasing loading rate.

4.5   Repeated relaxation tests of the austenitic and the ferritic material

The purpose of the repeated relaxation tests was to investigate how ferritic and austenitic grades behave in the situation where the bolts are reloaded after a certain period has passed after the first loading procedure. Reloading is a common practice in construction of steel structures with preloaded slip-resistant bolt connections.

outokumpu

TORNIO R&D CENTER

Creep and stress relaxation behavior of stainless
steel plates at room temperature
Timo Manninen, Johan Pilhagen

2018-0042
2017-01-02
Technical report
Public

Page 47 of 69

_____

As discussed in the literature study [1], room temperature creep of metals has been explained by two competing theories: the strain hardening theory and the exhaustion theory. Both theories explain the decreasing creep rate observed in creep tests based on thermally activated movement of dislocations over different types of barriers to dislocation movement. These two theories do not, however, provide a clear answer to what happens when the test material is reloaded to the same original stress level after a relaxation period.

Figure 61 shows the results of a repeated 3x4hour repeated relaxation test conducted on grade 1.4404 plate material. The relaxation curve obtained in 12 hours monotonic relaxation test is shows as reference. The results show clearly that the amount of stress relaxation decreases in each subsequent relaxation period. The results of all repeated relaxation tests are summarized in Figures 62 and 63. Two different loading speed values, were used in the tests. The following characteristics can be observed by comparing the stress values shown in the figures:

- The amount of stress relaxation decreases in each subsequent relaxation period.
- The amount of stress relaxation increases with the speed of loading.

The influence of the loading speed is clearly visible in the Figure 64 which compares the difference in stress relaxation for the same material and same loading with different loading speeds. Figures 65 and 66 present a comparison of stress relaxation in continuous 12 hour tests and 4x3 hour tests. The figures illustrate that a major part of the stress relaxation occurring in the continuous 12-hour relaxation tests occurs in the first 3 hours. The ferritic 1.4003 seems to be less susceptible to stress relaxation compared to the austenitic 1.4404.
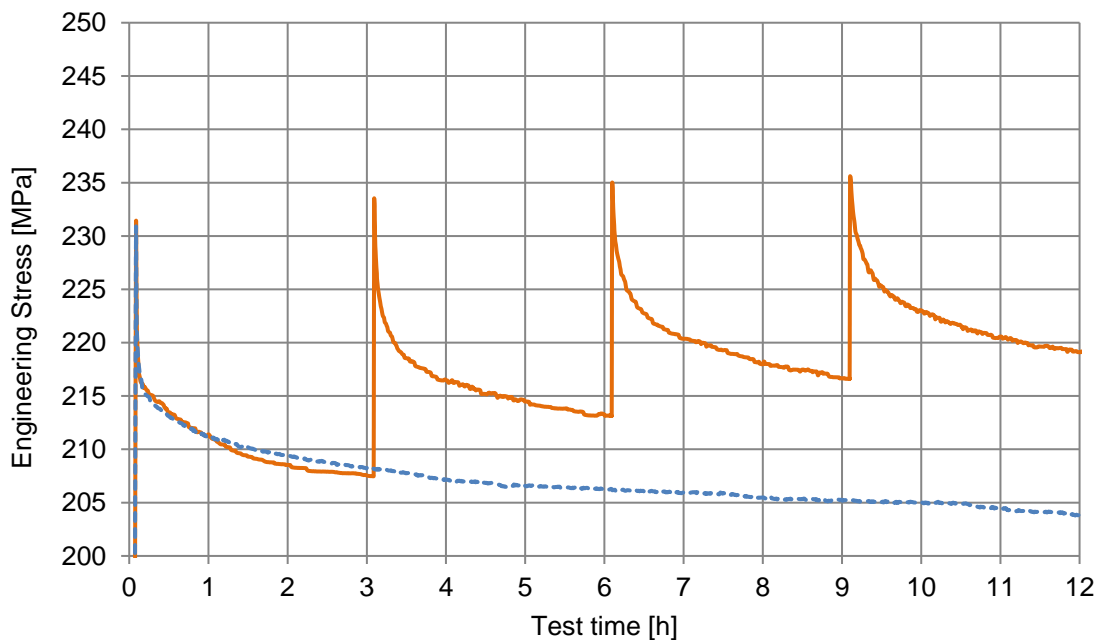
Figure 61. Repeated 4x3h relaxation test for grade 1.4404 plate material. The stress relaxation curve measured on continuous 12h loading is shown as reference (dashed blue line). The loading speed was 0.5 MPa/s and the load level corresponds to the 82.5 % of the 0.2 % proof stress of the material.

TORNIO R&D CENTER

Creep and stress relaxation behavior of stainless
steel plates at room temperature
Timo Manninen, Johan Pilhagen

2018-0042
2017-01-02
Technical report
Public

Page 48 of 69
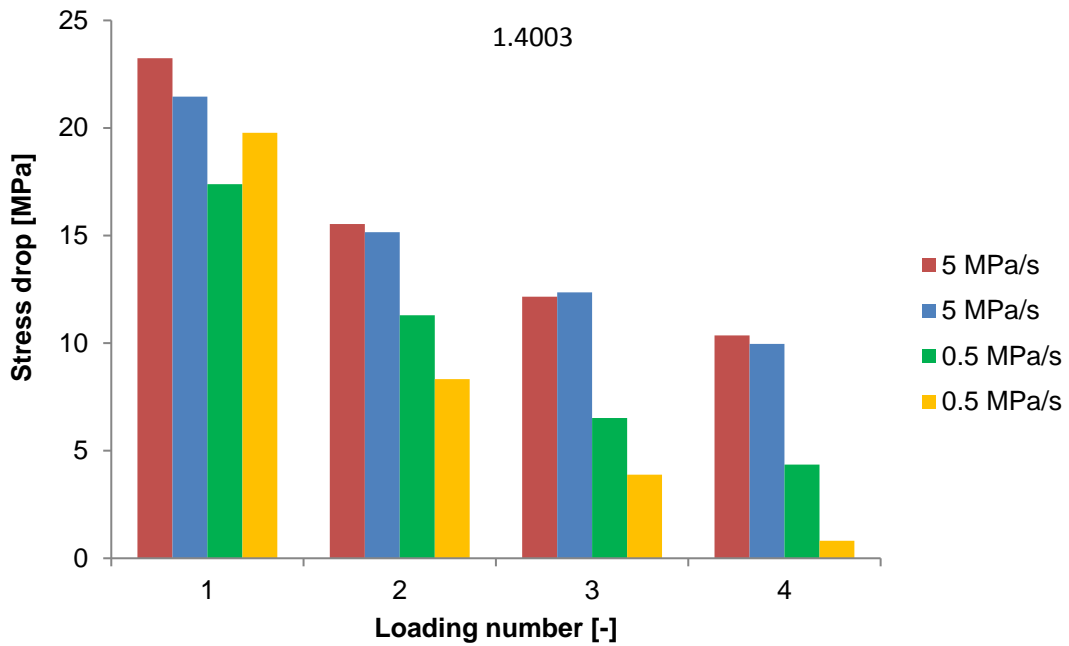
Figure 62. Stress drop in each subsequent relaxation period on 4x3h repeated relaxation tests for grade 1.4003 plate material. The same loading speed, given in the legend, was used on all repeats.
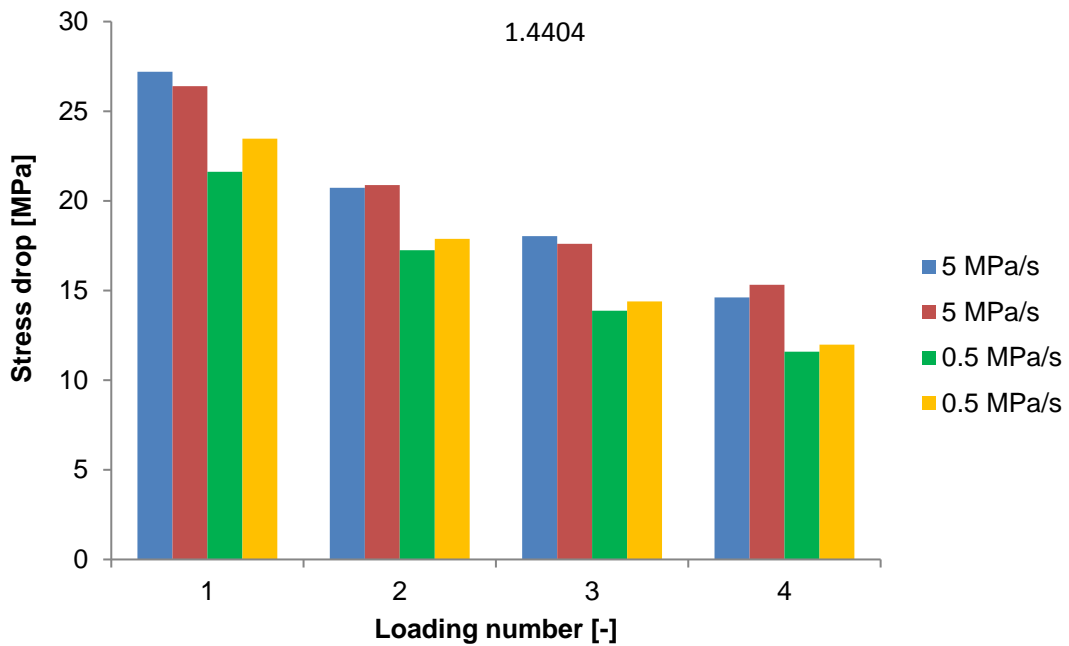
Figure 63. Stress drop in each subsequent relaxation period on 4x3h repeated relaxation tests for grade 1.4404 plate material. The same loading speed, given in the legend, was used on all repeats.

	Creep and stress relaxation behavior of stainless	2018-0042	Page 49 of 69
outokumpu	steel plates at room temperature	2017-01-02	
	Timo Manninen, Johan Pilhagen	Technical report	
TORNIO R&D CENTER		Public	

_____
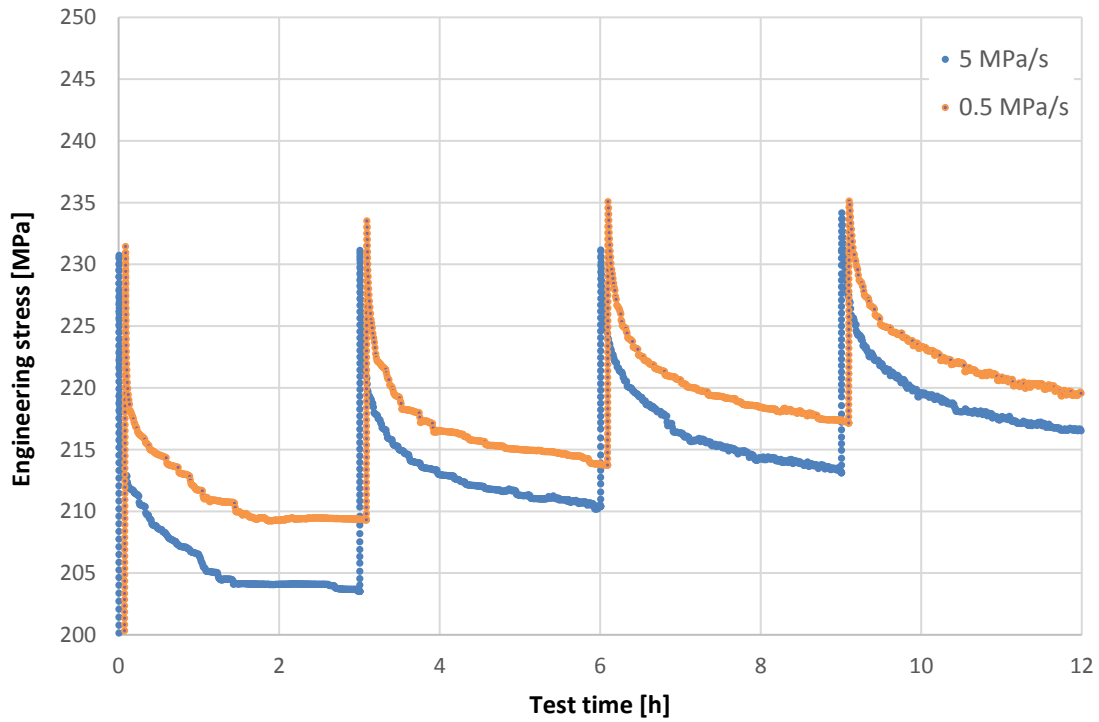
Figure 64. Stress relaxation in repeated 3x4h relaxation tests carried out with different loading speeds for grade 1.4404 plate materials.
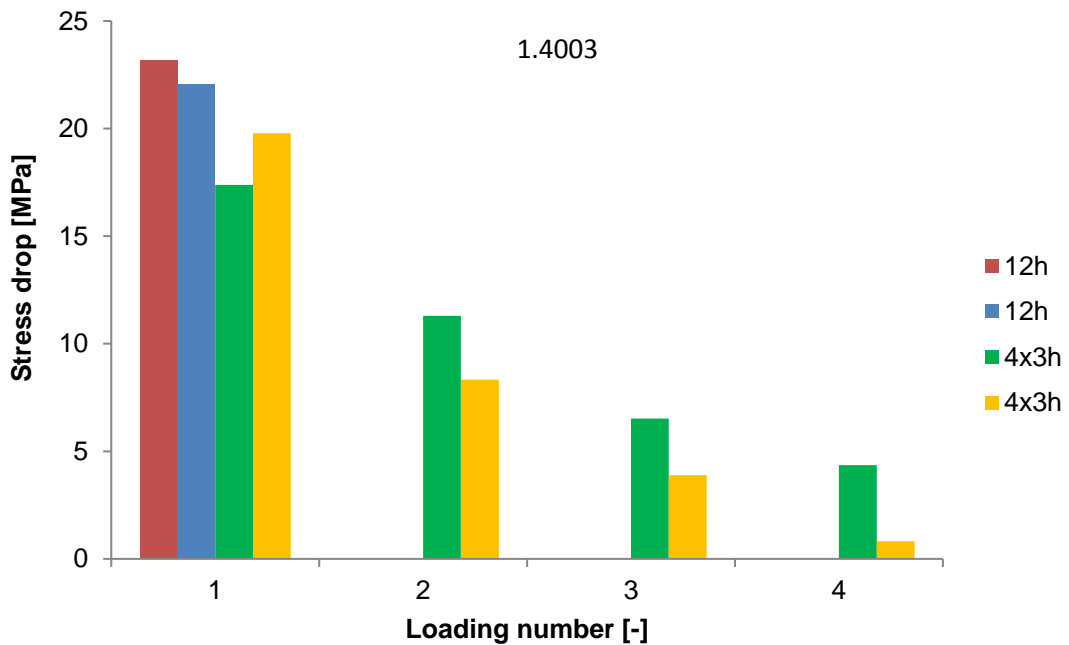
Figure 65. Stress drop in continuous 12h test and repeated 4x3h test for grade 1.4003 material. The same loading speed 0.5 MPa/s was used in these tests.

outokumpu	Creep and stress relaxation behavior of stainless steel plates at room temperature Timo Manninen, Johan Pilhagen	2018-0042 2017-01-02 Technical report Public	Page 50 of 69

TORNIO R&D CENTER

_____

Figure 66. Stress drop in continuous 12h test and repeated 4x3h test for grade 1.4404 material. The same loading speed 0.5 MPa/s was used in these tests.

	Creep and stress relaxation behavior of stainless steel plates at room temperature	2018-0042	Page 51 of 69
outokumpu	steel plates at room temperature	2017-01-02	
	Timo Manninen, Johan Pilhagen	Technical report	
TORNIO R&D CENTER		Public	

_____

4.6   Short and long-term creep testing of the duplex materials

The load levels σ, the resulting initial strain ε_0 and test durations used for the creep testing can be seen in Table 16.

Table 16 Mean values for the load level (σ), the mean strain after the initial loading (ε_0) and the test duration for each test.

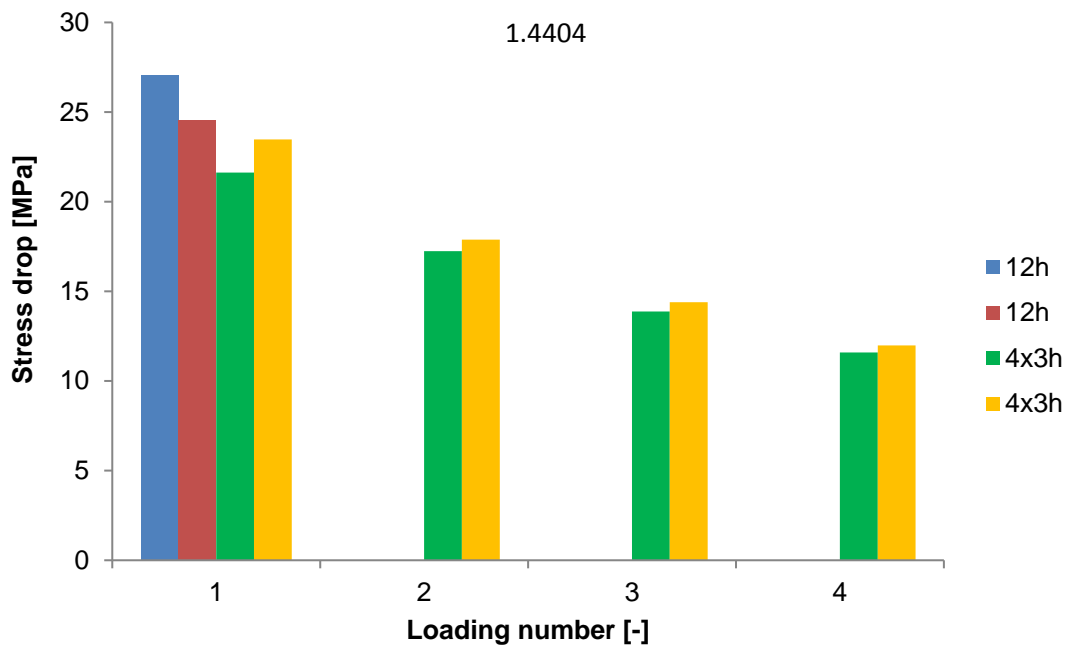| Grade	Loading rate	σ, x$R_{p0.2}$	σ, MPa	ε_0, %	t, h
1.4162	10^{-4} 1/s	0.65	330.0	0.17	20,20
		0.83	418.7	0.25	20,20
		1.00	508.8	0.51	20,20
	10^{-5} 1/s	0.65	330.9	0.18	151,161
		0.83	419.9	0.27	161,161
		1.00	509.2	0.62	144,161
	2 MPa/s	0.50	254.5	0.13	12,12,12
		0.65	330.8	0.18	100,100
		0.83	419.8	0.27	9.1,12,12,100
		1.00	508.9	0.55	12,12,12
		1.20	610.7	4.54	20,20,20
1.4462	10^{-4} 1/s	0.65	401.8	0.22	20,20
		0.83	509.9	0.31	5.7, 20
		1.00	618.8	0.76	20,20
	10^{-5} 1/s	0.65	402.4	0.22	161,168
		0.83	510.6	0.32	160,162
		1.00	613.3	1.15	140,140
	2 MPa/s	0.50	309.4	0.16	12,12,12
		0.65	402.3	0.22	100,100
		0.83	510.5	0.32	12,12,12,100
		1.00	618.9	0.67	12,12,12
		1.20	742.5	8.68	20,20,20

The creep results can be seen in Figure 67 and Figure 68. The time was adjusted with the time for loading for removing the difference in time due to initial loading times. The creep was high in the beginning but quickly slowed down with increasing time.

Creep was observed at 0.50x$R_{p0.2}$ for both duplex materials for the two first hours of testing. After that the creep rate was likely too low to be observed with the test setup and testing duration. The negative creep was likely attributed to changes in the ambient temperature, as previously discussed in chapter 3.5.

With increasing load level, the creep increased. The effect of changing ambient temperature was clearly observed at the 0.65x$R_{p0.2}$ load level. With further increased load level the influence on changing ambient temperature decreased and was not observed at the 1.00x$R_{p0.2}$ and at the 1.20x$R_{p0.2}$ load levels.
The amount of creep seemed influenced by the initial loading rate there the faster loading rate resulted in the highest creep and the slowest loading rate in the lowest creep.

The creep results show fairly low scatter between repeats, except for the 1.4462 at the 1.00xR_{p02} load level with 10^{-5} 1/s loading rate. This was due to two slightly different levels of load, 618.9 MPa and 607.7 MPa, where the lower load resulted in lower creep. No secondary creep was observed.
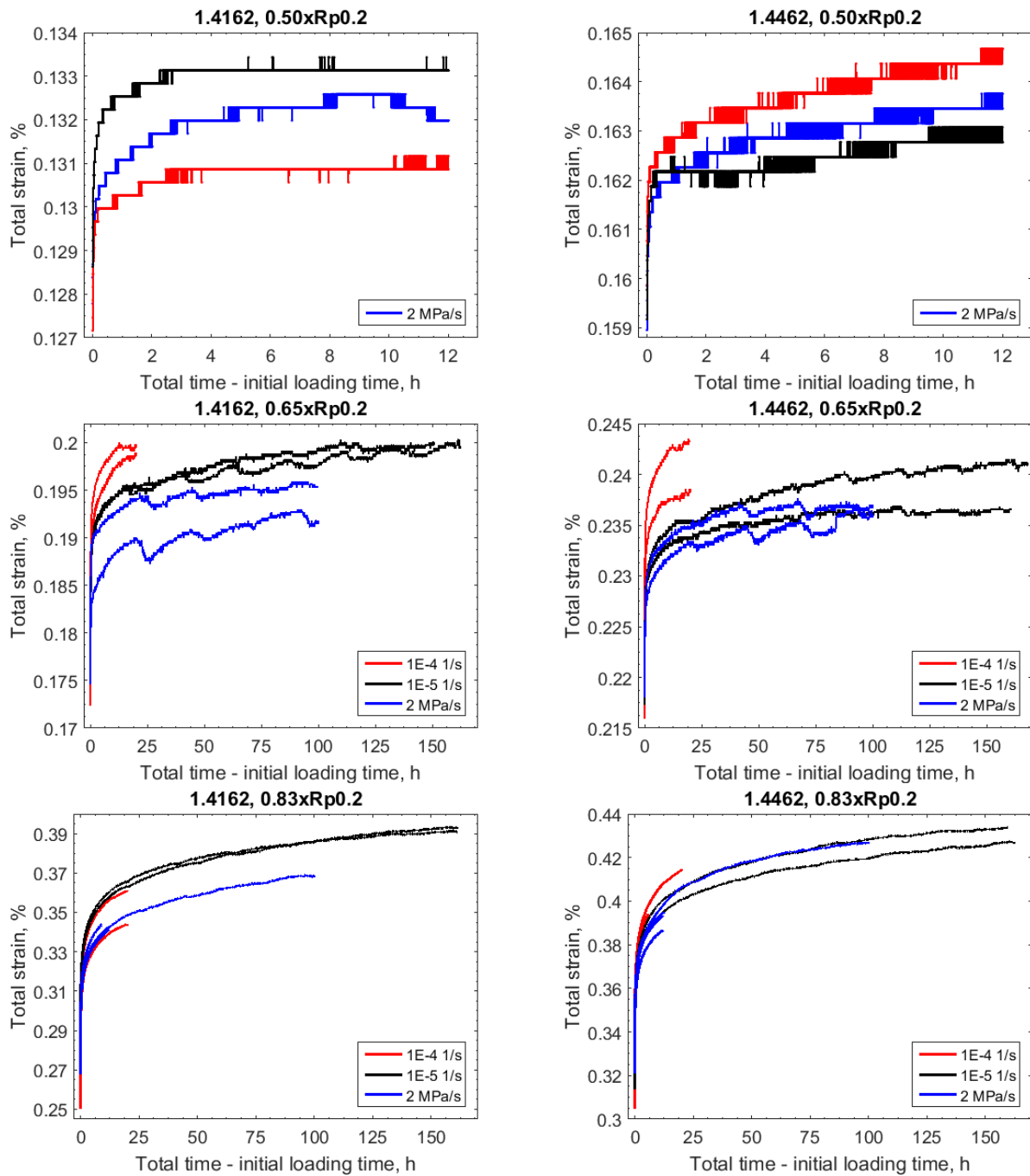
Figure 67 Room temperature creep results for load levels of 0.50 to 0.83xR$_{p0.2}$. For the 0.50xR$_{p0.2}$ load level the different colors represent individual measurements.

outokumpu ○

TORNIO R&D CENTER

Creep and stress relaxation behavior of stainless
steel plates at room temperature
Timo Manninen, Johan Pilhagen

2018-0042
2017-01-02
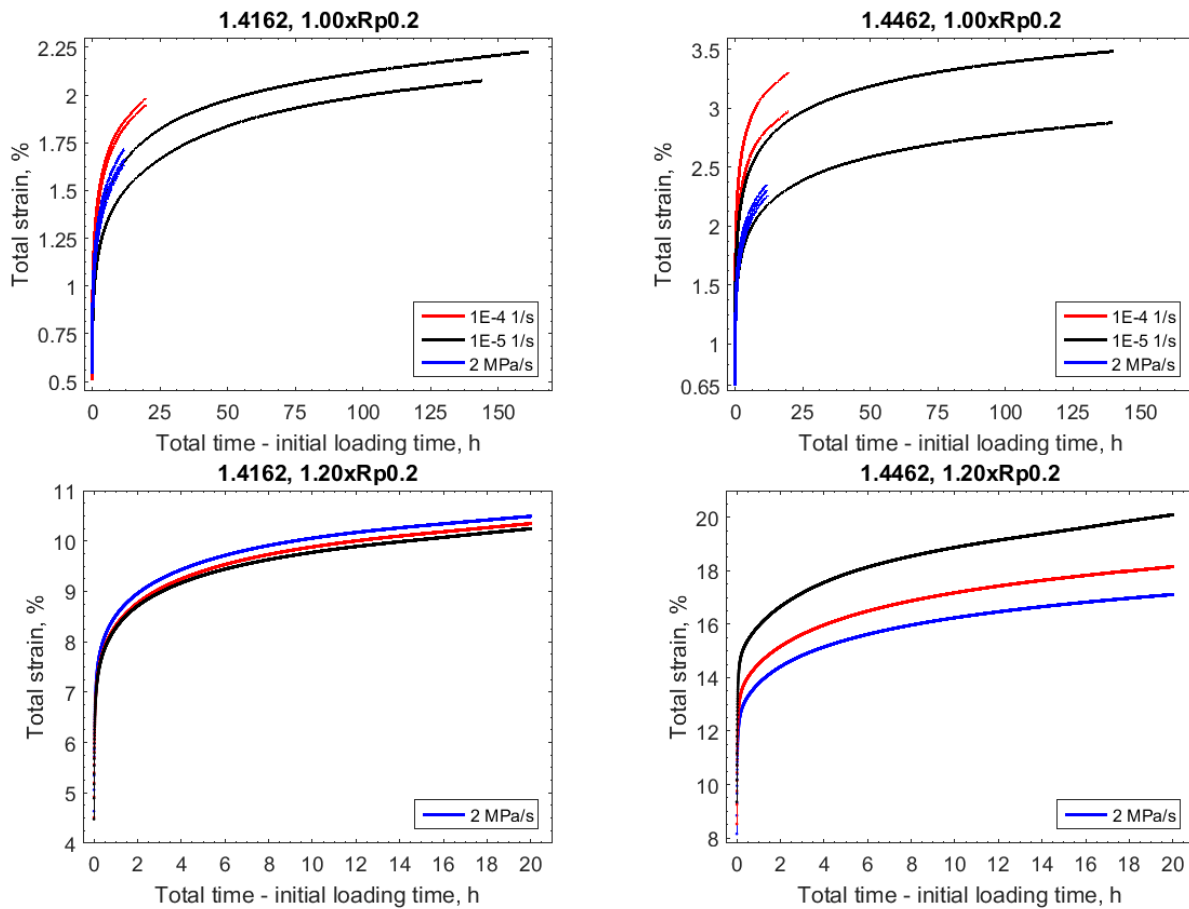Technical report
Public

Page 53 of 69

Figure 68 Room temperature creep results for load levels of 1.00 and 1.20xR$_{p0.2}$. For the 1.20xR$_{p0.2}$ load level the different colors represent individual measurements.

4.7 Summary of the creep test results

Figure 69 shows the creep results for the investigated stainless steels at room temperature condition. The inelastic strain was defined as the total strain minus the elastic strain (Hooke's law). The immediate plastic strain that occurs during the loading stage is included in the inelastic strain. Therefore, the creep strain is always smaller than the inelastic strain in the y-axis. The inelastic strain after 0.5 hour of testing is showed. The reason for comparing the inelastic strains and at the start of 0.5 hour was to be able to compare the different grades with different proof stress and to compare the dead weight testing with the testing in the servo mechanical testing machine.

At the 0.50×Rp0.2 creep load, creep deformation was observed for all the tested stainless steel grades. After 2.5 h of testing, the inelastic strain became constant indicating that the creep rate was below the resolution of the testing systems.

The ferritic grade, except at the 0.50×Rp0.2 load level, exhibit lower inelastic strain than the austenitic. The two duplex grades exhibited the lowest amount of inelastic strain for the two lowest load levels. At the 0.825×Rp0.2 load level the two duplex grades showed increased inelastic strain compared to the austenitic and ferritic grades. At the 1.00×Rp0.2 load level the two duplex grades exhibited the highest inelastic strain. One part of the explanation was likely that the duplex grades had higher proof strength compared to the austenitic and ferritic grades (recall Table 2 and Table 4). This resulted in higher amount of strain during the initial loading which consequently resulted in larger contribution of plastic strain to the inelastic strain due to the continuous yielding behavior of stainless steel. The mean contribution of plastic strain to the inelastic strain at the 1.00xRp0.2 load level was 33 % for the duplex grades where the 1.4462 had the highest contribution of plastic strain in the initial loading stage.
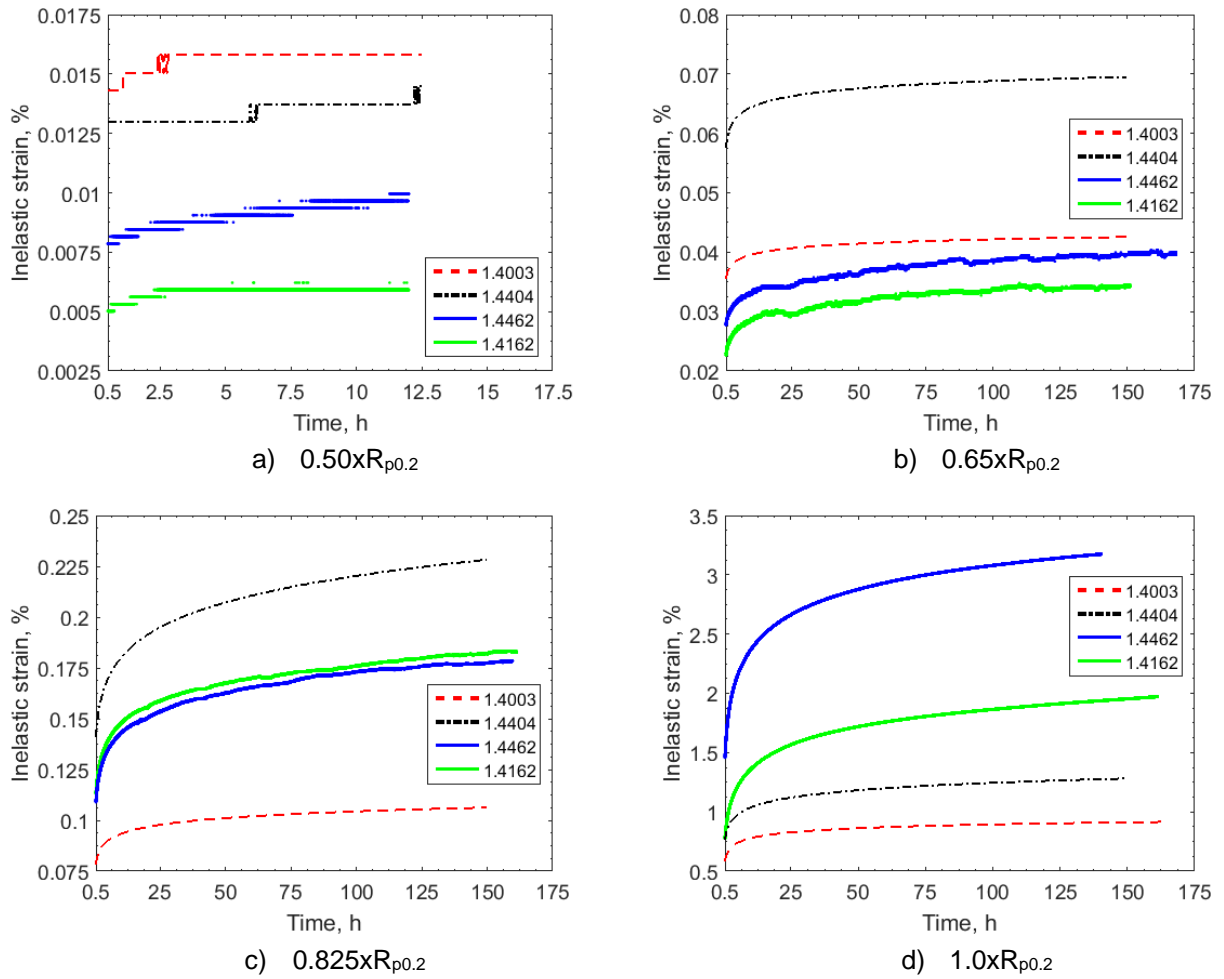
_____

Figure 69 Comparison of the resulting inelastic deformation for the different materials.

5.   Empirical models for the creep deformation

5.1   The austenitic and the ferritic grade

According to the literature study [1], room-temperature creep deformation of many pure metals and alloys can be described by the logarithmic creep model

$$\varepsilon = \alpha \ln(t) + \beta \quad \Leftrightarrow \quad \dot{\varepsilon} = \alpha t^{-1} \tag{11}$$

where parameters *α and β* may depend on the stress level. Therefore, regression analysis was carried out to investigate if the room temperature creep deformation of the ferritic and austenitic test materials studied in the present work can be also described by the logarithmic creep model.

First, the test results obtained in the tests with the same load level were collected and presented as ordered pairs of observations

$$\{(x_1, y_1), (x_2, y_2), ..., (x_n, y_n)\} \quad where \ x_i = \frac{t_{ref}}{t_i} \ and \ y_i = \dot{\varepsilon}_i \tag{12}$$

where the reference time value was t_{ref} = 1h. Then regression analysis was carried out to investigate if the linear model

$$y = \alpha \cdot x \tag{13}$$

appropriately describes the observations. The regression analysis was always conducted twice. After the first regression analysis, a small number outliers were removed based on the Grubbs test. Then the regression analysis was repeated with the cleaned data set. The statistical analyses were carried out using the Minitab software.

The results of the regression analysis are summarized in the Tables 17 - 20. The results show that the model is appropriate for the measurement data and describes the data well. The coefficient of determination slightly decreases in the long-term creep tests carried out with low load levels. This is clearly caused by the measurement noise (experimental error) rather than inappropriateness of the model. Figure 70 shows the measurement data and the regression model for the case with smallest coefficient of determination. The figure shows with a doubt that the regression line describes reasonably well the general trend in the measurement data even in this case.

Table 17. Summary of regression analysis of short-term creep test data for the grade 1.4003 material.

Stress level (x Rp0.2)	α (1/h)	R² (%)	P (-)
0.65	$(2.30 \pm 0.10) \cdot 10^{-5}$	98.8	< 0.001
0.825	$(5.40 \pm 0.10) \cdot 10^{-5}$	99.6	< 0.001
1	$(7.34 \pm 0.27) \cdot 10^{-4}$	93.4	< 0.001
1.2	$(1.59 \pm 0.01) \cdot 10^{-3}$	99.7	< 0.001

TORNIO R&D CENTER

Creep and stress relaxation behavior of stainless
steel plates at room temperature
Timo Manninen, Johan Pilhagen

2018-0042
2017-01-02
Technical report
Public

Page 56 of 69

_____

Table 18. Summary of regression analysis of short-term creep test data for the grade 1.4404 material.

Stress level (x Rp0.2)	α (1/h)	R² (%)	P (-)
0.65	$(2.20 \pm 0.15) \cdot 10^{-5}$	91.1	< 0.001
0.825	$(1.09 \pm 0.04) \cdot 10^{-4}$	92.0	< 0.001
1	$(1.04 \pm 0.01) \cdot 10^{-3}$	99.8	< 0.001
1.2	$(1.90 \pm 0.01) \cdot 10^{-3}$	99.9	< 0.001

Table 19. Summary of regression analysis of long-term creep test data for the grade 1.4003 material.

Stress level (x Rp0.2)	α (1/h)	R² (%)	P (-)
0.65	$(1.70 \pm 0.05) \cdot 10^{-5}$	88.1	< 0.001
0.825	$(4.70 \pm 0.15) \cdot 10^{-5}$	91.6	< 0.001
1	$(6.69 \pm 0.03) \cdot 10^{-4}$	99.9	< 0.001

Table 20. Summary of regression analysis of long-term creep test data for the grade 1.4003 material.

Stress level (x Rp0.2)	α (1/h)	R² (%)	P (-)
0.65	$(2.00 \pm 0.10) \cdot 10^{-5}$	98.8	< 0.001
0.825	$(1.25 \pm 0.02) \cdot 10^{-4}$	99.6	< 0.001
1	$(8.80 \pm 0.04) \cdot 10^{-4}$	93.4	< 0.001
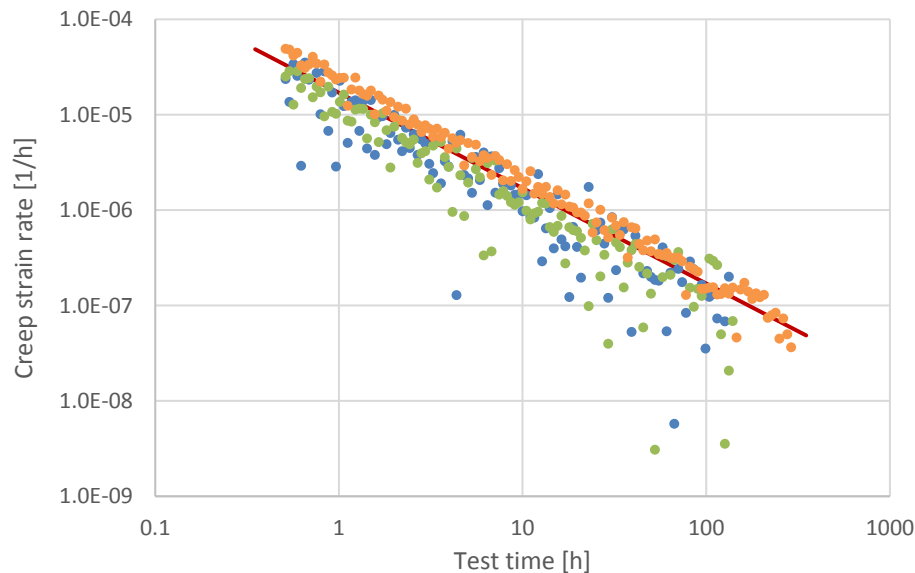
Figure 70. Measurement data and the regression model for the case with smallest coefficient of determination, i.e. long-term creep test of 1.4003 with the load level of 0.65xRp0.2.

The dependency of model parameter α on the load level is shown in Figures 71 and 72. The parameter α appears to be a nonlinear function of normalized stress. The value of α does not seem to follow any simple analytical function. Therefore, the values of α might be best described by interpolating between the observations shown in the Figures 71 and 72. The interpolating functions are given in Table 21. In the table,

_____

the pre-exponential factor α_0 equals to $\alpha_0 = 1.0 \; h^{-1}$ and the load level, i.e. stress divided by the 0.2 % proof stress of the material, is denoted by *s*.

Table 21. Interpolating functions for α as a function of load level s.

Steel grade	Load level	Interpolator
1.4003	0.65 – 0.825	$\alpha = \alpha_0 \exp[-14.30 + 5.34\,s\,]$
	0.825 – 1.0	$\alpha = \alpha_0 \exp[-22.31 + 15.04\,s\,]$
	1.0 – 1.2	$\alpha = \alpha_0 \exp[-11.36 + 4.10\,s\,]$
1.4404	0.65 – 1.0	$\alpha = \alpha_0 \exp[-17.87 + 10.92\,s\,]$
	1.0 – 1.2	$\alpha = \alpha_0 \exp[-10.37 + 3.42\,s\,]$

According to Kassner et al. [2,3], parameter α is a bilinear function of applied stress with a change of slope at the 0.2 % proof stress. In the present work, parameter α was a nonlinear function of applied stress rather than a linear one. But also in the present work, the general trend between α and the applied stress seemed to change at the 0.2% proof stress. Therefore, the present results are partially consistent with the findings by Kassner.

Figure 71. Stress dependency of the parameter α of the logarithmic creep model in short-term and long-term constant load creep tests for grade 1.4003 plate material.

_____

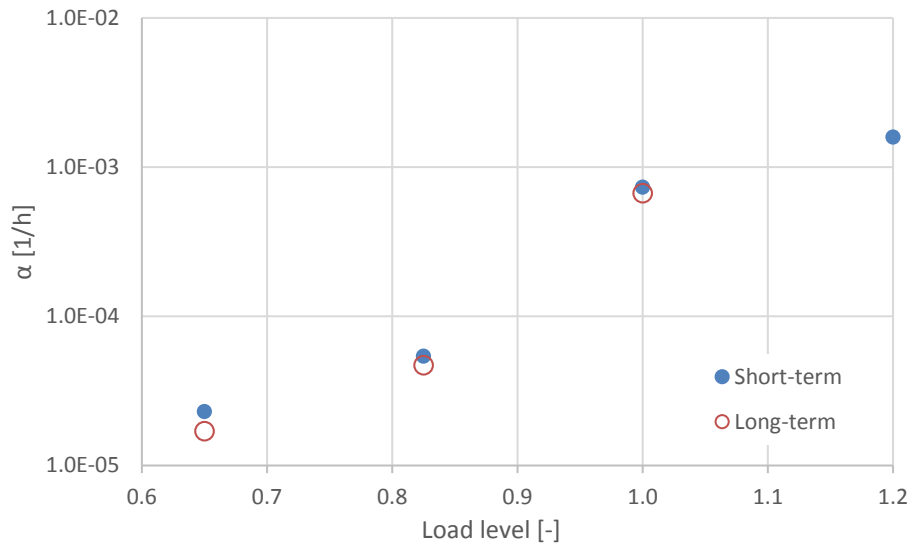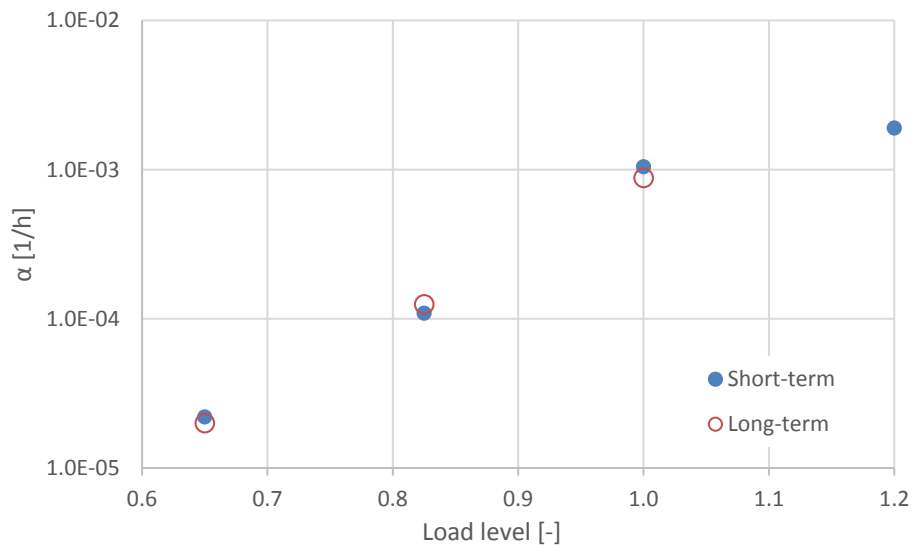*Figure 72. Stress dependency of the parameter α of the logarithmic creep model in short-term and long-term constant load creep tests for grade 1.4404 plate material.*

5.2 The duplex grades

To investigate if the tested duplex plates also had logarithmic creep behavior, the creep rate was determined. If the slope of the creep rate curves in the double logarithmic scale was found to be $k = -1$, then the creep was logarithmic. If $k \neq -1$ then the creep is usually defined as power-law creep [2]. Figure 73a shows the strain rate during the uniaxial tensile creep testing of the lean duplex grade at the 1.00xRp0.2 load level. Three distinct regions could be found: the first region (I) was the initial loading which in this case was constant strain rate of 10^{-5} 1/s, the second region (II) was the initial creep region where the creep rate rapidly decreases and the third region (III) was the creep rate region where the creep rate could be described by equation (11). Apparently, equation (11) does not describe the initial creep behavior.

The logarithmic creep rate region was independent of the initial loading rate as seen in Figure 73b which shows the creep rate for the three different initial loading rates. The initial loading rate determines the strain at the specified load and the maximum creep rate obtained during testing. Figure 73c shows the influence of the load level on the creep rate. The rapid decrease in creep rate during the initial creep region (II) was observed to depend on the load level where a high load level had lower creep rate drop which resulted in an elevated logarithmic creep rate (higher α value) which results in higher amount of inelastic strain. The creep behavior for the austenitic and ferritic grade in the present work was also found to be logarithmic. The 1.4462 duplex plate had similar creep behavior as the 1.4162, see Figure 73d.
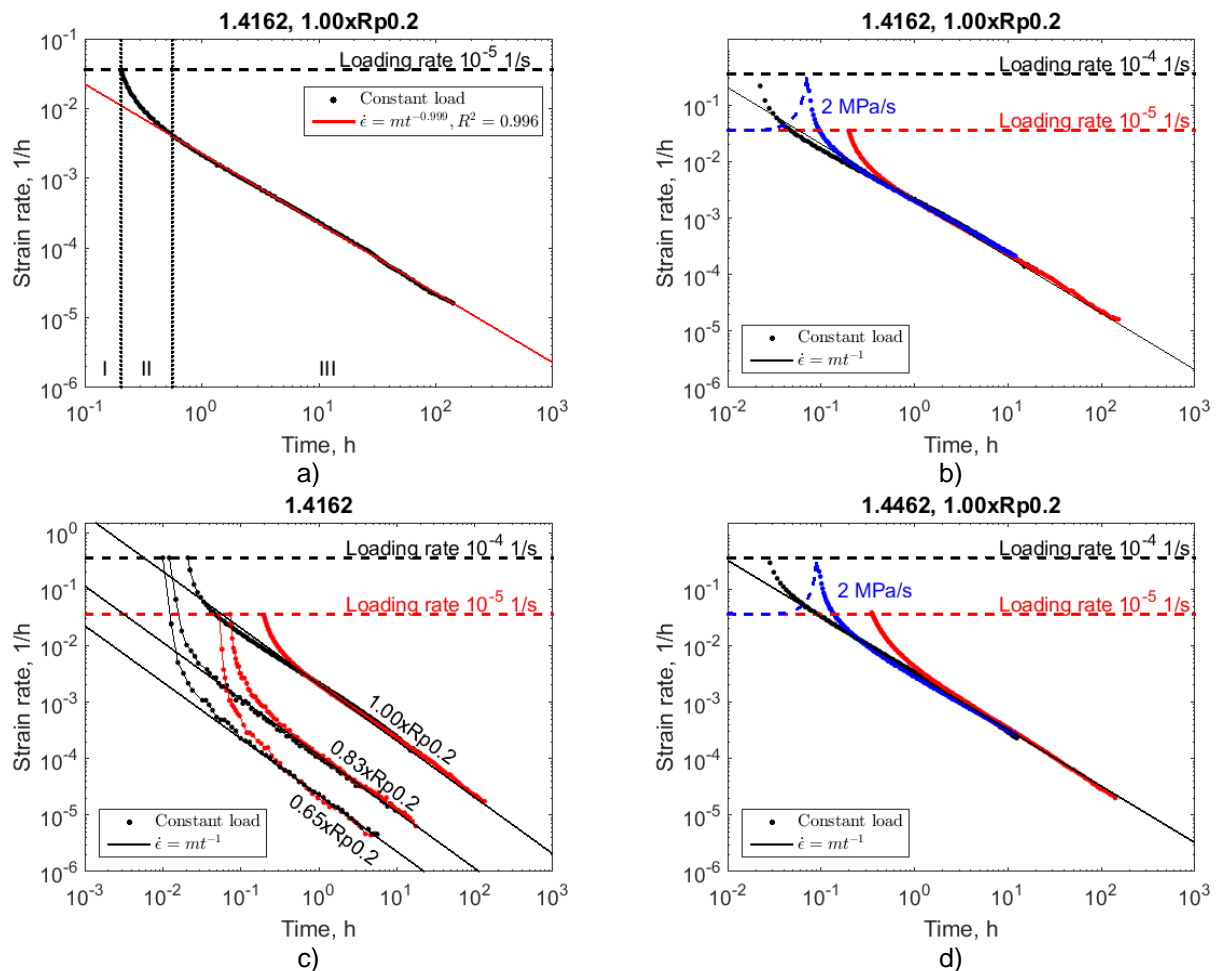

Figure 73 The creep rate during uniaxial creep testing. a) logarithmic creep behavior in region III, b) influence of the initial loading rate, c) influence of the load level, d) similar creep behavior for 1.4462. m = α in equation (11).

outokumpu

TORNIO R&D CENTER

Creep and stress relaxation behavior of stainless steel plates at room temperature
Timo Manninen, Johan Pilhagen

2018-0042
2017-01-02
Technical report
Public

Page 60 of 69

_____

Table 22 and Table 23 show the found coefficient of *k* and *α* for the two tested duplex plates. The *k* and *α* was found from linear least square fitting of the creep rate in the third region (III). K is the slope in double logarithmic scale.

Table 22 Found coefficients for k and m according to equation (2) for 1.4162.

Stress lvl, $xR_{p0.2}$	Loading rate	Mean of k	CV of k, %	Mean of α	CV of α, %
0.50	2 MPa/s	-1.07	4.0	6.89E-06	18.6
	2 MPa/s	-0.98	5.5	2.00E-05	2.3
0.65	1E-4 1/s	-0.99	2.6	2.54E-05	3.5
	1E-5 1/s	-1.00	2.3	2.25E-05	0.1
Mean		**-0.99**	**3.9**	**2.26E-05**	**10.0**
	2 MPa/s	-1.00	2.1	1.13E-04	1.3
0.83	1E-4 1/s	-0.99	0.3	1.10E-04	6.6
	1E-5 1/s	-0.98	0.3	1.22E-04	2.3
Mean		**-0.99**	**1.71**	**1.14E-04**	**5.5**
	2 MPa/s	-0.91	0.9	1.99E-03	3.1
1.00	1E-4 1/s	-0.93	0.9	2.10E-03	2.2
	1E-5 1/s	-0.98	2.4	2.12E-03	6.8
Mean		**-0.93**	**3.2**	**2.06E-03**	**5.3**
1.20	2 MPa/s	-1.01	0.75	7.22E-03	0.9

Table 23 Found coefficients for k and m according to equation (2) for 1.4462.

Stress lvl, $xR_{p0.2}$	Loading rate	Mean of k	CV of k, %	Mean of α	CV of α, %
0.5	2 MPa/s	-0.88	12.03	6.87E-06	8.4
	2 MPa/s	-1.0	4.6	2.04E-05	1.6
0.65	1E-4 1/s	-1.06	2.3	2.20E-05	7.4
	1E-5 1/s	-1.02	1.4	1.99E-05	3.6
Mean		**-1.02**	**4.3**	**2.08E-05**	**6.6**
	2 MPa/s	-1.00	2.5	1.08E-04	6.8
0.83	1E-4 1/s	-1.00	1.5	1.18E-04	5.6
	1E-5 1/s	-1.00	1.2	1.24E-04	6.0
Mean		**-1.00**	**2.0**	**1.14E-04**	**8.8**
	2 MPa/s	-1.00	0.6	2.99E-03	0.8
1.00	1E-4 1/s	-1.02	1.1	3.45E-03	3.8
	1E-5 1/s	-1.03	3.4	3.42E-03	16.1
Mean		**-1.01**	**2.2**	**3.24E-03**	**11.6**
1.2	2 MPa/s	-0.82	3.9	9.83E-03	3.8

The *k* value was in good agreement with -1 for most of the tests. At the 0.50xRp0.2 load level there was only few data points that could be used as the creep rate quickly became too low to be observed with the used equipment, therefore the agreement with -1 was less good at this load level. At the 1.00xRp0.2 load level for the 1.4162 the value of k was slightly less than -1. This may be due to testing issues and not a different material behavior. For the load level at 1.20xRp0.2 for the 1.4462 plate the found *k* value significantly differed from *k = -1* for all three tests, see Figure 74. At this load level, the maximum strain during the creep testing was similar to the measured uniform elongation from the tensile testing. Perhaps at this level of strain the creep behavior is better described by a power-law behavior than a logarithmic. This difference was not observed for

outokumpu

TORNIO R&D CENTER

Creep and stress relaxation behavior of stainless steel plates at room temperature
Timo Manninen, Johan Pilhagen

2018-0042
2017-01-02
Technical report
Public

Page 61 of 69

_____

the 1.4162 plate. The engineering strain at start of the creep testing (constant load) was 4.5 % for the 1.4162 compared to 8.7 % for the 1.4462, recall Table 16. This may be explained by higher work hardening for the 1.4162 compare to the 1.4462 (i.e. less strain was obtained for 1.4162 for achieving similar $xR_{p0.2}$ load level).
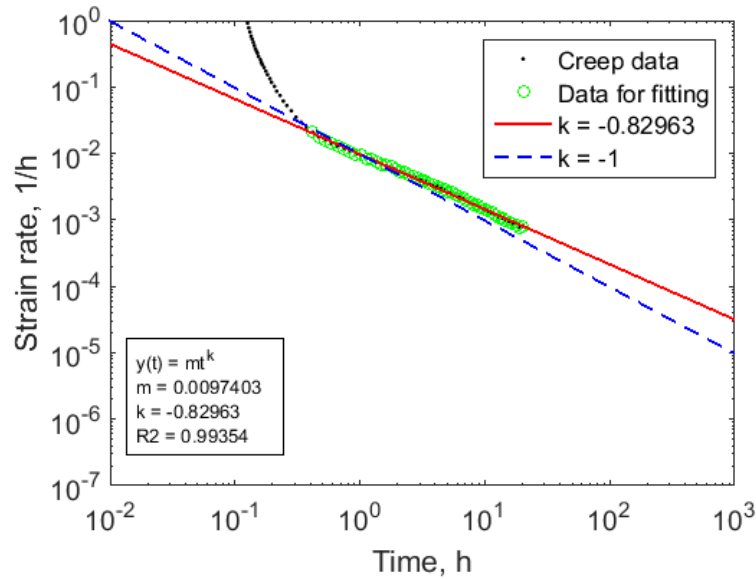

Figure 74 Different creep-rate behavior for 1.4462 at the 1.20xRp0.2 load level.

In the work by Alden [4] room temperature creep of 304 austenitic stainless steel sheet was examined. The conclusion from that work was that the creep behavior was significantly influenced by the initial loading rate. Higher loading rates resulted in higher creep deformation and vice versa. The results from this work indicates a similar behavior as seen in Table 24. This table shows the contribution of creep strain to the total strain for the 1.4162 plate at the 1.00xRp0.2 load level for the three different loading rates. The creep strain was defined as the total strain (Figure 68) minus the strain due to the initial loading (Table 16). The II region gives a minor contribution and was not clearly correlated to the loading rate. For the III region, the creep strain was dependent on the loading rate thus indicating that the room temperature creep behavior for duplex stainless steel is influenced by the initial loading rate.

Table 24 Creep strain as function of loading rate. ε_0 is the initial strain, II and III according to Figure 73a.

		Creep strain, %			Total strain, %	
Loading rate	ε_0, %	II	III, 12 h	III, 20 h	12 h	20 h
2 MPa/s	0.55	0.36	0.77	na	1.68	na
10^{-4} 1/s	0.51	0.25	1.09	1.17	1.85	1.93
10^{-5} 1/s	0.62	0.32	0.63	0.74	1.58	1.69

---

6. A state of the art viscoplastic constitutive model

The first generation of theories for creep deformation of metals, known as the classic creep theories, are analytical equations capable of describing the evolution of creep strain under instantaneously applied constant load. The logarithmic creep law discussed in the previous chapters is an example of a classic creep model.

The classic creep models are generally targeted for modelling situations which closely resemble tests that are used for investigating the creep characteristic of materials in the laboratory. In these tests, the loading is indeed applied instantaneously and maintained accurately at the constant value throughout the whole testing period.

Many applications, however, involve varying creep loads. The load may e.g. be applied gradually over a longer period. Creep or stress relaxation may then occur during the loading stage when the load is continuously increasing. The load may be also applied in two or several steps allowing creep or stress relaxation to occur between the increments. Creep deformation in the highly stressed regions of the structure also often lead to redistribution stresses in the structure. Additionally, changes in the external loading and thermal expansion may also result in changes in the creep load.

The classic creep models are generally not well-suited for describing material behavior under varying loads. Therefore, a second generation of creep models, known as viscoplasticity with internal state variables, started developing in the mid 1960's. In this approach, internal state variables, denoted here by β_i, are used to describe the evolution of the microstructure of the material. The creep rate $\dot{\varepsilon}_c$ is described as a function of observable variables (e.g. stress, creep strain and temperature) and internal state variables β_i.

$$\dot{\varepsilon}_c = \dot{\varepsilon}_c(\sigma, \varepsilon_c, T, \beta_i) \tag{14}$$

The creep constitutive law *(14)* is complemented with evolution laws for the internal state variables.

$$\dot{\beta}_i = \dot{\beta}_i(\sigma, \varepsilon_c, T, \beta_i) \tag{15}$$

The viscoplastic models with internal state variables are unified theories. The immediate and time dependent plastic deformations are treated as one inelastic strain component. The time-independent plasticity is obtained as a limiting case.

In low temperature creep and plasticity, dislocation glide is the dominating deformation mechanism. Therefore, the material behavior is determined by the strength of different barriers to dislocation motion such as:

A. interstitial and solute atoms,
B. grain boundaries,
C. precipitates,
D. density of mobile and sessile dislocations, and,
E. intergranular and intragranular residual stresses.

The hardening effects caused by solute atoms, grain boundaries and precipitates (A-C) do not evolve at room temperature. It follows that internal state variables are typically needed only for modelling the dislocation hardening and internal stresses in the microstructure. The number and type of internal state variables needed for describing these microstructural features varies widely depending on the specific application studied and on the desired level of complexity and accuracy of the model.

And extensive literature study was conducted as part of the work package five in the SIROCO project. In this literature study, available information on creep and stress relaxation behavior of stainless steel at room temperature was reviewed. The most important findings of the literature study can be summarized as follows:

- The physical mechanism responsible for creep and stress relaxation at low temperature in all types of steel is dislocation glide. The creep rate is dictated by the rate by which dislocations are capable of surmounting different types of obstacles assisted by thermal activation.

Creep and stress relaxation behavior of stainless steel plates at room temperature
Timo Manninen, Johan Pilhagen

2018-0042
2017-01-02
Technical report
Public

Page 63 of 69

TORNIO R&D CENTER

_____

- There are no fundamental differences in the room temperature creep behavior of materials with different crystal structure. Test materials with martensitic (BCT), ferritic (BCC) and austenitic (FCC) crystal structure behave in a qualitatively similar manner in the room temperature creep tests.

- The different methods that can be used for strengthening materials are not equivalent. Solid solution hardening by nitrogen or carbon alloying was less efficient way of increasing the creep resistance than hardening by cold-rolling.

- There exists a limiting stress value for the creep deformation. No creep can occur below the limit stress.

- The rate of creep deformation is a function of the overstress between the current stress and the creep limit.

- The creep limit increases due to work hardening during plastic deformation.

- The amount of creep deformation observed in creep tests depends on the loading rate used in the loading stage in the beginning of the test.

- The rate of creep deformation is closely related to the rate of work hardening in the material. Higher work hardening rate results in swifter deceleration of creep deformation.

- There is no difference between work hardening by creep test and work hardening in tensile testing. In spite of different deformation processes the material strain hardens by equal amount as long as the plastic strain is the same.

- The creep deformation causes the yield surface to undergo kinematic hardening with insignificant amount of isotropic hardening. This observation holds in creep testing of annealed materials with relative low stress levels in vicinity of the 0.2 % proof stress.

- No signs of secondary creep have been observed in room temperature testing.

The present state of the art in computational viscoplasticity was reviewed. The capability of different models in describing the features outlined above was assessed. Based on the assessment, a model referred henceforth as the Chaboche model was chosen as the constitutive model for modelling the room temperature creep and stress relaxation of all stainless steel plate materials. The Chaboche model is widely used both in academia and in industry for modelling cyclic plasticity. Furthermore, this model has been successfully used for modelling room temperature stress relaxation of AISI 316 type austenitic stainless steel [5–7].

The Chaboche model is a unified model. The immediate and time dependent plastic deformations are treated as one inelastic strain component. The time-independent plasticity is obtained as a limiting case. The model uses two internal state variables for describing the material hardening behavior. One internal state variable is a tensorial back-stress $\boldsymbol{\alpha}$ used for describing kinematic hardening of the material. The other state variable R accounts for isotropic hardening. Parametrized evolution laws are given for each internal variable. The back-stress is commonly described as a sum of components $\boldsymbol{\alpha}^{(i)}$

$$\boldsymbol{\alpha} = \sum_{i=1}^{N} \boldsymbol{\alpha}^{(i)} \tag{16}$$

Parametrized evolution laws are given for each internal variable. The evolution of kinematic hardening components is described by

$$\dot{\boldsymbol{\alpha}}^{(i)} = \frac{2}{3} C_i \, \dot{\boldsymbol{\varepsilon}}^p - \gamma_i \, \boldsymbol{\alpha}^{(i)} \, \dot{\bar{\varepsilon}}^p \tag{17}$$

where N is the number of kinematic hardening components, $\dot{\boldsymbol{\varepsilon}}^p$ is the rate of plastic strain tensor and $\dot{\bar{\varepsilon}}^p$ is the equivalent plastic strain. C_i and γ_i are material parameters. The scalar isotropic hardening component R follows the evolution law

$$\dot{R} = b(Q - R) \, \dot{\bar{\varepsilon}}^p \tag{18}$$

The rate of equivalent plastic strain is given by the power law viscosity function

$$\dot{\bar{\varepsilon}}_p = \langle \frac{\|\sigma - \alpha\|_{VM} - R - k}{D} \rangle^n \tag{19}$$

where D, k and n are material parameters. The norm $\|\cdot\|_{VM}$ denotes the Von Mises yield function. The McCauley brackets <·> guarantee that there exists an elastic limit below which no inelastic deformation occurs. The elastic limit also denoted the threshold for the onset of creep deformation and the limit at which stress relaxation ceases.

In the Chaboche model the observed hardening behavior is divided into kinematic and isotropic parts. It follows that identification of the material parameters for this model typically requires tests in which the direction of loading is reversed such as tension-compression tests. This kind of testing has not been carried out in work package 5. However, it is well-known that the transition from purely kinematic hardening to combined isotropic and kinematic hardening takes place in the vicinity of 1% plastic strain in most engineering materials. Therefore, it can be assumed that the rate independent hardening is purely kinematic hardening until the transition point at 1% plastic strain.

In the present application, the inelastic strains are expected to remain well below the transition point. The constitutive model was nevertheless extended to yield realistic prediction for the material behavior over the whole range that can be experimentally investigated with uniaxial tension tests. This will provide stable numerical calculation also in the possible case that a high stress concentration might occur in a localized region in the finite element model. Furthermore, this will also enable numerical experiments with hypothetical cold-worked plate materials.

After the transition point at 1% of plastic strain, the observed hardening was divided using a constant ratio in the kinematic hardening and isotropic hardening components. For single phase plate materials 1.4003 and 1.4404 it was assumed that the hardening consists of 60% of kinematic hardening and 40% of isotropic hardening following the experimental findings of Feaugas [8,9]. For the dual phase materials 1.4162 and 1.4462, it was assumed that the hardening is purely isotropic after the transition point.

Creep and stress relaxation behavior of stainless
steel plates at room temperature
Timo Manninen, Johan Pilhagen

2018-0042
2017-01-02
Technical report
Public

Page 65 of 69

TORNIO R&D CENTER

_____

A numerical method was developed for identifying the parameters of the Chaboche model based on the results of extensive materials testing carried out in the present work. The identification method has three stages:

I. Identification of the parameters D and n in the viscosity function (19). The 0.2 % proof stress values measured in tensile tests conducted with different constant loading rates in the range from 10^{-6} 1/s to 10^{-2} 1/s were used for the identification.

II. Identification of the hardening parameters in (17) and (18). The true stress vs. logarithmic plastic strain curves measured in tensile tests conducted with different constant loading rates in the range from 10^{-7} 1/s to 10^{-2} 1/s are used for identification. The rate-dependent part of stress is subtracted from the stress response using the viscosity function.

III. Fine tuning of model parameters by means of tensile test, creep test and relaxation test data. The simulated test results are compared with experimental results and parameters are adjusted manually based on expert judgement.

The developed numerical method was used to determine the Chaboche model for all four plate materials. The identified material parameters are summarized in *Table 25*.

Table 25. Chaboche model parameters for plate materials. The initial elastic limit is given by parameter k.

Grade	D (MPa)	n (-)	C_1 (MPa)	γ_1 (-)	C_2 (MPa)	γ_2 (-)	C_3 (MPa)	γ_3 (-)	Q (MPa)	b (-)	k (MPa)
1.4404	110	15.0	45949	591.4	617031	6765.3	1434	2.5	380	2.5	73
1.4003	130	11.0	623733	5855.1	17430	558.6	1680	10.8	104	10.8	106
1.4462	313	24.3	947349	11334.6	252038	1222.1	2971	60.0	723	2.8	106
1.4162	329	30.2	483769	4875.7	102445	975.3	6766	180.8	649	3.5	109

The results of long-term relaxation tests conducted by VTT were also used for fine tuning the material parameters of 1.4404. A report on the long-term relaxation tests is included as an appendix. Further information about calibration of the material parameters can be found in the work package 5 task 5.5 final report [10].

outokumpu

TORNIO R&D CENTER

Creep and stress relaxation behavior of stainless steel plates at room temperature
Timo Manninen, Johan Pilhagen

2018-0042
2017-01-02
Technical report
Public

Page 66 of 69

_____

7. Conclusions for preloaded connections

Room temperature creep deformation under uniaxial constant load was observed for the investigated stainless steels. The amount of creep deformation increased with increasing load level and likely also with increasing initial loading rates. At load levels around $0.5 \times R_{p0.2}$ the two duplex grades had the least susceptibility for creep but at around load levels of $1.0 \times R_{p0.2}$ the they had the highest susceptibility for creep. This indicates that in general, higher 0.2 % proof strength gives higher resistance to room temperature creep. But the actual creep behavior at absolute loads close to and above the proof strength seems to greatly depend on the yielding behavior. The ferritic 1.4003 had in overall the least susceptibility for creep.

However, the amount of creep deformation in the plates of preloaded stainless connections then greatly depends on the level of stress in the plates due to the preloading of the bolts. The preloading force in the bolt can be considered independent of the plate material. Therefore, level of stress in the plate is less significant for plates materials with higher yield strength. It has been estimated that for the preload ($F_{p,C}$) used in this project, the maximum through-thickness load levels were $0.71 \times R_{p0.2}$ for the austenitic plates, $0.66 \times R_{p0.2}$ for the ferritic plates, $0.49 \times R_{p0.2}$ for the lean duplex plates and $0.40 \times R_{p0.2}$ for the duplex plates. The approximate creep deformation after equivalent time (normalized to the austenitic sheet, i.e. 1.0) would then be 2/7 for the ferritic sheet, 1/25 for the lean duplex plate and <1/25 for the duplex plate, recall Figure 69. Thus, for the used preload in this project, the susceptibility for creep were (from highest to lowest): the austenitic, the ferritic, the lean duplex and the duplex material.

Table 26 shows 30 min of measured loss of preload in instrumented preloaded connections (reused bolts) together with extrapolation to 50 years [11]. There was no significant difference in loss of preload between ferritic and duplex stainless steel connections while the austenitic stainless steel connection had a higher loss of preload. The higher loss of preload for the austenitic connection would then be explained by the higher susceptibility for creep at the used preload. When using new bolts, the extrapolated loss increased to 8 % indicating that it is the stress relaxation in the bolt [12] that mainly contributes to the loss of preload in a stainless steel preloaded connection and not the creep deformation in the plates. This hypothesis is further strengthened when comparing with the structural carbon steel set-up (S355 with reused HV10.9 bolts) as the S355 steel is usual regarded as creep resistant at room temperature conditions.

Table 26 Measured and extrapolated loss of preload (mean values) from instrumented preloaded connections (reused bolts) [11]. BUMAX 109 bolts for the stainless steels and HV10.9 for the carbon steel.

Grade	30 min, %	50 years, %
1.4404 (austenitic)	2.0	5.7
1.4003 (ferritic)	1.1	2.5
1.4162 (lean duplex)	1.0	2.5
1.4462 (duplex)	0.9	2.5
S355	0.9	2.5

Similar observations was made by Tendo et al. [13], where type 304 austenitic grade was used in similar preloaded connections (carbon steel bolts). The 0.2 % proof strength was 265 MPa and when using 304N plates with the higher 0.2 % proof strength of 394 MPa, the measured loss of preload was significantly decreased and was similar to a structural carbon steel set-up. Finite element modeling was used for obtaining good agreement between modeling and measurements when using equation (11) for describing the creep behavior.

The higher loss of preload for the austenitic plate can be reduced by using higher strength splice plates (e.g. temper rolled austenitic plates) [13]. This decreases the amount of stress in the plates, and consequently, the amount of creep deformation.

The results of repeated relaxation tests suggest that repeated retightening of bolts can be used to reduce the loss preload. The same results also showed that the amount of stress relaxation increases with increasing loading speed. Therefore, preloading of bolts should preferably be carried out as slowly as possible.

_____

The uniaxial tensile creep testing affects the entire specimen cross-section whereas the stress under a washer in a preloaded connection is not uniformly distributed [14]. There is also indication that the creep behavior is different in tensile or compressive state, where the compressive stress state results in less creep [15]. Thus, the uniaxial tensile creep testing can be used for examining the material behavior under constant load but may not directly relate to the loss of preload in a preloaded connection.

	Creep and stress relaxation behavior of stainless steel plates at room temperature	2018-0042	Page 68 of 69
outokumpu	Timo Manninen, Johan Pilhagen	2017-01-02 Technical report	
TORNIO R&D CENTER		Public	

_____

8. Summary

- Room temperature creep was observed for the tested austenitic, ferric and duplex stainless steels at load levels at and above $0.50 \times R_{p0.2}$.
- No secondary creep was observed.
- The creep was greatly influenced by the load level.
- By analyzing the creep rate, three different deformation regions could be observed: (I) the initial loading, (II) the initial creep deformation and (III) the creep deformation that could be described by logarithmic creep.
- The logarithmic creep region was dependent on the load level but independent on the initial loading rate.
- The tested austenitic, ferritic and the two duplex grades had logarithmic creep behavior.
- In general, higher 0.2 % proof strength gives higher resistance to room temperature creep. But the actual creep behavior at absolute loads close to and above the proof strength seems to greatly depend on the yielding behavior.
- Although one can observe creep in uniaxial tensile testing, the stress in plates in a preloaded connection is too low to give any significant contribution to the loss of preload.
- The results from instrumented preloaded connections, the creep testing in this report and the stress relaxation testing of bars shows that the main contribution to the loss of preload in a preloaded stainless steel connection was the stress relaxation of the bolts.
- A state of the art viscoplastic material model was developed for modelling the creep and stress relaxation behavior of stainless steels at room temperature.

9. References

[1] T. Manninen, E. Jacobsen, J. Pilhagen, SIROCO Deliverable WP5, Task 5.1. Literature Study on Creep and Stress Relaxation of Stainless Steel at Room Temperature, Tornio, Finland, 2016.

[2] M.E. Kassner, K. Smith, Low temperature creep plasticity, Journal of Materials Research and Technology. 3 (2014) 280–288.

[3] M.E. Kassner, P. Geantil, R.S. Rosen, Ambient Temperature Creep of Type 304 Stainless Steel, Journal of Engineering Materials and Technology. 133 (2011).

[4] T.H. Alden, Theory of Mobile Dislocation Density: Application to the Deformation of 304 Stainless Steel, Metallurgical Transactions A. 18A (1987) 87–62.

[5] J.L. Chaboche, G. Rousselier, On the plastic and viscoplastic constitutive equations - Part I : Rules developed with internal state variable concept, Journal of Pressure Vessel Technology. 105 (1983) 153–158.

[6] J.L. Chaboche, G. Rousselier, On the plastic and viscoplastic constitutive equations - Part II : Application of the internal state variable rules to the 316 stainless steel, Journal of Pressure Vessel Technology. 105 (1983) 159–163.

[7] J. Lemaitre, J.-L. Chaboche, Mechanics of solid materials, Cambridge university press, 1994.

[8] X. Feaugas, On the origin of the tensile flow stress in the stainless steel AISI 316L at 300 K: back stress and effective stress, Acta Materialia. 47 (1999) 3617–3632.

[9] C. Gaudin, X. Feaugas, Cyclic creep process in AISI 316L stainless steel in terms of dislocation patterns and internal stresses, Acta Materialia. 52 (2004) 3097–3110.

[10] P. Hradil, T. Manninen, J. Pilhagen, N. Baddoo, A. Chen, SIROCO Deliverable WP5 Task 5.5. Report on numerical model calibration, Espoo, Finland, 2017.

[11] N. Stranghöner, N. Afzali, P. de Vries, E. Schedin, J. Pilhagen, S. Cardwell, Slip-resistant bolted connections of stainless steel, Steel Construction. 10 (2017) 333–343. doi:10.1002/stco.201710044.

[12] J. Pilhagen, SIROCO Deliverable, WP5 Task 5.3. Report on creep and stress relaxation behavior of stainless steel bars and bolts: Mechanical properties and stress relaxation of stainless bolts, Avesta, Sweden, 2017.

[13] M. Tendo, K. Yamada, Y. Shimura, Stress relaxation behavior at high-tension bolted connections of stainless-steel plates, Journal of Engineering Materials and Technology. 123 (2001) 198–202.

TORNIO R&D CENTER

Creep and stress relaxation behavior of stainless
steel plates at room temperature
Timo Manninen, Johan Pilhagen

2018-0042
2017-01-02
Technical report
Public

Page 69 of 69

_____

[14] T. Manninen, SIROCO Deliverable WP5, Task 5.0. Estimation of Load Level for the Short Term Dead
Weight Creep Tests on 1.4404 plates, Tornio, Finland, 2014.

[15] W. Schmidt, H. Dietrich, Einfluss einer kaltverformung auf den zusammenhang zwischen
raumtemperaturekriechen und Bauschinger-effekt, Thyssen Edelst. Techn. Ber., 7. Band, 1981, Heft 1,
pp. 41-54.

10.   Appendices

A. Report on relaxation tests on 1.4404 austenitic stainless steel by VTT.

European Commission

Research Programme of the Research Fund for Coal and Steel

Technical Group: TG 8

Creep and Stress Relaxation Behaviour of Stainless Steel Plates at Room Temperature

SIROCO Task 5.1

Annex to Deliverable D5.2

Author: Juhani Rantala, VTT

Date: May 17, 2017

Table of contents

1 Objective

The idea in the project planning phase was to conduct creep relaxation tests for 1.4404 stainless steel plates with a maximum duration of 2 hours per test. The test material was planned to be delivered by Outokumpu Oy. The test data would be used for developing a relaxation model which could then be used in the FE analysis of the stainless steel bolts.

2 Test material

A 500x500 mm plate of 1.4404 with a thickness of 8mm was received from Outokumpu Oy.

3 Test specimens

It was decided that VTT would use same type of so-called dog-bone specimens as Outokumpu Oy as shown in Fig. 1. However, for creep testing it is better to use pin loading with a diameter of at least as big as the width of the specimen. Therefore, it was decided to machine the holes to diameter 20 mm. Wire erosion with CNC-control was used for the cutting. It was decided that the following amount of specimens will be machined:

- 4 specimens machined in L-direction
- 4 specimens machined in T-direction

Residual stresses caused out of plane bending of some specimens in L-direction. At the very edge of the plate there was in-plane bending and between the specimen about 4 mm of out-of-plane bending as seen in Fig. 2. Therefore, Outokumpu Oy sent five additional ready-made specimens machined in the L-direction.

Fig. 1. The test specimen drawing delivered by Outokumpu Oy.

Fig. 2. Bending caused by residual stresses during wire erosion.

4 Test equipment

A relaxation test would normally be carried out in a servo-mechanical (or servo-hydraulic) testing machine with a precise strain control. During the test the specimen will be loaded to the required strain level, which would then be kept constant during the entire test. This requires a very good stability of the servo-control and the extensometer. VTT does have such machines, but because the relaxation tests for the Siroco project were planned to last between one day and one week per specimen, the total amount of testing hours became so large that the machines used for fracture mechanics testing could not be allocated to the Siroco project. Therefore, instead a servo-mechanical Instron 1361 was used, see Fig. 3. The shift to strain control caused load shocks and three specimens were bent, and this problem with the machine could not be rectified. Therefore, the tests were run in position control, adjusting the strain signal (see Fig. 4) by manual adjustment of the actuator position. This resulted in a surprisingly good stability and it was possible to carry out the test programme.

The specimens were loaded to an initial stress (not to initial strain like it should be according to the definition) in position control and then the strain signal was followed manually and the position of the piston was adjusted manually so that the strain signal was kept within the required scatter band. When a test was started in the morning, it was necessary to adjust the machine during the working day and a couple of times in the evening, but not during the night. During the test the following signals were recorded: time, load, strain, temperature and the actuator displacement.

The decision not to make the holes for the pin loading bigger than the width of the specimen (20 mm) was found to be a lucky choice because during the relaxation test the material around the loading pin holes deformed and made the manual control of the test much easier. The reason for this is the following: a relaxation specimen and the test machine can be seen as two springs in series. When the stress of the test specimen reduces, the elasticity of the test machine (the stronger spring) tends to pull the specimen above the specified strain, which then has to be compensated by the active servo-control of the test machine. Now that we did not have a servo-controlled machine, the deformation of the specimen ends did part of this job and as a result in most of the tests the strain was kept within the required tolerances of ASTM E328.

Fig. 3. The servo-mechanical test machine used for the relaxation tests.

Fig. 4. The test specimen with a strain transducer and a thermocouple during the test (left) and the set-up used for the calibration of the strain transducer (right).

The test matrix is shown in Table 1. In the project planning phase it was specified that the relaxation tests should last for only two hours, but taking the long service-life of the bolt joints into consideration it is better to make the tests as long as practical. Therefore, the testing time was extended to maximum one week per specimen. The last (extra) test 4L5 was cancelled when the control electonics of the test machine broke down.

A typical loading curve is shown in Fig. 5. The displacement rate of the actuator was reduced in steps when approaching the required strain level. The reduction of rate is shown as small drops in the stress curve. An example of a typical load vs. strain curve is shown in Fig. 6. The relaxation takes place at the vertical part at the top right corner of the curve when the strain is kept constant and the load reduces as a result of relaxation.

Some example plots of strain and load vs. time plots are shown in Figs. 7-10. The ASTM E328 strain stability requirement of ± 25 µε (corresponds to ± 0.0025% of strain) are shown in these figures, indicated by red horizontal lines. In most of the cases the strain signal remained within these limits, but is some cases the strain signal exceeded the limits. If the diversion from the allowed range was short, one could make a compromise and still use the data for model fitting. In some cases the data at the end of the test went outside the limits and in such cases the beginning of the test can still be used for fitting, but the data outside the limits has to be cut. All the data used for modelling are shown in Fig. 11 in a double logaritmic plot.

Table 1. The relaxation test matrix

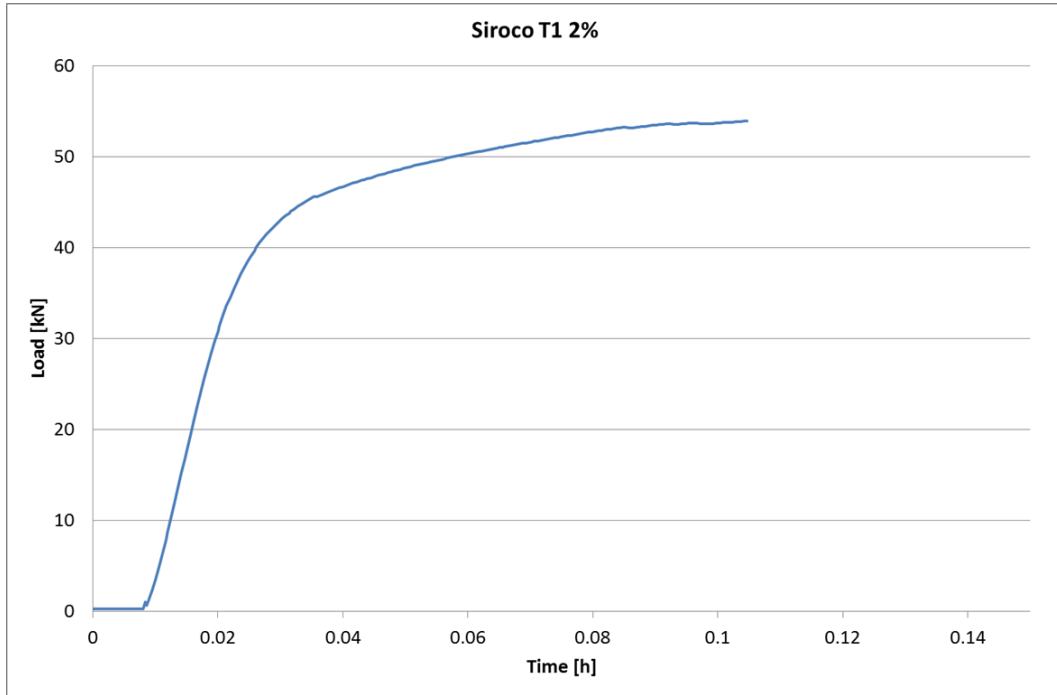| Specimen	Initial strain	Status	Duration
L1, L2, L3		invalid	
L4	2%	complete	20h
T1	2%	complete	35h
T2	1.16%	complete	57h
T3	0.36%	complete	23h
T4	0.12%	complete	104h
4L1	2%	complete	24h
4L2	1.16%	complete	68h
4L3	0.36%	complete	168h
4L4	0.12%	complete	166h
4L5	Extra 0.12%	spare	Cancelled

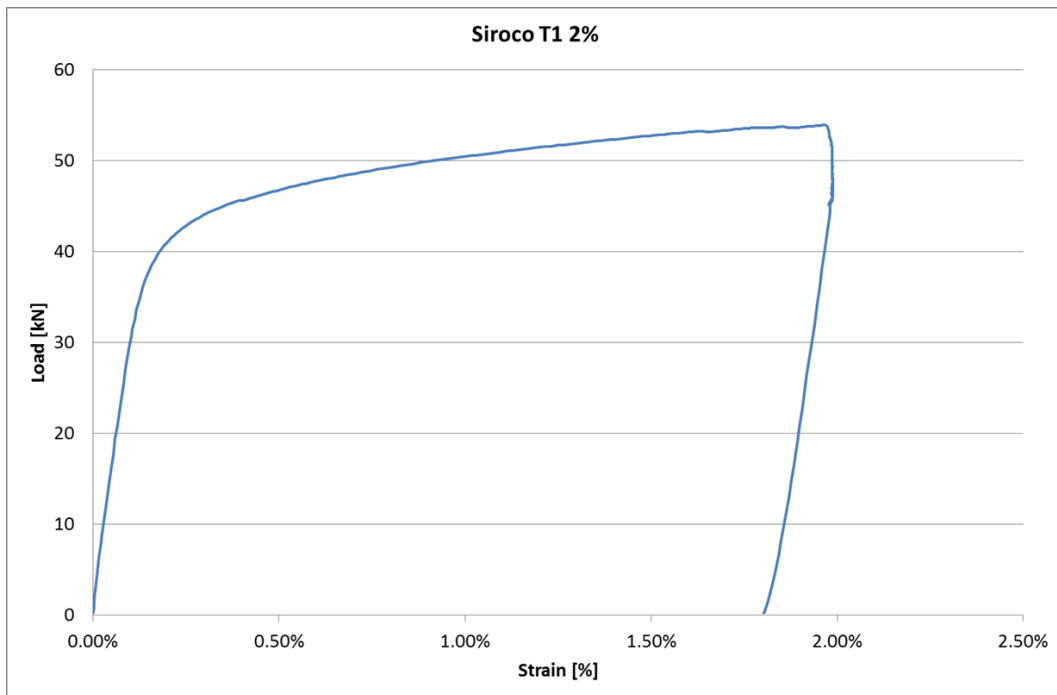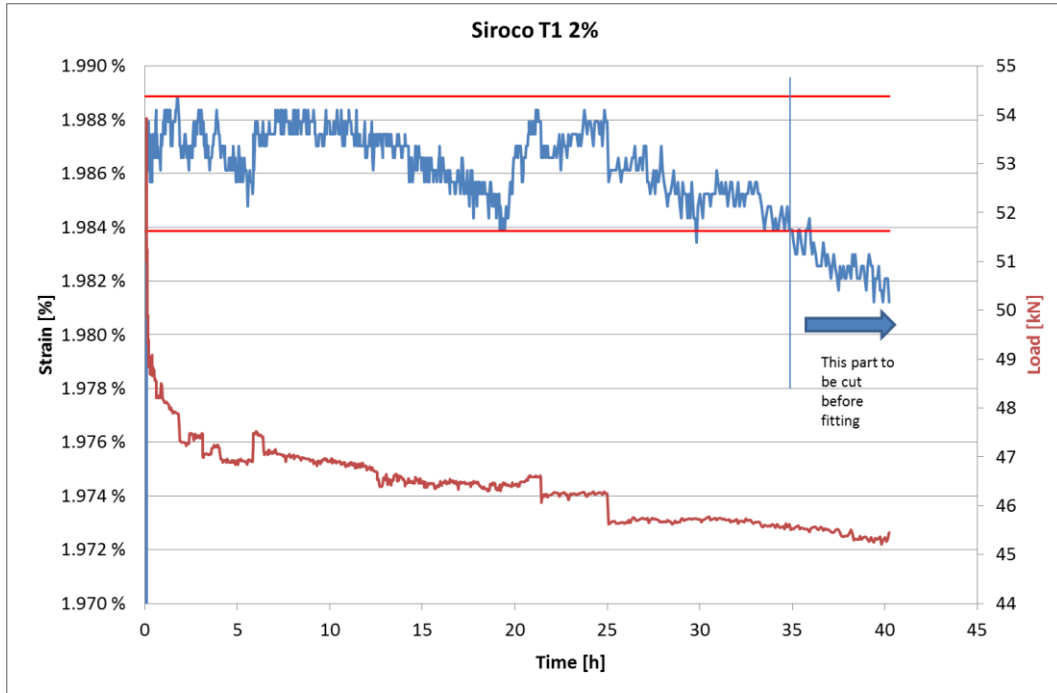*Fig. 5. A typical loading curve.*

Fig. 6. The full load vs. strain curve.

Fig. 7. Strain and load vs. time plot. The red horizontal lines represent the ASTM E328 strain stability requirement of ± 25 µε corresponding to ± 0.0025% of strain. Strain signal (top curve) in blue, load signal in brown (lower curve).
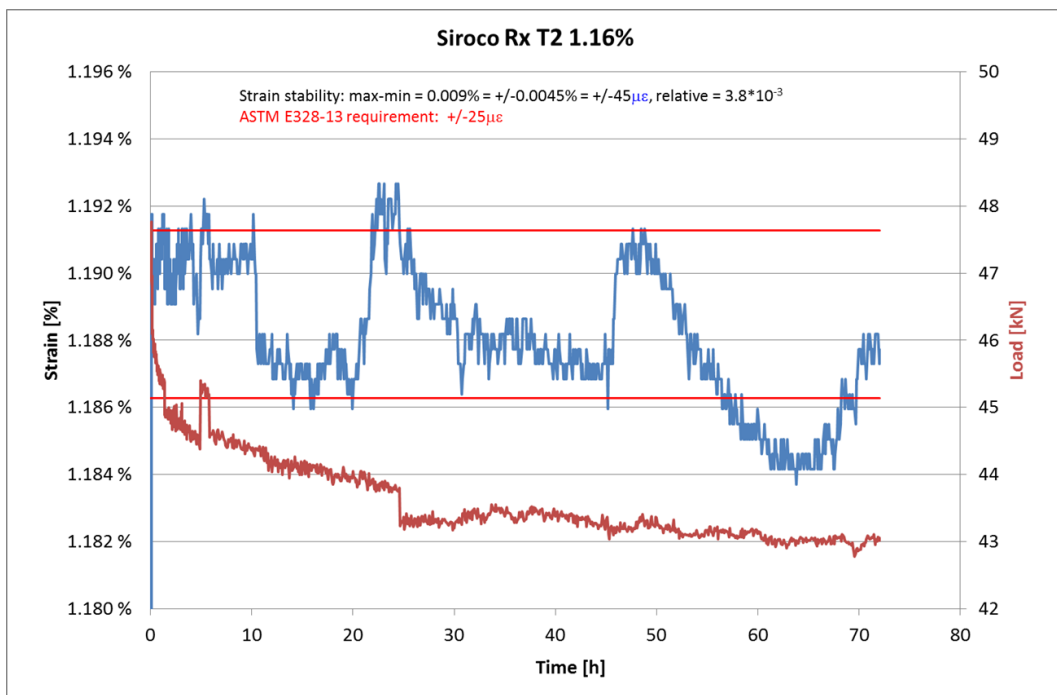

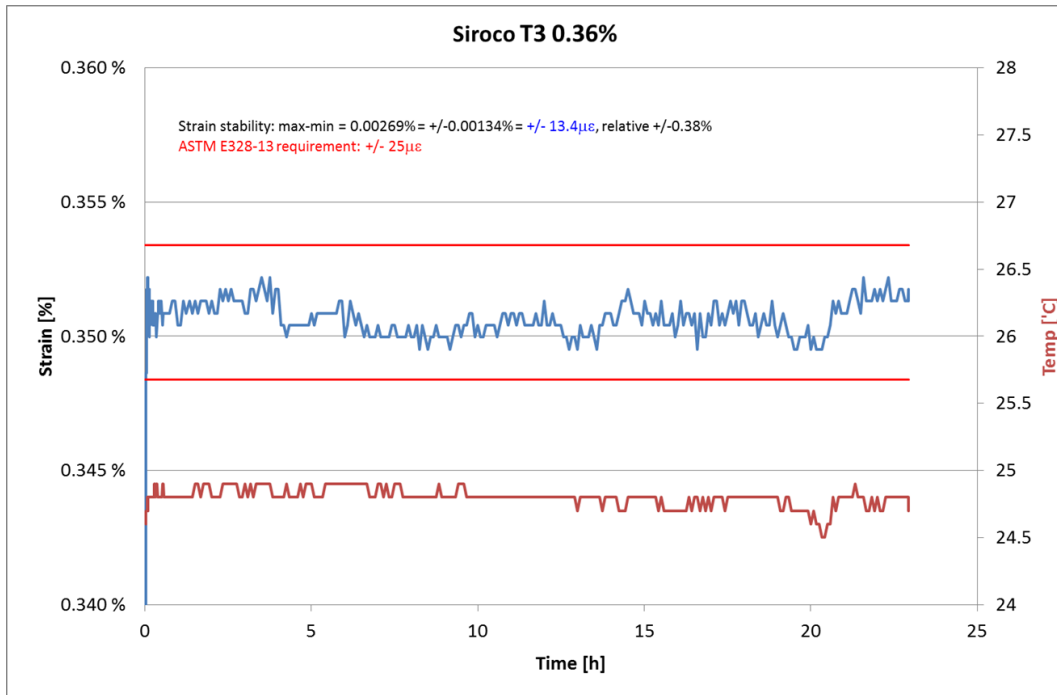*Fig. 8. An example of a test where the strain requirement was not met.*

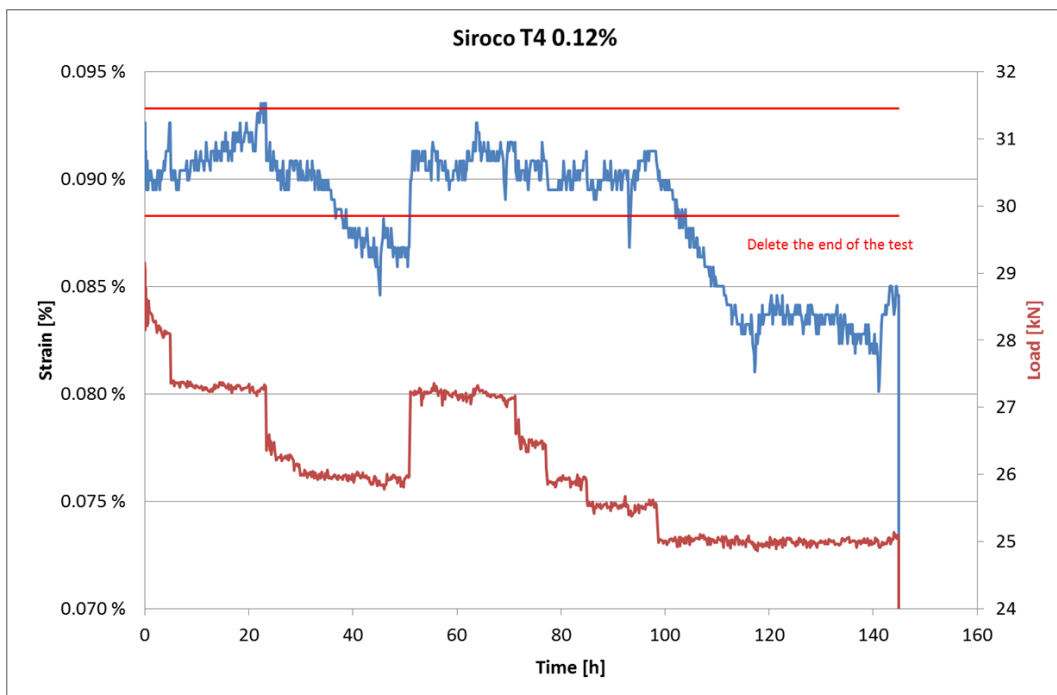*Fig. 9. Best example of strain stability in a 23 h test. The lower curve is temperature.*

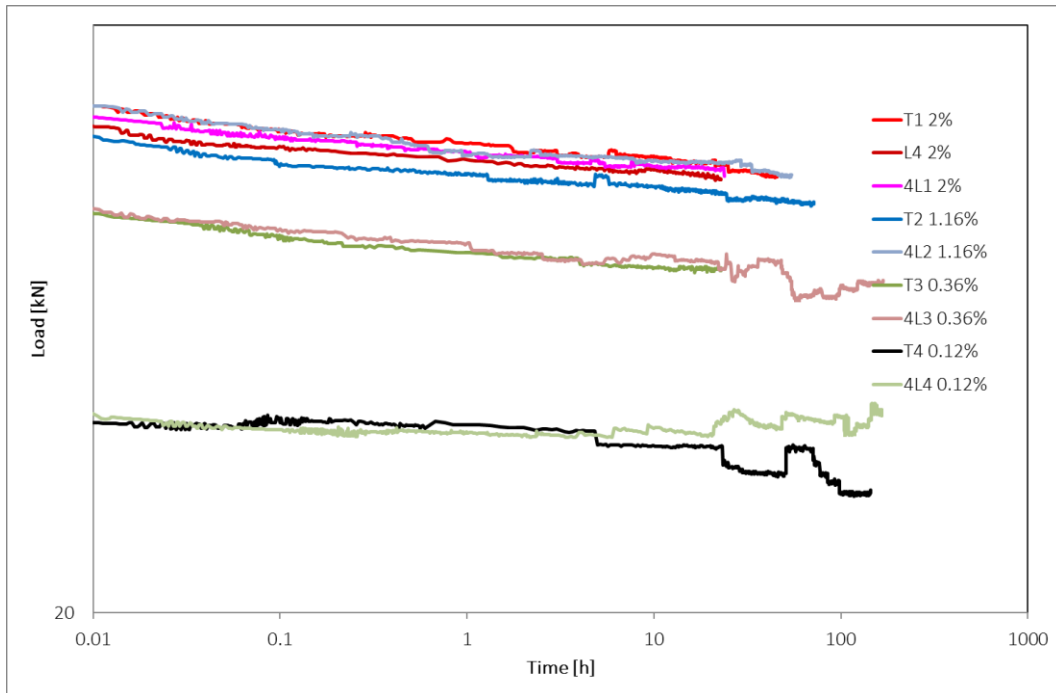*Fig. 10. Worst example of a long test with a small initial strain.*

Fig. 11. All relaxation results in a load vs. time plot.

5 Data fitting

The relaxation data was supplied in Excel format to the modelling people at VTT and the data was fitted by using suitable relaxation models. These results are reported in the report VTT-R-01467-17.